

DISSERTATION

HIERARCHICAL MODELS PROVIDE INSIGHT INTO
WILDLIFE AND DISEASE MANAGEMENT

Submitted by

Chris Geremia

Graduate Degree Program in Ecology

In partial fulfillment of the requirements

For the Degree of Doctor of Philosophy

Colorado State University

Fort Collins, Colorado

Spring 2014

Doctoral Committee

Advisor: N. Thompson Hobbs

P. J. White

Michael W. Miller

Jennifer A. Hoeting

Michael F. Antolin

Copyright by Chris Geremia 2014

All Rights Reserved

ABSTRACT

HIERARCHICAL MODELS PROVIDE INSIGHT INTO WILDLIFE AND DISEASE MANAGEMENT

Wildlife diseases can alter host populations with cascading effects throughout ecosystems and human economies that rely on those wildlife. Pathological effects can be the ultimate cause of wildlife population decline through depressing host reproduction and survival. Otherwise, less virulent pathogens can harm host populations indirectly, through management actions imposed on wildlife populations harboring diseases that harm people or their livelihoods. Hierarchical Bayesian methods provide a framework for factoring highly dimensional problems into lower dimensional ones. These techniques decompose a problem into data, the underlying process, and parameters, and identify uncertainty associated with each component. Appropriately quantifying uncertainty fosters clearer understanding of wildlife and disease management problems.

Bison *Bos bison* migrating from Yellowstone National Park into the state of Montana during winter and spring concern ranchers on lands surrounding the park because bison can transmit brucellosis (*Brucella abortus*) to cattle. Migrations have been constrained with bison being lethally removed or moved back into the park. I, and several coauthors (we) developed a state-space model to support decisions on bison management aimed at mitigating conflict with landowners outside the park. The model integrated recent GPS observations with 22 years (1990-2012) of aerial counts to forecast monthly distributions and identify factors driving migration. Wintering areas were located along decreasing elevation gradients and bison accumulated in wintering areas prior to moving to progressively lower elevation areas. Bison movements were affected by time since the onset of snow pack, snow pack magnitude, standing crop, and herd size. Migration pathways were increasingly used

over time, suggesting experience or learning influenced movements. To support adaptive management of Yellowstone bison, we forecast future movements to evaluate alternatives. Our approach of developing models capable of making explicit probabilistic forecasts of large herbivore movements and seasonal distributions is applicable to managing the migratory movements of large herbivores worldwide. These forecasts allow managers to develop and refine strategies in advance, and promote sound decision-making that reduces conflict as migratory animals come into contact with people.

Chronic wasting disease (CWD) is a fatal, neurodegenerative prion disease that affects members of the deer family (*Cervidae*). There is worldwide concern that the disease may harm ecosystems and human economies by causing demise of deer populations. Little is known about effects of the disease on population dynamics. We studied a mule deer population where CWD has been present for at least four decades. We developed a disease model to estimate the effect of CWD on population growth rate and extent that the epidemic is increasing. Our model integrated capture-mark-recapture histories of adult female mule deer during a four year study with long-term population monitoring data on abundance, composition, and CWD prevalence. Our model was capable of deciphering probabilities of infection and correct identification of infected individuals from disease tests.

We provide compelling evidence that prion epidemics can affect mule deer populations both locally and at coarse spatial scales. Chances of population decline were greatest at the wintering subpopulation scale, but differences in infection rate among subpopulations caused CWD to have virtually no effect on growth in some wintering subpopulations. At larger scales, deer populations showed some natural resistance against CWD by localizing areas of higher infection. Overall, disease effects were subtle and the protracted time-scale of the epidemic is likely much longer than the thirty year time span of our research. As a result, we could not identify the inevitable fate of deer populations with CWD. Our findings do suggest, in the nearer-term (e.g., decades), mule deer populations persisting at lower levels after disease establishment.

ACKNOWLEDGMENTS

I thank N. Thompson Hobbs, P.J. White, Michael W. Miller, Jennifer A. Hoeting, Micahel F. Antolin, Lisa L. Wolfe, Rick Wallen, Doug Blanton, Nathan L. Galloway, and Fred G. R. Watson for their assistance with preparation of the following dissertation chapters. The views and text of these chapters are those of mine and these coauthors.

This research was funded by the National Science Foundation (EF-00914489), the Colorado Division of Parks and Wildlife, and the National Park Service. I thank Yellowstone National Park staff including Dave Hallac; Colorado Division of Parks and Wildlife staff, including Mark Leslie, Janet George, Mark Vieira, Debbie Grossblat, and the Wildlife Health Program; Dave Younkin and Quick Silver Air; Colorado State University staff, including Caroline Krumm, Jill Lockett, Randall Boone, and Terry Spraker; and the community of Larimer County, Colorado.

TABLE OF CONTENTS

Abstract	ii
Acknowledgments	iv
Chapter 1: Introduction	1
Chapter 2: Integrating Individual- and Population- level data in a movement model of Yellowstone bison	3
Study Area	6
Methods	9
Movement Data	9
Aerial Counts	9
Model Covariates	9
Bison Utilization Distribution	10
Structural Connectivity	10
Statistical Approach	11
Process Model	11
Initial Conditions	13
Data Models	14
Parameter Models	15
Model Implementation	16
Predictions for Adaptive Management	17
Results	19
Assessment of Model Performance	19
Individual Animal Movements	21
Estimation of Population Level Parameters	22
Adaptive Management	26
Discussion	32

Chapter 3: A Mule Deer Population Persists with Enzootic CWD	38
Material and Methods	40
Study Area	40
Data Collection	41
Population Growth and Disease Trajectory	43
Data Analysis	45
Results	47
Discussion	59
Chapter 4: Age Drives CWD Ante Mortem Test Sensitivity in Mule Deer	64
Material and Methods	66
Data Collection	66
Background and Statistical Analysis Framework	67
Detailed Statistical Methods	68
Estimating the Chance of a False Negative Test	69
Results	70
Discussion	78
Chapter 5: Mobility and Clay Soils Underlie CWD Infection in Adult Female Mule Deer	82
Material and Methods	84
Data Collection	84
Disease Model	86
Developing Landscape- and Individual- Level Covariates	88
A. CWD Prevalence and Infection Risk	88
B. Clay Soils and Infection Risk	90
C. Migration and Infection Risk	91
D. Age and Infection Risk	92
E. Prnp Genotype and Infection Risk	93
Model Selection	93

Results	95
Discussion	105
Literature Cited	112
Appendix 1 Supplementary Material	132
Appendix 2 Supplementary Material	139
Appendix 3 Supplementary Material	149
Appendix 4 Supplementary Material	151

CHAPTER 1: INTRODUCTION

Wildlife diseases can alter host populations with cascading effects throughout ecosystems and human economies that rely on those wildlife. Pathological effects can be the ultimate cause of wildlife population decline through depressing host reproduction and survival. Otherwise, less virulent pathogens can harm host populations indirectly, through management actions imposed on wildlife populations harboring diseases that harm people or their livelihoods.

Brucellosis is a bacterial disease caused by *Brucella abortus* that may induce abortions or the birth of non-viable calves in livestock and wildlife. When livestock are infected it also results in economic loss from slaughtering infected cattle, increased testing requirements, and possibly, reduced marketability of cattle. Bison and elk in Yellowstone National Park are chronically infected with brucellosis. Feared transmission of brucellosis from bison to livestock has resulted in intensive management and reductions of bison exiting Yellowstone National Park. Implementing brucellosis management strategies is contingent on these seasonal migrations and understanding the forces that shape migratory movements can improve management. In Chapter 2, I and several coauthors (we) developed a movement model capable of forecasting seasonal bison distributions. We used this model to compare alternative strategies for managing the trans-boundary movements of Yellowstone bison.

In the remaining chapters, we focused on chronic wasting disease (CWD), an emergent, neurodegenerative prion disease that affects deer, elk, and moose throughout North America. CWD has raised worldwide concern because it can be transmitted among species of the deer family, is uniformly fatal, and the infectious agent, PrP^{Sc}, persists in the environment for long periods. Simulation models suggested that the consequence of CWD for deer populations could vary widely with predictions ranging from limited population decline and sustained low disease prevalence to widespread local extinction within decades of disease introduction. Empirical studies have shown CWD can depress growth rates of local populations with

remarkably high infection prevalence. Declines in deer abundance over larger spatial extents could pose debilitating effects on ecosystems and human economies, because deer populations play important roles in ecosystems, provide primary prey for large carnivores, and serve as a food resource to people. The inevitable consequence of CWD will only begin to play out over our lifetimes. Today's challenge is making decisions about CWD in the face of incomplete understanding.

We completed a four year capture-mark-recapture study of female mule deer to estimate survival and infection probability. In Chapter 3, we integrated these data with long-term information on deer abundance, demography, and CWD prevalence to estimate the effect of CWD on population growth rate. Disease tests on live animals were imperfect, which complicated estimating disease effects. In turn, we developed a disease model capable of identifying probabilities of infection, correct diagnosis, and uncertainties associated with each component. In Chapters 4 and 5, we analyzed our disease model in detail. Chapter 4 focused on factors affecting test accuracy and Chapter 5 evaluated individual effects on infection probability.

A unifying goal of my dissertation research was to illustrate the usefulness of hierarchical Bayesian modeling in gaining understanding from data collected from wildlife and disease management studies. Hierarchical Bayesian methods provide a framework for factoring highly dimensional problems into lower dimensional ones. These techniques decompose a problem into data, the underlying process, and parameters, and identify uncertainty associated with each component. I aimed to show how these approaches are general and can be applied to a variety of problems. I challenged myself to build better tools to address pressing wildlife and disease management concerns.

CHAPTER 2: INTEGRATING INDIVIDUAL- AND POPULATION- LEVEL DATA IN A MOVEMENT MODEL OF YELLOWSTONE BISON

Large herbivore movements occur at multiple scales of time and space. Annual migration is the manifestation of choices made at the regional scale that allow animals to respond to changes in resources that cannot be exploited year round (Senft et al., 1987; Fryxell and Sinclair, 1988). Migration is a regular, long distance pattern of movement typically observed in systems with predictable, seasonal fluctuations in environmental conditions (Mueller and Fagan, 2008). In montane environments, such movements along elevation gradients provide large herbivores access to newly emerging vegetation during the growing season resulting in increased long-term rates of energy gain (Albon and Langvatn, 1992; Wilmshurst et al., 1995; Mysterud et al., 2001; Hebblewhite et al., 2008). Migratory movements may also diminish predation pressure as animals move beyond the boundaries of predator territories (Laundre et al., 2001; Fortin et al., 2004; Hebblewhite and Merrill, 2007). Montane environments are characterized by a prolonged period when newly emerging vegetation is no longer available and decisions to move are often influenced by increased energetic costs of locomotion and foraging with snow pack establishment (Parker et al., 1984; Larter and Gates, 1991; Schaefer and Messier, 1995; Fryxell et al., 2004; Doerr et al., 2005). Within patch foraging movements are affected by localized heterogeneity, whereas migratory movements are typically driven by factors at the landscape-scale (Ball et al., 2001; D'Eon and Serrouya, 2005; Holdo et al., 2009; Zweifel-Schielly et al., 2009).

Human activities have fragmented landscapes throughout the world, severing historic pathways for migration of many species of large herbivores (Galvin et al., 2008; Hobbs et al., 2008). Rural landscapes supporting livestock production and agriculture often provide usable habitat for migrating large herbivores (Hansen and DeFries, 2007). Road development (Nellemann et al., 2001; Ito et al., 2005; Fox et al., 2009; Holdo et al., 2011), fencing (Fox et al., 2009; Bartlam-Brooks et al., 2011; Li et al., 2012), natural resource extraction (Sawyer

et al., 2009), and recreation-based development (Vistnes et al., 2004; Wittmer et al., 2007) now threaten many remaining long distance migrations (Berger, 2004). Furthermore, migratory wildlife may come into conflict with people beyond the boundaries of protected areas because wildlife transmit disease, damage property, or compete with livestock for forage. (Thouless, 1995; Plumb et al., 2009; Metzger et al., 2010). Severing migrations has had adverse demographic effects on large herbivores and there is increasing support at regional and global levels to preserve these natural phenomena (Berger, 2004). However, the interests of local economies often conflict with conservation goals. Maintaining migrations in the face of this conflict requires understanding the forces that shape migratory patterns.

Human hunting reduced plains bison (*Bos bison*) from an estimated 28 million animals to fewer than 100 by the end of the nineteenth century. Approximately 25 of these surviving bison occupied remote areas in Yellowstone National Park and the remainder were found in private preserves across the western United States. Beginning in 1902, a second herd was started in Yellowstone with 21 bison from two private reserves. Total bison abundance in Yellowstone has gradually increased through protection, husbandry, and relocation. Beginning in 1968, bison numbers were allowed to fluctuate in response to weather, predators, and resource limitations (Meagher, 1973). Seasonal movements were re-established as the population increased in size and expansion of the winter range was detected by the 1980s (Meagher, 1989). Yellowstone bison eventually began using lower elevation winter ranges outside the park in Montana where winter snow pack is less severe and it is easier to access forage. Range expansion much beyond the park boundary is now precluded by intense management intervention due to concerns of brucellosis transmission to cattle (White et al., 2011).

Approximately 60% of the Yellowstone bison population has been exposed to brucellosis, a bacterial disease caused by *Brucella abortus* that may induce abortions or the birth of non-viable calves in livestock and wildlife (Rhyan et al., 2009). When livestock are infected it also results in economic loss from slaughtering infected cattle, increased testing requirements,

and possibly, reduced marketability of cattle. The United States government and the state of Montana agreed to an adaptive interagency bison management plan (USDI and USDA, 2000a,b) for cooperatively managing the risk of brucellosis transmission from Yellowstone bison to cattle while conserving bison as a natural component of the ecosystem and allowing some bison to migrate out of the park. Before cattle are stocked in the area during summer, bison that migrated into Montana during winter are either hazed (i.e., moved) back into Yellowstone National Park, harvested by hunters, or captured and transported to slaughter (USDI and USDA, 2000a,b).

Adaptive management is a structured decision making approach for improving resource management by systematic learning from management actions and outcomes (Walters and Holling, 1990). It involves the exploration of alternatives for meeting objectives; prediction of outcomes from alternatives using current understanding; implementation of at least one alternative; monitoring of outcomes; and using results to update our knowledge and adjust actions (Williams et al., 2007). Adaptive management provides a framework for decision making in the face of uncertainty and a formal process for reducing uncertainty to improve management and outcomes over time.

White et al. (2011) provided an assessment of the Interagency Bison Management Plan that indicated migrations far exceeded expectations of initial models and approximately 3,200 bison were culled during 2001-2011. More than 20% of the population was removed during 2006 and 2008 which contributed to a skewed sex ratio, gaps in the population age structure, and reduced productivity, which could threaten the integrity of the population if continued (White et al., 2011). These authors and stakeholders recommended reduced culling of animals at park boundaries and increased tolerance in adjacent areas in the state of Montana to support sport hunting. Managers agreed to reduce large scale culls through gather-and-slaughter and requested a predictive model of trans-boundary movements to assess revised management alternatives.

Model development is a component of the structured decision-making process that brings together data and uncertainty through testable hypotheses representing our understanding of the system and effects of management alternatives. Uncertainty arises from our lack of understanding of the ecological process, measurement error, environmental variability, and our lack of complete control over management actions (Williams et al., 2007). Hierarchical models are particularly well suited for adaptive management because of the ability to appropriately incorporate data with different error structures and identify both observation error and process variance. Bayesian techniques provide a particularly clear method for constructing these models.

Here, we develop a hierarchical Bayesian model of regional scale movements of Yellowstone bison. The structural connectivity of the bison range is identified by differentiating the landscape into wintering areas linked by migration paths. We used a state transition approach (Caswell, 2001) in discrete time to estimate monthly distributions during 1990-2012 and to relate transition probabilities to environmental covariates. Future migrations are forecasted under different scenarios of environmental conditions and herd sizes to identify the timing and magnitude of movements, and assess the appropriateness of alternative management interventions. This approach of using Bayesian inference in support of adaptive management is applicable to addressing trans-boundary movements of wildlife worldwide.

Study Area

Yellowstone bison live in a single population of approximately 2,500-5,000 bison in at least two breeding herds (central and northern). The central herd occupies the central plateau of Yellowstone National Park, extending from the Hayden Valley and nearby grasslands in the east to the lower elevation and thermally influenced Gibbon (also referred to as Madison) River drainage and Hebgen Lake basin in the west (Figure 1). The central plateau is characterized by several large meadow complexes located along an east-west gradient of decreasing

elevation linked by narrow travel corridors which coincide with rivers. At the highest end, the Hayden Valley is characterized by highly productive upland grass communities with the majority of habitat classified as big sagebrush/Idaho fescue or silver sagebrush/Idaho fescue. Elevations exceed 2,450 m and snow water equivalents are more severe than alternative bison use areas, with refuge areas provided by windswept hills and geothermal influenced areas during winter. The mid-elevation Firehole River drainage (2,225 m) encompasses several interconnected, thermally influenced, geyser basins with ground cover dominated by sedges at the base of the basins and cool season grasses on the slopes. The Gibbon Valley and Hebgen Lake basin are a series of small and disjoint meadows spanning a decreasing gradient from 2,200 m in the east to 2,050 m at the western boundary of the park north of West Yellowstone, Montana.

The northern herd congregates in the Lamar Valley and on adjacent plateaus in northern Yellowstone during the breeding season (July 15-August 15; Figure 1). During the remainder of the year, these bison use habitats in the Yellowstone River drainage, which extends 100 km between Cooke City and the Paradise Valley north of Gardiner, Montana. This area is characterized by a large expanse of upland grassland meadows occurring along a decreasing elevation gradient from east (2,200 m) to west (1,650 m). This area has drier and warmer summers and less severe winters than the central interior of the park. There is limited geothermal influence and the majority of the habitat is characterized as big sagebrush/Idaho fescue or big sagebrush/sticky Idaho fescue. The western extent of these northern grasslands occurs near Gardiner, Montana. Although it is the least productive wintering range, it generally contains snow-free areas during most winters, so forage availability can be high even though production is low.

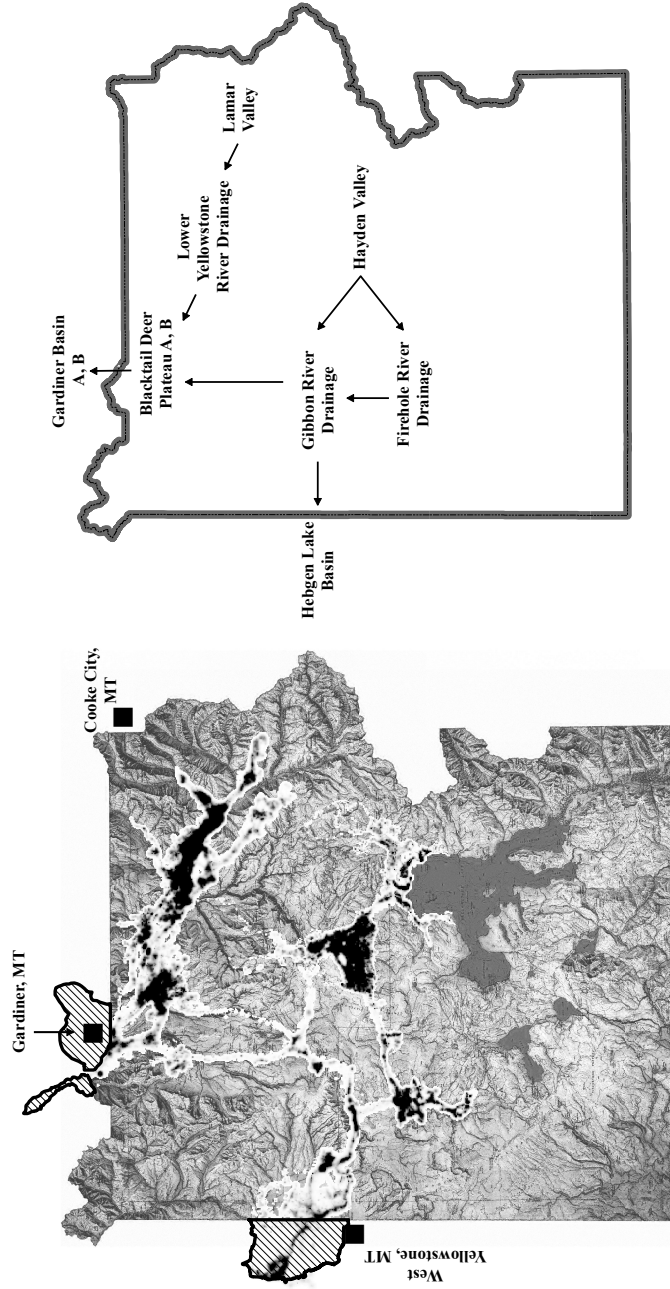


Figure 1: The left panel is a cumulative utilization distribution of bison use (darker colors represent increased use) in and surrounding Yellowstone National Park during 2004-2012. Hatched areas are out-of-park bison management areas where animals are harvested, gathered into livestock-like handling facilities, and can come into contact with cattle. The right panel is a graph of wintering areas and migration paths (arrows) that was created from the cumulative utilization distribution. The letters A and B indicate separate wintering areas for central and northern herd animals occupying the same geographic area. These wintering areas and migrations paths served as a basis for modeling movements.

Methods

Movement Data

Sixty-six bison >1 year of age were captured in autumn during 2004-2012 by immobilization with carfentanil and xylazine (Rhyan et al., 2009) or at handling facilities near the boundary of the park (USDI and USDA, 2000a,b). Individuals were fit with a store-on-board GPS collar (Telonics Inc. Mesa, Arizona) that collected between 2 months and 5 years of information. Bison were captured from the central herd during 2004-2012 and from the northern herd during 2006-2012. GPS devices were programmed to collect one location every 48 min during 2004-2005 and one location every 2 h during 2005-2012. A total of 512,621 locations were collected.

Migration paths used by bison in the central portions of Yellowstone generally passed through constricted regions at some point, and remotely triggered camera stations (PM-175, Silent Image, Reconyx Inc., Holmen, WI) were installed in these areas during November-April, 2010-2012 to record total numbers of bison and their direction of travel. Cameras were visited biweekly to download images and replace batteries. Pictures were viewed using Mapview (Reconyx Inc., Holmen, WI).

Aerial Counts

During 1990-2012, 136 aerial counts were completed to estimate population size where observers recorded the location and size of encountered bison groups during systematic surveying of wintering areas (Hess, 2002). Counts occurred monthly from 1990 to 1997, approximately quarterly from 1998 to 2006, and again monthly from 2007 to 2012.

Model Covariates

Three movement covariates were observed throughout the duration of this research. i) Herd Size: Between two and three annual aerial counts of bison on breeding areas were

completed to estimate herd sizes. ii) Snow Pack: Daily snow estimates were generated using a simulation model that predicted 28 m² resolution surfaces of snow water equivalents (Watson et al., 2006; Geremia et al., 2009). Daily snow surfaces of the bison utilization distribution area across the central and northern portions of park were averaged to single north and central values for each day of the year. We added these averaged, daily values across the year to create single, annual snow pack values for the northern and central regions. iii) Standing Crop: Standing crop estimates at the conclusion of the growing season were generated using a simulation model that predicted 30 m² resolution surfaces of modeled monthly net primary productivity from NASA's Carnegie-Ames-Stanford-Approach (Potter et al., 2007; Geremia et al., 2011). CASA, a biophysical ecosystem model, incorporates temperature, precipitation, solar radiation, vegetation cover, and the normalized differentiation vegetation index from Landsat satellite data as inputs during April through October (Potter and Klooster, 1999; Crabtree et al., 2009; Huang et al., 2010). Values were averaged across central and northern grassland regions of the bison utilization distribution for each year.

Bison Utilization Distribution

Brownian bridge movement models were used to approximate the continuous movement path of individual adult female bison between successive locations recorded by store-on-board global positioning system (GPS) devices (Horne et al., 2007). We created utilization distributions that were two dimensional gridded surfaces representing relative use according to frequency of visits to and movement rate through areas for each individual. A single cumulative utilization distribution for the entire population was created by summing across each individual utilization distribution (Sawyer et al. 2009; Figure 1).

Structural Connectivity

We used a graph theoretic approach to define the structural connectivity of Yellowstone bison (Urban and Keitt, 2001). We differentiated the landscape into a set of nodes that

were wintering areas connected by edges that were migration paths. Wintering areas and migration paths were determined by looking at the cumulative utilization distribution and identifying the two types of areas. GPS histories of individually marked animals were then examined to confirm our classification. Our graph included 10 wintering areas connected by 8 migration paths (Figure 1).

Statistical Approach

State-space models can be used to join stochastic models of observations with a stochastic model portraying the underlying mechanisms of movement (Patterson et al., 2008; Schick et al., 2008). In the state-space approach, we assume there is a time series of unobserved, true states such that the current state directly influences the state at the next time. A second time series, running in parallel, includes the observations of the true states. We assume the observations fail to represent the true state perfectly because they are made with error. Hierarchical Bayesian methods provide a framework for factoring highly dimensional problems into lower dimensional ones (Berliner, 1996). These techniques decompose a problem into data, the underlying process, and parameters, and identify uncertainty associated with each component. The following sections describe the decomposition of the problem into process, data, and parameter models.

Process Model

The true numbers of bison in wintering areas and movement probabilities between areas were estimated using a state-transition model (see also Harrison et al. 2006; Morrison and Bolger 2012) in discrete time (Figure 2). The model updated on a monthly time step. The initial spatial distribution of bison for each year was estimated during July when bison were congregated on breeding areas for the rut. Model updates were generated each subsequent month through peak migration which occurred when highest numbers of bison were located on alternative wintering areas. The column vector $z_{t,j}$ represents the true number of bison

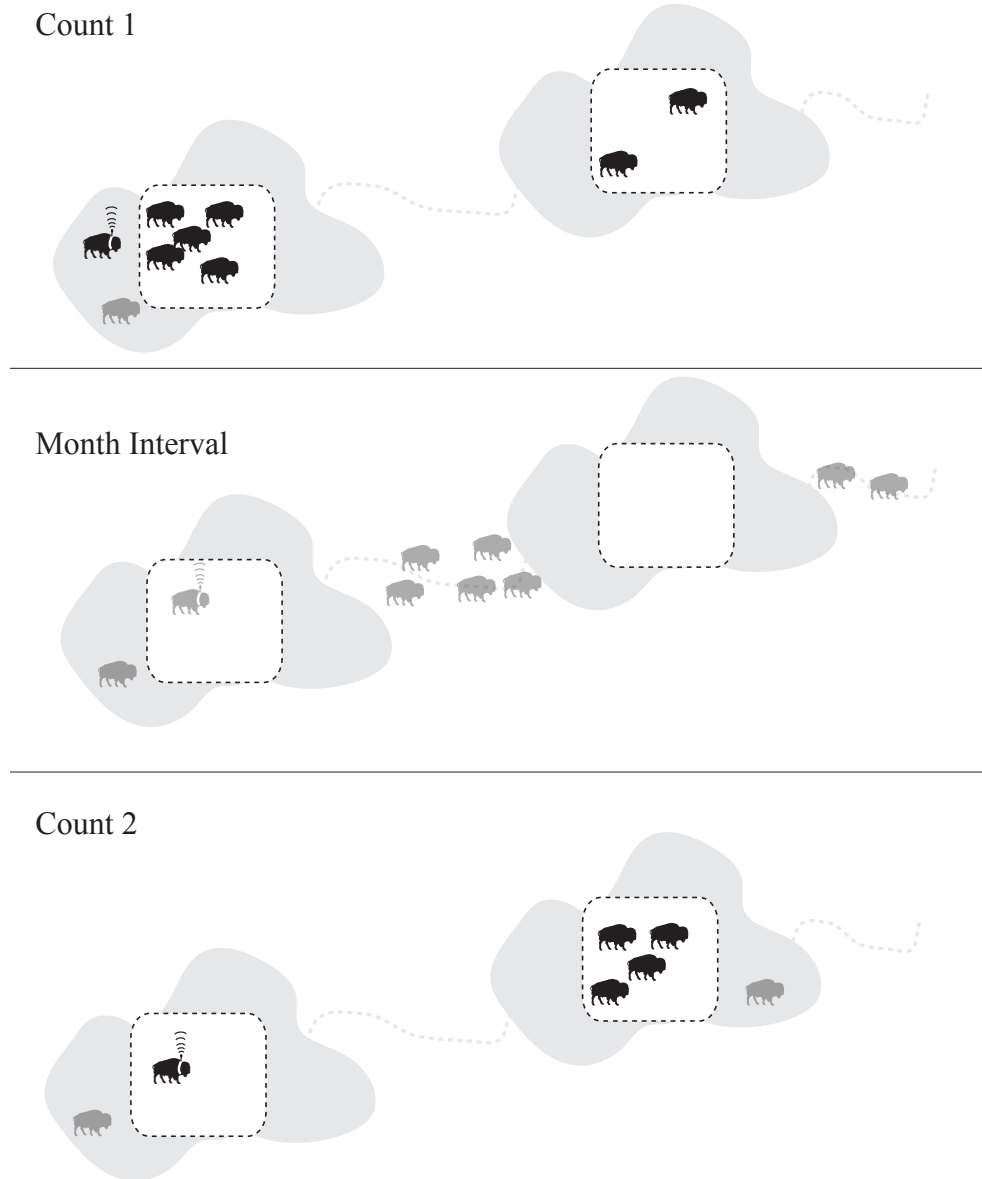


Figure 2: We present a conceptual figure of our model. **Top:** Aerial count units (square boxes with dotted line) did not completely overlap wintering areas (gray shaded region). Bison were observed in aerial count units or in wintering areas based on GPS devices fit to animals. Uncollared bison outside of count areas were not observed which we represent using the transparent icon. **Middle:** movements between wintering areas during the ensuing month were not observed. **Bottom:** One month later bison were again observed in aerial count units or or in wintering areas based on GPS devices fit to animals. Unobserved quantities including the true number of bison in wintering areas at the time of counting and movements between counts were estimated. These unobserved quantities (e.g., movements) were related to covariates mainly reflecting food availability.

in each wintering area during month t and year j . The matrix \mathbf{A} represents transitions of bison between wintering areas (e.g. survival and movement along migration paths) during Δt (Appendix 1). We assume the i^{th} element of $\mathbf{z}_{t,j}$ follows a gamma distribution with rate β and shape $\mathbf{A}_i \mathbf{z}_{t-1,j} \beta$ where \mathbf{A}_i is the i^{th} row of \mathbf{A} . The parameters of the gamma distribution are the rate and shape which correspond to the mean $\mathbf{A}_i \mathbf{z}_{t-1,j}$ and process variance $\frac{1}{\beta} \mathbf{A}_i \mathbf{z}_{t-1,j}$ using moment matching (Appendix 1).

Survival and movement determined the number of bison remaining in each wintering area at the next time step. The monthly probability of survival is ϕ and the monthly movement probability along the i^{th} migration path is γ_i . Each movement probability is related to covariates using the logistic model that reflect increased energetic costs of locomotion and foraging during winter (Appendix 1). These covariates include days since the onset of snow cover, annual snow pack magnitude, herd size, standing crop at the conclusion of the growing season, and year of study. Days since the onset of snow cover is represented using a quadratic term. This allows movement probabilities to reach minima corresponding to optimal times of the year for wintering area use. Year was included as a covariate to allow annual movement probabilities to steadily increase or decrease throughout the duration of our research.

Initial Conditions

The number of bison in each wintering area at the current time $\mathbf{z}_{t,j}$ was conditioned on the number of bison at all previous times, but could be expressed by conditioning only on the most recent time. Then, the joint distribution of the movement process could be factored as $[\mathbf{z}_{1:t,j}] = [\mathbf{z}_{t,j} | \mathbf{A} \mathbf{z}_{t-1,j}] [\mathbf{z}_{t-1,j} | \mathbf{A} \mathbf{z}_{t-2,j}] [\mathbf{z}_{t-2,j} | \mathbf{A} \mathbf{z}_{t-3,j}] \dots [\mathbf{z}_{1,j}]$. We needed to specify prior distributions on the initial numbers of bison in each wintering area $\mathbf{z}_{1,j}$ during each year. We chose informative priors that were based on the numbers of bison observed during initial counts, where $\log(\mathbf{z}_{1,j}) \sim \text{N}(\log(\mathbf{y}_{1,j}), 0.5)$ (Appendix 1).

Data Models

Aerial counts did not occur exactly one month apart and we adjusted our process model to have a variable time step. Model updates occurred on the day of counting or on the 15th day of the month when counts did not occur. To align the intervals in the process model with the intervals in observed counts, transition probabilities were scaled by the fraction of elapsed time to the monthly time step. We defined $\Delta t_{t,j}$ as this proportion and scaled survival using $\phi^{\Delta t_{t,j}}$ and movement using $1 - \gamma_i^{\Delta t_{t,j}}$. For example, if counting occurred 45 days (e.g. 1.5 months) after the previous model update, then survival during that interval was estimated as $\phi^{1.5}$ and movement as $1 - \gamma_i^{1.5}$.

Counts of wintering areas were assumed to follow a Poisson-gamma mixture distribution. Count areas overlapped wintering areas and the relation matrix \mathbf{B} was created to align counting and wintering areas (Appendix 1). The vector $\boldsymbol{\lambda}_{t,j}$ was the true average number of bison in count areas during month t and year j and $\mathbf{y}_{1_{t,j}}$ was the observed count. We assumed the k^{th} element of $\boldsymbol{\lambda}_{t,j}$ follows a gamma distribution with rate α and shape $\mathbf{B}_k \mathbf{z}_{t,j} \alpha$ where \mathbf{B}_k is the k^{th} row of \mathbf{B} . Then, each element of $\mathbf{y}_{1_{t,j}}$ follows a Poisson distribution with intensity $\boldsymbol{\lambda}_{t,j}$ (Appendix 1). The shape parameters of the gamma distribution correspond to the mean ($\mathbf{B} \mathbf{z}_{t,j}$) and observation variance ($\frac{1}{\alpha} \mathbf{B} \mathbf{z}_{t,j}$) using moment matching. Our specification assumed that observers had perfect detection during counting which was based on >0.97 sightability reported by Hess (2002). Discrepancies between process model predictions and counts were attributed to sampling error, such as bison moving outside of count unit boundaries or incomplete surveying of units due to inclement weather.

Monthly locations of all bison fit with GPS devices were assumed to follow a multinomial distribution with the vector $\mathbf{y}_{2_{t,j}}$ as the number of individually marked bison located in each wintering area during month t and year j . Multinomial probabilities were the proportion of bison in each wintering area predicted by the process model where the probability for the i^{th} wintering area was $z_{t,j,i} / \sum_i z_{t,j,i}$ (Appendix 1).

Covariates were treated as being measured with error. We assumed observations (\mathbf{x}) of annual snow pack magnitude, standing crop at the conclusion of the growing season, and herd size followed normal distributions. The vector $\boldsymbol{\mu}_{x_j}$ represented latent snow, herd, and standing crop conditions during year j (Appendix 1). The vector $\boldsymbol{\sigma}_x$ had one element for each latent covariate type (Appendix 1). Informative prior distributions were chosen for standard deviations of snow pack magnitude and standing crop conditions (see Parameter Models). Up to three replicate observations of herd sizes were recorded annually and diffuse prior distributions were specified for standard deviations of herd sizes (See Parameter Models). Covariates were standardized to improve model convergence, reduce auto correlation, and facilitate comparison of covariate effects. Because covariates were treated as latent quantities, standardization occurred during each MCMC update. The difference of each current covariate value and mean of all current covariate values were divided by the standard deviation of all current covariate values.

Parameter Models

We assumed that monthly survival followed a Beta(97,0.98) distribution based on previous research identifying survival in Yellowstone bison using mark-recapture techniques (Geremia et al., 2009). Note, the posterior distribution of the survival parameter was identical to the prior distribution and, as a result, we do not discuss this result further. Snow model generated metrics were produced for sites corresponding with four SNOTEL stations located within and surrounding Yellowstone. Predictions were compared to reported values to create informative N(1.60,0.10) prior distributions for log standard deviations of snow conditions. Standing crop measures were collected at the conclusion of the growing season from across Yellowstone and compared to forage model predictions to create informative N(1,0.10) prior distributions for log standard deviations of standing crop conditions. Otherwise, the diffuse prior distribution N(0,1000) was assumed for all model parameters including: the logistic model coefficients relating covariates to movement probabilities; the log parameters of

gamma distributions for the true (β) and observed (α) numbers of bison occupying wintering areas; the log means (μ_{x_j}) of annual herd size, snow, and standing crop conditions; and the log standard deviations of herd size conditions (σ_x ; Appendix 1).

Model Implementation

Marginal posterior distributions of latent states and parameters were estimated using Markov chain Monte Carlo (MCMC) methods. Samples were drawn from the posterior distribution of each parameter and latent state using a hybrid Gibbs sampler with Metropolis-Hastings steps. All analyses were completed using program R (R Core Development Team 2013) and we included code to simulate data and implement our model in the Supplemental Material.

Each of three MCMC chains was run for 500,000 iterations and the first 250,000 iterations were discarded to allow for burn-in. We confirmed convergence using the Gelman and Rubin test statistic by assuring that the potential scale reduction factor was <1.02 for each variable (Gelman and Rubin, 1992). Trace plots of marginal posterior distributions were inspected to ensure reasonable exploration of the parameter space. Metropolis-Hastings acceptance rates were tracked to assure values near 0.40.

Posterior predictive checks help assess whether observed data are consistent with the model (Gelman et al., 1996; Gelman and Hill, 2007). Posterior predictive realizations of count observations were obtained during each MCMC update after the burn-in period. These realizations can be conceptualized as replicated data produced by the model. We assessed how replicated data resembled the distribution of the real data by defining test statistics and calculating Bayesian p-values as the proportion of MCMC iterations for which the test statistic of the replicated data was more extreme than the observed data. One test statistic was created as the proportion of bison in each count area to indicate discrepancies in central tendency. Mean squared error was defined as an additional test statistic to indicate discrepancies in dispersion.

Posterior predictive realizations of counts should exhibit a strong linear relationship to observed counts. We estimated the posterior predictive distribution of r between the observed and replicated data during each MCMC iteration after the burn-in period. Out-of-sample prediction was also used to assess model performance by comparing predicted numbers of bison moving along migration paths to numbers of bison recorded using remote camera stations.

Predictions for Adaptive Management

Bayesian inference provides a framework for prediction that estimates the uncertainty in the model parameters, process error, and observation error (Clark, 2007). The same model that is used for estimating the parameters is used to make predictions. This is done by conditioning the predictive distribution of future numbers of bison in wintering areas on the parameters, process error, and future covariate variables. Because these covariate variables are not known in advance, an additional source of uncertainty enters which we refer to as scenario uncertainty (Clark, 2007). Future snow and standing crop conditions can be conditioned on what has been observed. For example, \tilde{x} is a predicted covariate and we assume \tilde{x} follows a normal distribution with the mean and standard deviation of previously observed snow or standing crop conditions. It is more challenging to estimate future herd sizes which depend on herd size during the previous year \tilde{x}_{j-1} , population growth $\tilde{\lambda}$, and removals \tilde{r}_j such that $\tilde{x}_j = \tilde{\lambda}(\tilde{x}_{j-1} - \tilde{r}_j)$. Population growth can be estimated as a derived quantity in our model by calculating this quantity for each year since 1990. Then, predictions of $\tilde{\lambda}$ follow a normal distribution with the mean and standard deviation of these derived quantities. Management reductions occur through hunting, or gather-and-consignment where bison are moved into livestock facilities and shipped to slaughter, terminal pastures, or research or quarantine facilities. Managers have complete control over gather-and-consignment, since riders on horseback are used to haze targeted animals into processing facilities. Therefore, we do not need to incorporate uncertainty in \tilde{r} for predicting removals occurring through

gather-and-consignment. However, there is uncertainty in predicted hunter success because not all bison occupying hunting districts are harvested by hunters. Observations during 2005-2012 indicated that it is reasonable to assume that the probability of harvest of bison occupying hunt areas follows a Beta(1,5) distribution. Using these steps, we were able to incorporate all reasonable sources of scenario uncertainty in forecasting future movements.

Bison distributions were forecasted for the 15th of each month during August-March on the northern portions and August-May on the central portions of Yellowstone during 2013 through 2017. Starting bison population size during August 2013 was assumed as 4,170-4,230 (approximately 1,600 central and 2,600 northern) based on aerial counting. Five management alternatives were compared including:

1. Low Hunting: supporting recent levels of public and treaty hunting that included 50 total permits issued during early (November-January) and late (February-March) seasons.
2. Moderate Hunting: increased hunting that included 50 permits issued for the western management area and 300 permits for the northern management area during early and late seasons.
3. Moderate Consignment: gather-and-consignment of up to 350 bison near the northern park boundary during early March.
4. Aggressive Consignment: gather-and-consignment of up to 1,000 bison near the northern park boundary during early March.
5. Moderate Hunting - Supplemental Consignment: hunting as described in alternative 2 with supplemental gather-and-consignment during early March such that total removals do not exceed 350 bison

Plumb et al. (2009) recommended maintaining the bison population between 2,500-4,500 to satisfy collective interests concerning the park's forage base, bison movement ecology,

retention of genetic diversity, brucellosis risk management, and prevailing social conditions. Furthermore, White et al. (2011) found that increased conflict with humans occurred in Montana when more than 500 bison exit either park boundary. We established three constraints on model output; that total population size was kept between 2,500-4,500, that individual herd size was between 1,250-1,750 animals, and that the number of migrants (excluding harvests and culls) was below 500.

Results

Assessment of Model Performance

We begin by assessing model performance to confirm that our model appropriately portrayed bison movements. Comparison of posterior predicted realizations of counts to 819 real count observations indicated a r value of 0.82 (0.79 - 0.85, 95% credible interval). The Bayesian p-value of the proportion of bison in any single count area assessed across all count observations was 0.30, but the Bayesian p-value based on mean squared error was <0.01 . These test statistics show that our model was able to generate replicated data with similar average numbers of bison in wintering areas as the observed data. However, mean squared error between replicated data and true numbers of bison in each wintering area was greater than mean squared error between the observed data and true numbers of bison. Replicated MSE values were likely larger because errors propagate across levels of the modeling hierarchy. Overestimating uncertainty at the parameter level produces overdispersed estimates of latent states and subsequent replicated data would be overdispersed compared to the observed data. This finding was not unexpected given the large numbers of parameters and latent states that were estimated.

Derived quantities of numbers of bison moving along migration paths were compared to observations recorded by remotely triggered camera stations. Our process model only allowed for one directional moves along edges that linked nodes representing wintering areas. Camera

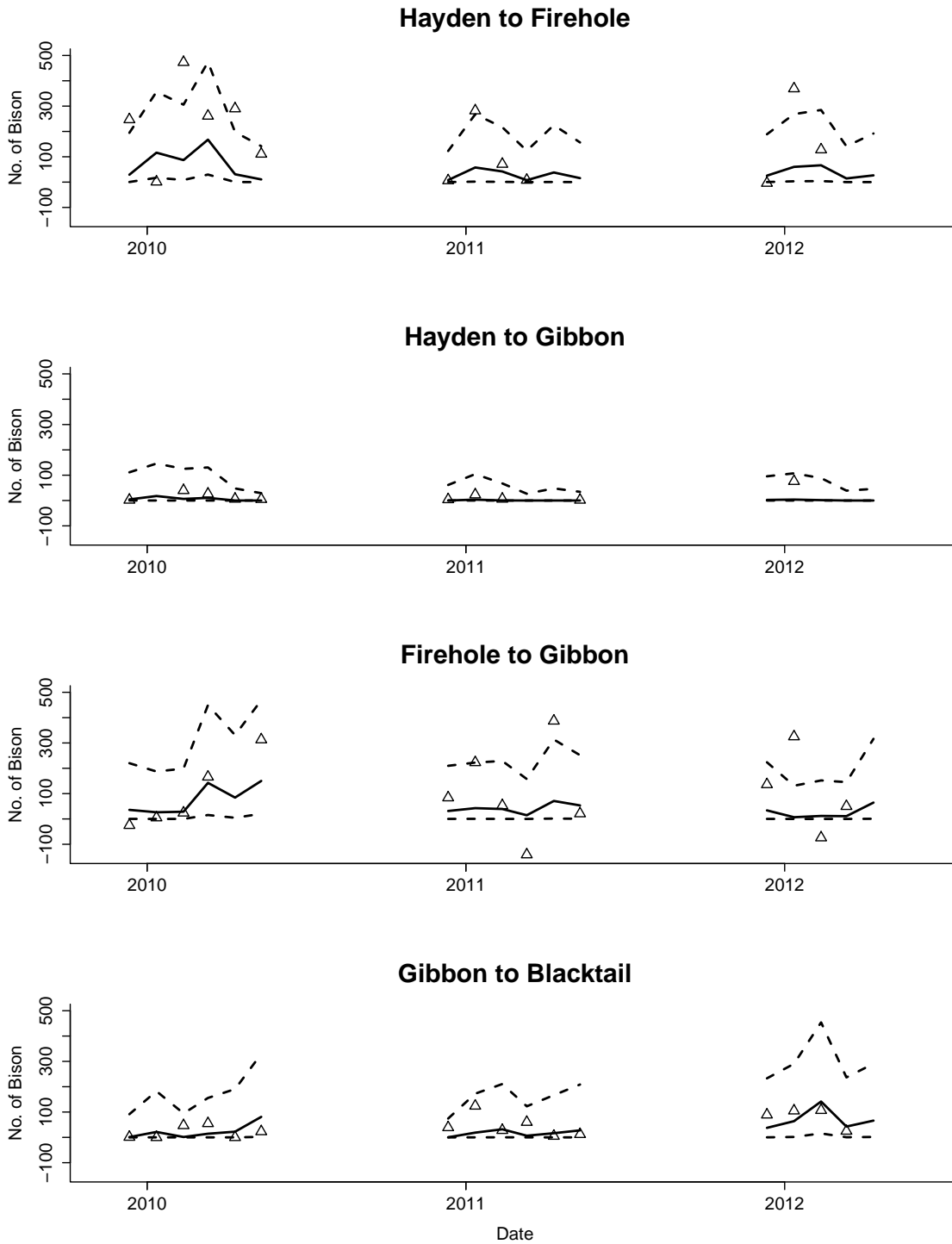


Figure 3: Estimated numbers of bison moving along migration paths were generated as derived quantities and compared to net observed movements recorded by remote camera stations (triangles) during November 2009 - March 2012 . Solid and dotted lines represent medians and 95% credible intervals of model predictions.

observations identified that back-and-forth movements occurred. However, net movements were in the direction of the process model in 94% (51/55) of monthly observations and generally within 95% credible intervals of derived quantities (Figure 3). Thus, our model was capable of predicting movements similar to those recorded by an independent data set.

Process variance was estimated as $\frac{1}{\beta}\mathbf{A}_i\mathbf{z}_{t-1,j}$ and aerial counting error was estimated as $\frac{1}{\alpha}\mathbf{z}_{t,j,k}$ using moment matching. Each of these quantities depended on numbers of bison in wintering areas (Table 3). To provide an illustration of the relative contribution of each of these sources of uncertainty, a process model prediction mean of 500 animals in a wintering area corresponded to a 95% credible interval of 230-861 animals truly present. The corresponding average count would be 490 with a standard deviation of 251 (Figures 4 and 5).

Individual Animal Movements

Individual animal movement histories were used to develop a graph of wintering areas and migration paths from the cumulative distribution of bison use. Alternative graphs of wintering areas and migration paths were compared against GPS histories of adult female bison. We identified a graph (Figure 1) that matched >90% of monthly locations of individual animals, which served as our state-transition matrix for predicting monthly distributions and movements. This graph was appropriate for the entire study period because migration routes were re-established by 1990 after nearly a century of recovery and population increase (Meagher, 1989, 1998). Also, telemetry locations of adult female bison recorded since 1995 (Fuller et al., 2007; Olexa and Gogan, 2007; Geremia et al., 2009) indicated that identified migration paths were present and used extensively during our study.

Radio collared adult female bison from the central herd congregated in non-forested areas of the Hayden Valley for the breeding season, after which most animals began to regularly travel between the Hayden Valley and alternative areas along the north shore of Yellowstone Lake and within the Pelican Valley. During most years, all animals exited these higher

elevation areas directly to the Firehole River drainage by the conclusion of winter. Some brief return movements to the Hayden Valley occurred, and a few bison directly accessed the Gibbon River drainage from the Hayden Valley. From the Firehole River drainage, bison accessed several disjoint meadows along the Gibbon and Madison rivers. Movements were fluid between these areas, resulting in low residence time in any single meadow. Bison next moved towards the western park boundary (23 of 46 bison fit with GPS devices) or accessed the western portion of the grasslands in northern Yellowstone by moving north along the road connecting Mammoth Hot Springs and the interior of the park (23/46). Most females from the central herd exhibited strong fidelity to breeding sites and wintering areas (40/46). However, six individuals that migrated to the northern portions of Yellowstone moved to the Lamar Valley during the following summer, interbreeding with the northern herd.

Use of northern Yellowstone by adult female bison fit with telemetry devices showed that animals fluidly moved across an approximately 40-km region along the Lamar River from Cache Creek in the east to west of the confluence of the Yellowstone River in the west. Use was concentrated in the eastern portions of this area and adjacent higher elevation slopes during the breeding season and early autumn, and concentrated in the western portions during winter. During some years, most, if not all individuals, moved northwest to the Blacktail Deer Plateau. Several movement corridors connected these areas. Bison also moved further north to the lower-elevation Gardiner basin during many of these years. These movements were made along several pathways that followed the Yellowstone and Gardner rivers. Females from the northern herd exhibited strong fidelity to breeding sites (19/20), but within-year variation in use of wintering areas. Only a single individual from the northern herd was observed using the central interior of the park.

Estimation of population level parameters

Monthly estimated abundance of bison on wintering areas suggested that migrations followed a movement cascade, with animals moving progressively from higher to lower elevation

areas. Abundance on breeding areas that corresponded to the highest elevation wintering areas steadily decreased after the conclusion of the rut in September. Abundance on mid-elevation wintering areas peaked during migration periods, suggesting these areas were used much like stop-over sites. Abundance on wintering areas at the termination of migration paths peaked during May and June in the Hebgen Lake basin and during February-April in the Gardiner basin. Similar numbers of bison tended to remain on higher elevation wintering areas at the conclusion of migration periods along central migration paths (Figure 4). The timing, magnitude, and extent of movements along northern migration paths was more variable between years. Most, if not all, bison remained on middle elevation wintering areas during some years, with nearly all animals exiting to the lower elevation areas during others (Figure 5).

We found strong seasonality of monthly movement probabilities along central migration paths based on days since the onset of snow cover (Table 1). Movement probabilities reached minima during the migration period, supporting that early migrants exhibited higher probabilities of movement to subsequent wintering areas. Minima corresponded to optimal times of use of wintering areas, which occurred at similar days after snow onset each year. Thereafter, movement probabilities rapidly increased. Seasonality of movement probabilities along northern migration paths was less apparent (Table 2), with increased inter-annual variation related to herd size, snow pack magnitude, and standing crop (Figures 6 and 7).

The size of the northern herd was related to increases in monthly movement probabilities. There was a 0.85 probability that the northern herd covariate coefficient was greater than zero for movements between the Lamar Valley and the lower Yellowstone River drainage and a 0.87 probability for movements between the Lower Yellowstone River drainage and Blacktail Deer Plateau. The effect of central herd size was less clear. Movement probabilities from the breeding area for the central herd decreased with herd size, suggesting that larger herd sizes prolonged congregation on the breeding area. Perhaps bison cooperatively displace snow, thereby facilitating foraging and locomotion early in winter. Central herd animals moved

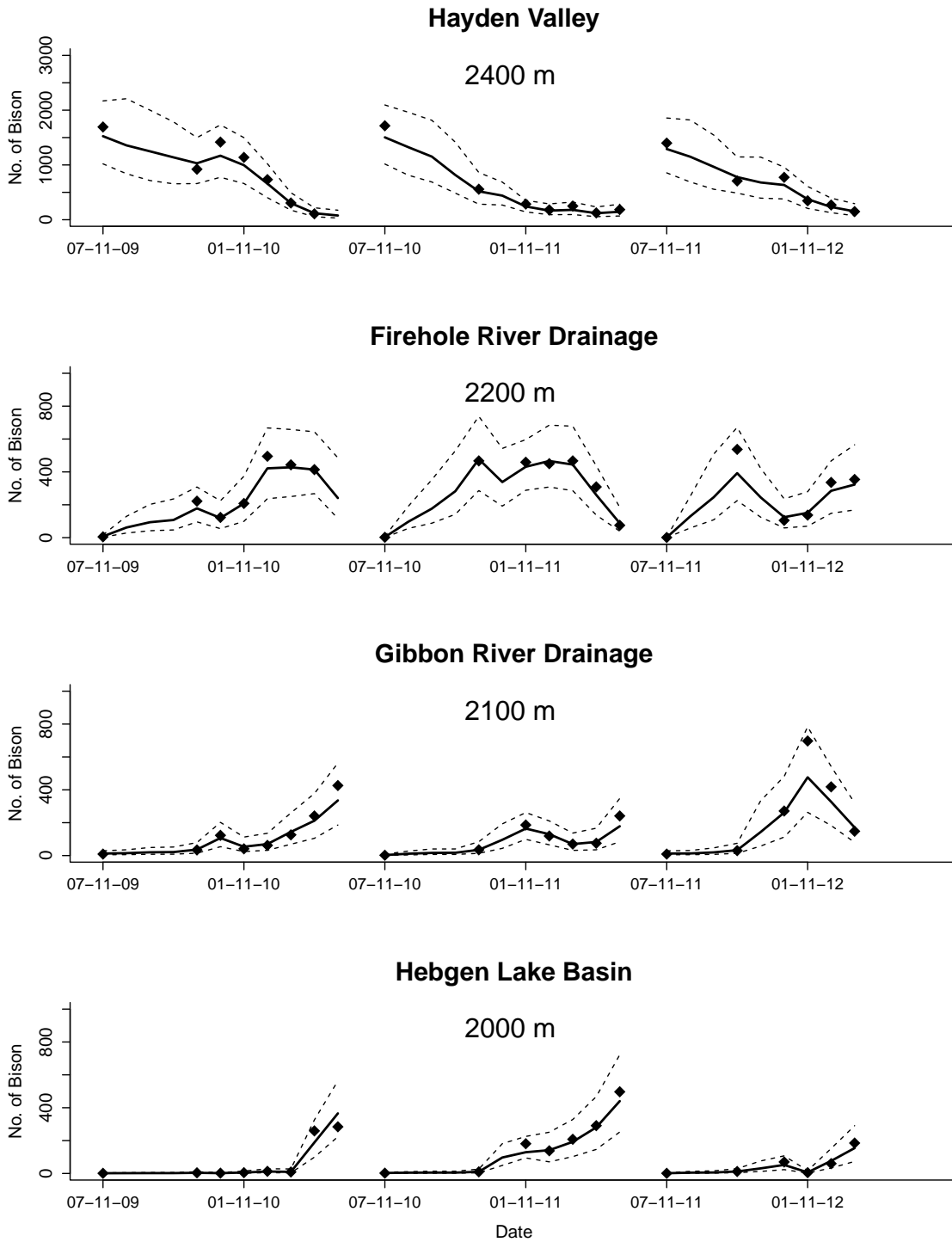


Figure 4: Counts (dots), mean (solid lines) and 95% credible intervals (dotted lines) of marginal posterior distributions of numbers of bison occupying wintering areas in central Yellowstone during July 2010 - May 2012. Breaks in lines represent times when bison were returning to breeding areas for the rut. Panels are aligned from top to bottom to show progressively lower elevation wintering areas.

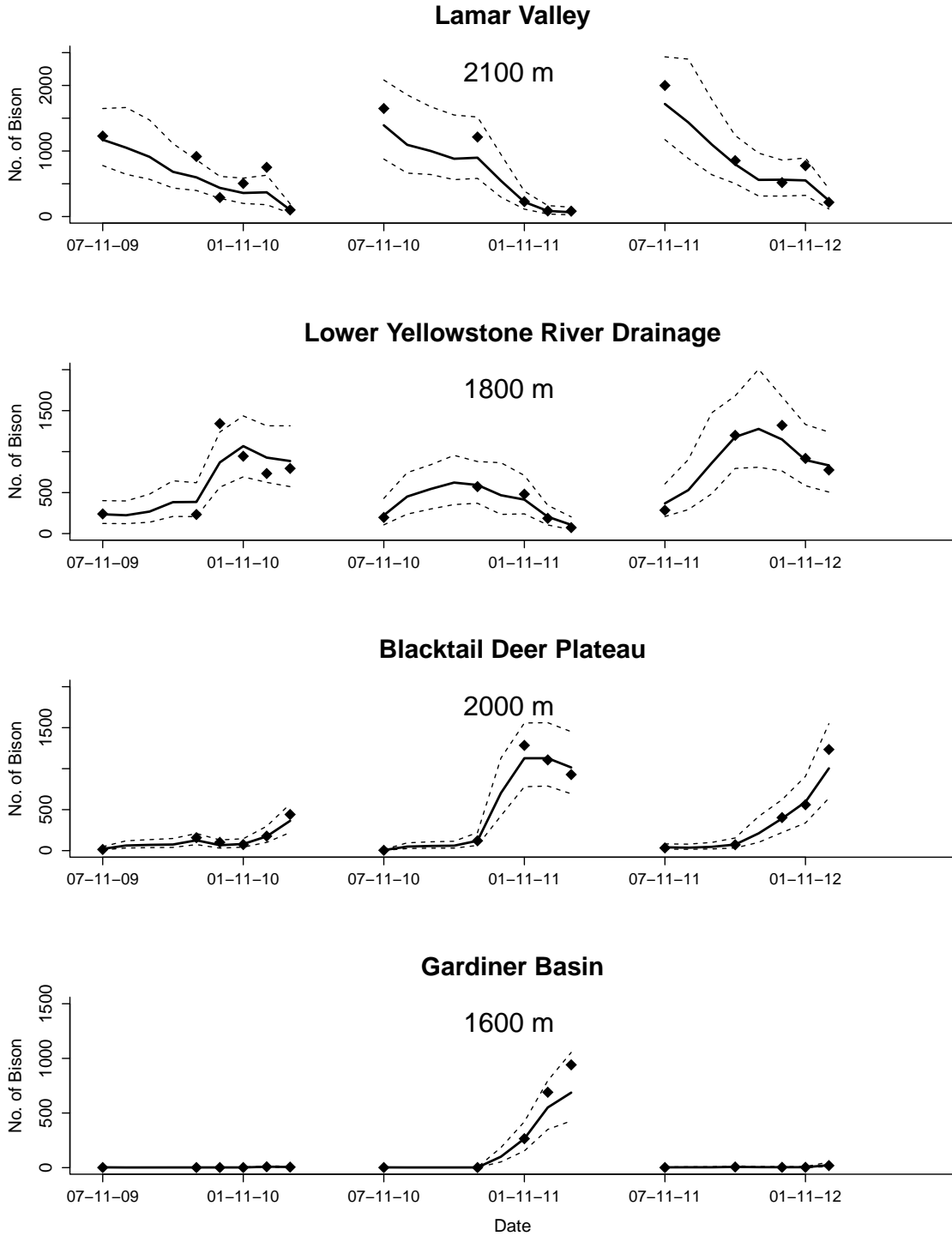


Figure 5: Counts (dots), mean (solid lines) and 95% credible intervals (dotted lines) of marginal posterior distributions of numbers of bison occupying wintering areas in northern Yellowstone during July 2010 - May 2012. Breaks in lines represent times when bison were returning to breeding areas for the rut. Panels are aligned from top to bottom to show progressively lower elevation wintering areas.

to the northern or western park boundaries from the Gibbon River drainage. Movements towards the northern park boundary were believed to be infrequent prior to the central herd increasing in size after large-scale reductions during 1996-97 (Gates et al., 2005). We found 0.90 probability that the central herd covariate coefficient was greater than zero for movements to the north and 0.89 probability that the central herd covariate was less than zero for movements to the west. Thus, as the central herd increased in size, use of the northern migration pathway increased (Table 1).

Snow pack magnitude was related to increased monthly movement probabilities along northern migration paths, with a 0.94 probability that the northern snow pack covariate coefficient was greater than zero for movements between the Lower Yellowstone River drainage and Blacktail Deer Plateau and a 0.86 probability for movements between the Blacktail Deer Plateau and Gardiner basin (Table 2). Snow pack magnitude effects were in opposition across central migration paths. Snow was related to increased movements from the Hayden Valley to the Firehole River drainage (0.89 probability) and the Gibbon River drainage to the Heben Lake basin (0.81 probability), but decreased movements from the Firehole to Gibbon River drainages (1.00 probability; Table 1). The Firehole River drainage is characterized by thermally influenced areas that likely offset the negative effects of snow on accessing food.

The effects of standing crop at the conclusion of the growing season were ambiguous. While nearly all coefficients were in the expected direction with increases in standing crop related to decreased per capita movements, all credible intervals broadly spanned zero (Tables 1 and 2). Monthly movement probabilities along most central migration paths increased through the duration of our research and probabilities from the Blacktail Deer Plateau to the Gardiner basin decreased (Tables 1 and 2)

Adaptive Management

Continued large-scale gather-and-consignment (alternative 4), as has occurred sporadically since the inception of the Interagency Bison Management Plan, exhibited the highest

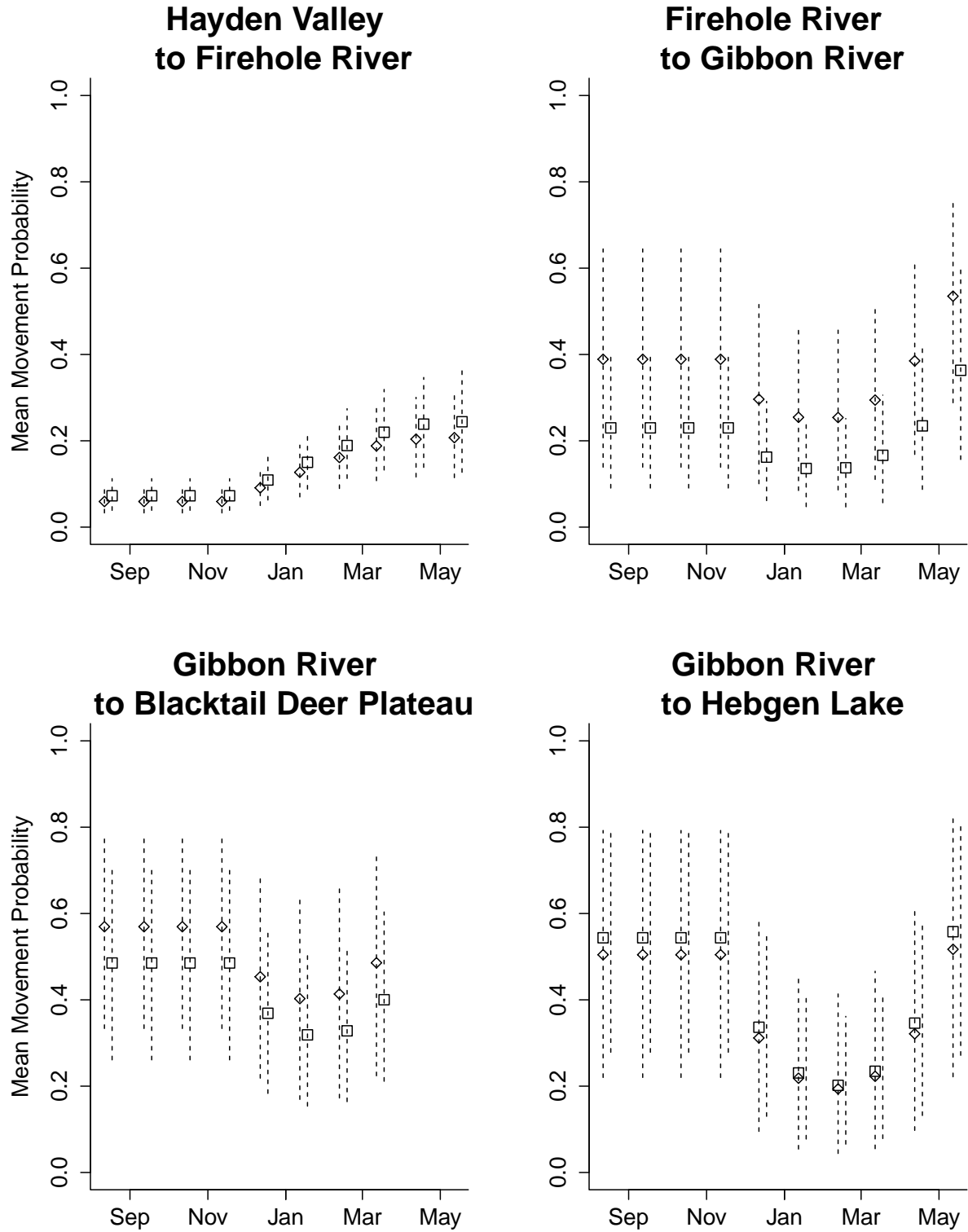


Figure 6: Mean posterior predicted monthly movement probabilities along migration paths in central Yellowstone assuming below-average (diamond) and above-average (square) covariates. Dotted lines represent 85% quantiles (Table 1).

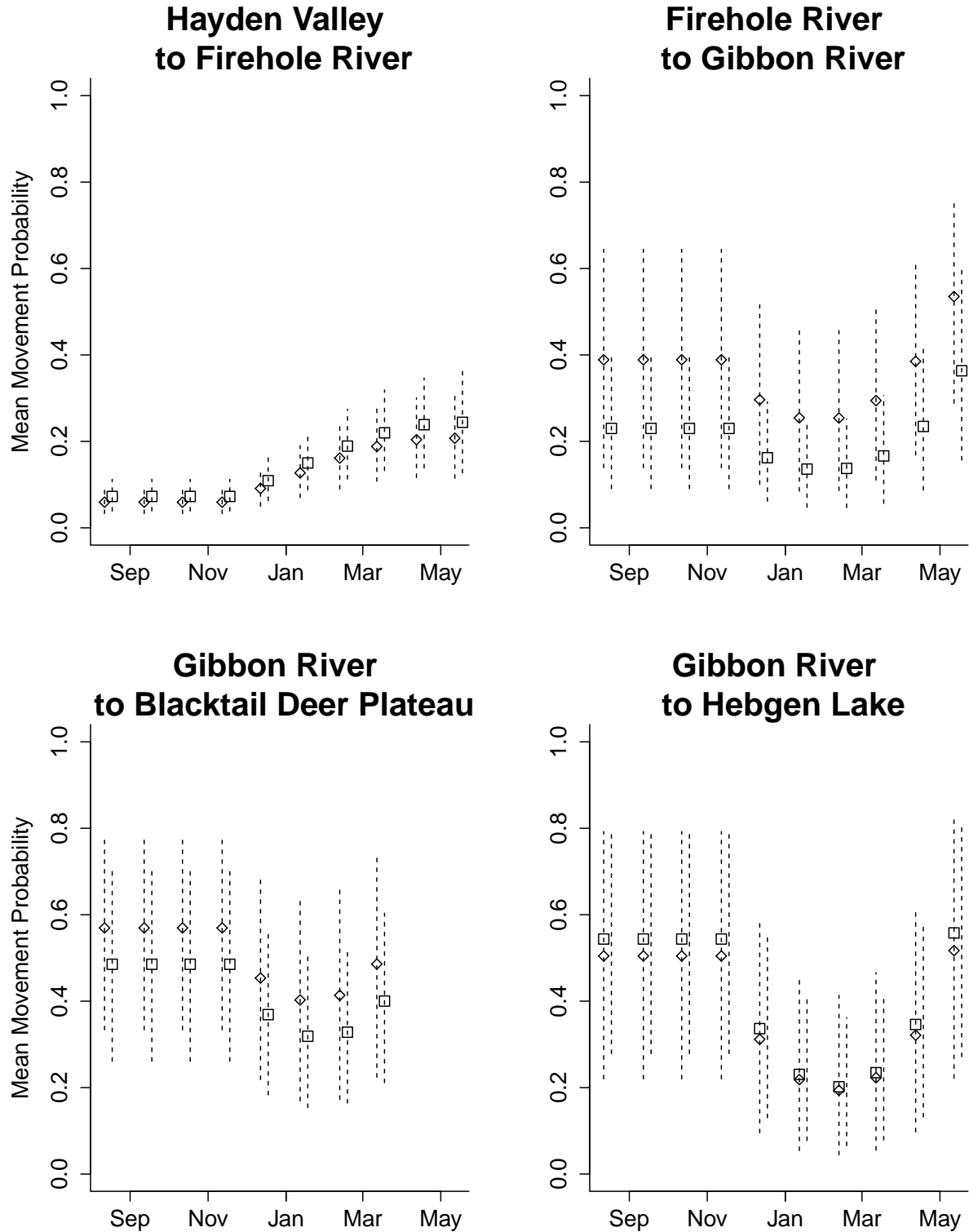


Figure 7: Mean posterior predicted monthly movement probabilities along migration paths in northern Yellowstone assuming below-average (diamond) and above-average (square) covariates reflecting food availability. Dotted lines represent 85% quantiles (Table 1).

Table 1: Posterior estimates of logistic model coefficients of monthly movement probabilities along central Yellowstone migration paths. Bold text indicates covariates with >0.85 probability of an effect.

Migration path	parameter	median	0.025%	0.975%	Migration path	parameter	median	0.025%	0.975%
Hayden to Firehole					Firehole to Gibbon				
	intercept	-1.91	-2.24	-1.62		intercept	-2.21	-3.11	-1.61
	snow onset	0.74	0.48	0.99		snow onset	-0.25	-0.80	0.41
	snow onset (2 order)	-0.27	-0.56	-0.01		snow onset (2 order)	0.62	0.25	1.03
	herd size	-0.17	-0.38	0.03		herd size	0.06	-0.38	0.50
	snow pack severity	0.13	-0.08	0.33		snow pack severity	-0.19	-0.59	0.18
	standing crop	-0.02	-0.25	0.19		standing crop	-0.35	-0.84	0.05
	year of study	0.03	-0.21	0.27		year of study	0.30	-0.09	0.78
Gibbon to Blacktail					Gibbon to Hebggen				
	intercept	-2.55	-1.99	-1.50		intercept	-2.24	-3.11	-1.61
	snow onset	-0.14	-0.66	0.32		snow onset	-0.78	-1.45	-0.22
	snow onset (2 order)	0.78	0.07	1.48		snow onset (2 order)	1.06	0.55	1.72
	herd size	0.21	-0.17	0.60		herd size	-0.27	-0.78	0.21
	snow pack severity	-0.16	-0.49	0.14		snow pack severity	0.18	-0.23	0.61
	standing crop	-0.02	-0.39	0.34		standing crop	0.01	-0.53	0.48
	year of study	0.77	0.30	1.24		year of study	0.44	-0.11	1.08

Table 2: Posterior estimates of logistic model coefficients of monthly movement probabilities along northern Yellowstone migration paths. Bold text indicates covariates with >0.85 probability of an effect.

Migration path	parameter	median	0.025%	0.975%
Lamar to Lower Yellowstone	intercept	-1.20	-1.88	-0.66
	snow onset	0.36	-0.74	1.02
	snow onset (2 order)	-0.87	-2.16	0.17
	herd size	0.29	-0.25	0.84
	snow pack severity	-0.05	-0.26	0.15
	standing crop	-0.16	-0.47	0.16
	year of study	-0.10	-0.71	0.51
Lower Yellowstone to Blacktail	intercept	-2.20	-2.74	-1.73
	snow onset	-0.17	-0.67	0.31
	snow onset (2 nd order)	-0.84	-0.20	0.39
	herd size	0.36	-0.28	1.04
	snow pack severity	0.19	-0.05	0.44
	standing crop	0.14	-0.24	0.52
	year of study	-0.14	-0.87	0.54
Blacktail to Gardiner	intercept	-0.47	-1.06	0.14
	snow onset	-0.26	-0.69	0.14
	snow onset (2 order)	0.39	-0.29	1.07
	herd size	-0.11	-0.54	0.28
	snow pack severity	0.13	-0.12	0.39
	standing crop	0.03	-0.38	0.48
	year of study	-0.68	-1.05	-0.35

Table 3: Posterior estimates of model parameters representing process uncertainty and observation error. Process uncertainty and counting error are functions of estimated parameters where \mathbf{A} is a transition matrix of movement and survival probabilities, $\mathbf{z}_{t,j}$ is a column vector of true numbers of bison in each wintering area during month t and year j , and k are count areas.

parameter	definition	median	0.025%	0.975%
β	process uncertainty ($\frac{1}{\beta}\mathbf{A}_t\mathbf{z}_{t-1,j}$)	0.018	0.016	0.021
α	counting error ($\frac{1}{\alpha}\mathbf{z}_{t,j,k}$)	0.012	0.011	0.013
$\sigma_x(\text{central})$	herd abundance	141.97	114.61	181.37
	snow pack magnitude	5.16	4.20	6.38
	standing crop	2.20	1.81	2.68
$\sigma_x(\text{northern})$	herd abundance	165.60	132.67	216.72
	snow pack magnitude	7.28	5.85	8.74
	standing crop	2.20	1.81	2.68

probability of reducing herd sizes below targeted levels (Table 4). Alternatives that relied exclusively on hunting were least likely to meet decision criteria (alternatives 1 and 2). Under low levels of hunting (alternative 1), herd sizes increased and there was a high probability of more than 1,500 migrants moving beyond park boundaries. Issuing more annual hunting permits (alternative 2) increased the probability of meeting decision criteria. However, there was large variation in forecasted herd sizes due to broad uncertainty in hunter success rate.

Supplementing increased numbers of state and tribal hunting permits with moderated late winter gather-and-consignment (alternative 5) provided the highest certainty of meeting key management criteria over the next five years (Table 4). Under this alternative tribal members would be afforded greater opportunity for the consumption of bison as food, and the associated cultural and spiritual benefits. By issuing 350 permits each year, we forecasted average hunter harvests of more than 100 animals each of the next five winters. In turn, numbers of bison removed by gather-and-consignment were reduced by one-half compared to scenarios that excluded hunting. Reduced numbers of bison removed through gather-and-consignment mitigates social conflicts that arise from slaughtering wild animals. Also, managers are provided increased flexibility for pursuing non-lethal alternatives, such as transport to quarantine facilities for eventual supplementation of tribal, private, and publicly owned bison populations throughout North America.

Under alternative 5 (hunting and consignment) and a starting population near 4,200 bison, we found a 29% chance of more than 500 and 10% chance of more than 1,000 animals exiting the northern park boundary (in addition to removals) within one year. After five years, we forecasted a 18% chance of more than 500 animals and only 5% chance of more than 1,000 animals exiting the northern park boundary. Consistent hunting supplemented with gather-and-consignment of bison increased the chances that future migrations do not surpass levels that are generally accepted by prevailing social conditions. At the same time, harvests and culls did not remove all migrants during most years. Consequently, managers would be afforded the opportunity to selectively remove animals through gather-and-consignment.

Culls could be targeted at desired age and sex classes to offset potential adverse effects of selective hunting (e.g., by sex or herd) or reduce brucellosis infection through removing individuals capable of transmitting infection to livestock or other wildlife (Treanor et al., 2011; White et al., 2011).

In contrast to the northern park boundary, management alternatives that reduced herd sizes to the targeted range of 1,250-1,750 animals did little to moderate numbers of bison migrating to the western park boundary. Further, these movements coincided with the calving period when bison are most likely to transmit brucellosis by shedding infectious material onto the landscape through parturition. Therefore, successful trans-boundary management must focus on spatio-temporal separation of livestock and bison, rather than on removing migrants through harvest or gather-and-slaughter. Fencing or hazing bison away from areas soon to be occupied by cattle, and targeted gather-and-haze of bison from these potential conflict areas, should create this separation. Also, current management policies attempt to gather-and-haze all bison back into the park by May 15th. However, movement probabilities out of the park peak at this time, thereby complicating management efforts. Fostering increased tolerance in regions where bison cannot come into contact with cattle until bison naturally return to breeding areas may be a sensible alternative.

Discussion

We provide a first assessment identifying regional scale movements of bison throughout Yellowstone and nearby areas of Montana. This research extends existing work that determined relationships between numbers of bison exiting the park, herd sizes, snow pack severity, and forage production (Gates et al., 2005; Bruggeman et al., 2009; Kilpatrick et al., 2009; Geremia et al., 2011). We used a hierarchical approach, which allowed us to bring together detailed movement history data collected on individual animals over relatively brief periods of time with long term monitoring data of seasonal distributions, and account for

Table 4: Forecasted conditions during the next five years assuming a starting population size of 4,200 animals and annual management alternatives of issuing 1) 50 and 2) 350 hunting permits; gather-and-consignment of up to 3) 350 and 4) 1,000 bison; and using harvests and gather-and-consignment to remove up to 350 animals.

Key Criteria	Alternative 1		Alternative 2		Alternative 3		Alternative 4		Alternative 5	
	Year 1	Year 5								
Probabilities of Numbers of Bison in Conflict Areas (excluding removals)										
>500 Gardiner basin	0.52	0.72	0.45	0.56	0.30	0.19	0.11	0.02	0.29	0.19
>500 Hebgén Lake basin	0.31	0.35	0.31	0.34	0.34	0.39	0.34	0.36	0.31	0.33
>1,000 Gardiner basin	0.20	0.44	0.15	0.26	0.10	0.05	0.02	<0.01	0.10	0.05
Probabilities of End-of-Winter Herd Sizes within Desired Conditions										
1,250-1,750 northern	0.17	0.11	0.18	0.14	0.19	0.20	0.21	0.20	0.20	0.20
1,250-1,750 central	0.21	0.21	0.21	0.20	0.21	0.20	0.21	0.20	0.21	0.20
2,500-3,500 park wide	0.51	0.38	0.51	0.43	0.52	0.49	0.53	0.48	0.52	0.50
Average Annual Harvests										
Gardiner basin		114		130		0		0	119	98
Hebgén Lake basin (mean)		31		32		0		0	31	32
Average Annual Gather-and-Consignments										
Gardiner basin	0	0	0	0	268	241	449	265	153	145

uncertainty resulting from each component. By treating this as a hierarchical problem, we were able to estimate monthly distributions during more than two decades in the face of incomplete data, and identify changes in monthly movement probabilities between bison wintering areas. Our approach allowed a clearer understanding of the forces that shape migratory patterns, which is necessary for managing trans-boundary movements of wildlife where there are disease, property, or safety concerns.

Bison select habitats that facilitate group formation to reduce predation risk and support cooperative displacement of snow (Fortin et al., 2009). Meagher (1998) referred to this phenomenon as a desire for bison to maintain their social bonds. We found that bison were congregated on high elevation breeding areas at the conclusion of the rut. Foraging efficiency in these areas likely declined as food was consumed and snow accumulated, and bison made coordinated movements to lower elevation areas which provided improved access to food. Animals rapidly accumulated in lower elevation areas. As food accessibility declined in these areas due to consumption and snow accumulation, animals moved to progressively lower elevation areas.

The net effect of snow and herd size conditions on northern migration pathways resulted in dramatic year-to-year differences in numbers of bison moving to the Gardiner basin wintering area. This finding is corroborated by previous research that indicated snow, standing crop, and herd size as significant predictors of numbers of bison exiting Yellowstone (Gates et al., 2005; Kilpatrick et al., 2009; Geremia et al., 2011). We found little net effect of snow and herd size conditions on monthly movement probabilities along central migration pathways. Central herd animals moved to wintering areas that span park boundaries across all observed central herd sizes. More animals moved sooner with larger herd sizes, which corroborates earlier work by Bruggeman et al. (2009) and increases were proportional to changes in herd size.

Our findings could be interpreted as snow acting as a stronger control on movements in northern Yellowstone. However, snow conditions are clearly more severe in central Yellow-

stone with earlier and deeper snow pack establishment (Meagher, 1973; Gates et al., 2005; Watson et al., 2006; Geremia et al., 2009), and our northern snow covariate levels averaged 32% lower than central snow conditions. Covariate levels were standardized, such that we compared the effect of a condition relative to the average. We believe that snow conditions in central Yellowstone reached levels that affected movements each year. Therefore, year-to-year variations had little additional effect.

Emergent seasonal distributions during years characterized by above or below average snow conditions were similar in central Yellowstone and variable in northern Yellowstone. Fidelity to summering and wintering locations declines as conditions affecting foraging become less predictable (Mueller and Fagan, 2008). Wildebeest (*Connochaetes taurinus*) in the Serengeti provide an excellent example, where animals make nomadic movements during the wet season tracking highly unpredictable vegetation dynamics in response to rainfall (Holdo et al., 2009). When conditions affecting foraging are highly predictable from year-to-year, experience and learning play an increasingly important role in movement decision-making (Bailey et al., 1996; Mueller and Fagan, 2008). Such behavior has been observed in large herbivores in snow-limited environments, including elk (*Cervus elaphus*; Morgantini and Hudson 1988; Hebblewhite et al. 2008), mule deer (*Odocoileus hemionus*; Nicholson et al. 1997), white-tailed deer (*Odocoileus virginianus*; Nelson and Mech 1991), pronghorn (*Antilocapra americana*; White et al. 2007) and caribou (*Rangifer tarandus*; Mueller et al. 2011).

It is difficult to determine if moving herbivores are responding to food or basing decisions on experience. We did not directly test if experience affected movements in our model. GPS histories of central herd adult female bison indicated that animals increased fidelity to movement patterns with age which is suggestive of learning. We also found strong year effects on most central Yellowstone migration paths suggesting that routes became increasingly entrenched over time. The central herd reached record abundance in 2005, which coincided with a winter characterized by above-average snow pack. Concurrently, changes in management policy allowed increased use of the Hebgen Lake basin wintering area, which

afforded bison access to newly emerging vegetation while high elevation areas remained snow covered. Range expansion as the result of food limitation caused by the record population abundance and above-average snow pack is likely what facilitated bison in pioneering new areas. Movements out of the central interior to northern portions of the park and expanded use of areas adjacent the western park boundary became established and likely persisted due to experience and learning.

Posterior predictive checks indicated that our model accurately estimates the mean. Unsurprisingly, the variance estimates are slightly too large. Snow pack estimates were averaged over the entire year across large areas. Snow is a highly local variable and consideration of snow in each wintering area per month may provide better spatial-temporal resolution of the covariate. Additional covariates could be developed as we continue this research. For example, wolves (*Canis lupus*) were reintroduced to Yellowstone during 1995-97. Wintering areas with increased wolf occurrence during times of increased snow may affect bison movements. Elk numbers have also declined substantially since the return of the wolf, which may provide increased foraging opportunities for bison. It would also be interesting to develop a metric for management pressure to test if bison are learning and possibly avoiding certain types of interventions. However, additional data are needed before these covariates based on recent changes in the system can be adequately addressed.

Our research suggests population size and out-of-park abundance objectives can be met using hunting and gather-and-consignment, with removal actions limited to bison that exit the northern boundary. Spatial and temporal separation of livestock and bison that exit the western boundary has effectively prevented disease spillover. Beyond Yellowstone our research provides some general insight of managing migratory wildlife populations in fragmented landscapes. Managers should acknowledge that they have limited control, because movements are themselves affected by unpredictable variation (e.g., weather). As a result, a clear single best management strategy does not exist or is not identifiable. Instead, it is essential to work over short time frames with continual reassessment of management guide-

lines and outcomes. Management is further complicated when animals seasonally occupy protected areas such as National Parks. These areas serve many purposes, one of which is providing visitors with an opportunity to view wildlife in a natural setting. Management interventions (e.g., culls, harvests, sterilization, contraception) are often limited within these areas, with the unintended consequence of population growth which increases movements and the chances of episodic reductions outside these protected areas. Learning and experience may affect movements by allowing a behavior like the use of a migration path or wintering area to become increasingly entrenched. If a particular learned behavior increases conflict, it may be reasonable to target animals that exhibit the behavior for removal. We developed a tool to make probabilistic forecasts of migratory ungulate distributions. These forecasts promote sound decision-making by allowing managers to develop and refine strategies in advance. Models are unique to each situation, but the framework we used is applicable to the global concern of managing wildlife in fragmented habitats.

CHAPTER 3: A MULE DEER POPULATION PERSISTS WITH ENZOOTIC CWD

Epizootics can affect the health and stability of host populations, ecosystems, and human economies (McCallum and Dobson, 1995; Daszak et al., 2000). Rinderpest provides the case example where episodic viral outbreaks led to dramatic declines in buffalo *Syncerus caffer* and wildbeest *Connochates taurinus* populations in the Serengeti with cascading effects on predator-prey and grassland dynamics (Sinclair and Arcese, 1995). More recent examples include marine epizootics that are reducing the abundance of reef-building corral species and altering community structure and ecosystem processes (Harvell et al., 1999, 2002; Bruno et al., 2003), as well as chytrid fungus that is associated with a worldwide amphibian taxa decline (Daszak et al., 2003). Chronic wasting disease (CWD) is a transmissible spongiform encephalopathy that occurs naturally in members of the deer family (*Cervidae*) of North America (Prusiner, 1998; Williams and Young, 1992). CWD has been detected in nineteen states and two Canadian provinces. It continues to be identified in wild deer populations across a wider geographic extent (Williams et al., 2002; Miller and Conner, 2005; Saunders et al., 2012a).

CWD has raised worldwide concern because it can be transmitted among species of the deer family, is uniformly fatal, and the infectious agent persists in the environment for long periods (Williams and Young, 1992; Williams, 2005). The infectious agent of CWD, PrP^{Sc}, is a malformed variant of host prion protein. PrP^{Sc} appears to replicate by temporarily interacting with normally formed host prion, PrP, to cause mis-folding and new infectious agent (Williams and Young, 1992; Ryou, 2007). Horizontal transmission likely contributes to disease spread (Miller and Williams, 2003) and infectious material can be excreted through feces, saliva, and urine (Mathiason et al., 2006; Tamgüney et al., 2009; Gough and Maddison, 2010; Haley et al., 2011). Indirect transmission through an environmental reservoir plays an important role in infection dynamics (Miller et al., 2004; Mathiason et al., 2009). Direct transmission is also believed to occur (Miller et al., 2000).

Simulation models suggested that the consequence of CWD for deer populations could vary widely (Gross and Miller, 2001; Wasserberg et al., 2009; Almberg et al., 2011). Predictions ranged from limited population decline and sustained low disease prevalence to widespread local extinction within decades of disease introduction. Outcomes varied as a result of differences in assumptions about controls on the number of new infections, including the relative importance of direct and indirect transmission, decay rate of infectious agent in the environment, habitat configuration, and host social behavior, gender, and age (Miller and Conner, 2005; Farnsworth et al., 2006; Miller et al., 2008; Wasserberg et al., 2009; Gear et al., 2010; Almberg et al., 2011; Storm et al., 2013).

Empirical studies have shown CWD can depress growth rates of local populations with remarkably high infection prevalence (Miller et al., 2008; Edmunds, 2013). Declines in deer abundance over larger spatial extents could pose debilitating effects on ecosystems and human economies because deer populations play important roles in ecosystems, provide primary prey for large carnivores, and serve as a food resource to people. Studies implemented over larger geographic extents are needed to better understand the course of CWD infections and fate of deer populations. Such research is hard to implement because of the timespan of CWD epidemics and magnitude and distribution of deer populations. It necessitates integration of long-term monitoring information with detailed short-term studies, and collaborative efforts between wildlife management agencies and research institutions.

The origin of CWD in wild deer populations is unknown. The initial case in a wild mule deer *Odocoileus hemionus* was documented in the Red Feather-Poudre River mule deer population of north-central Colorado and southern Wyoming in 1985 (Spraker et al., 1997). At that time, CWD had likely been present for at least two decades (Miller et al., 2000). State management agencies targeted the Red Feather-Poudre River mule deer population for long-term population monitoring and disease surveillance. Consequently, this population provides an opportunity to study host and pathogen dynamics long after disease establishment and provide some indication of how recently detected CWD epidemics may progress.

We conducted research to understand the effect of CWD on the growth rate of the Red Feather-Poudre River mule deer population. Capture-mark-recapture techniques were used to estimate infection rates and survival. Fertility estimates were determined from age and sex surveys. Three decades of population counts enabled us to estimate deer density and confirm model predicted growth rates. Previous disease tests from harvested and culled deer allowed us to compare our findings to disease prevalence up to fifteen years ago. We determined the effect of CWD on population growth under current infection levels and evaluated the degree to which the CWD epidemic is increasing.

Materials and Methods

Study Area

The Red Feather-Poudre River mule deer population is estimated near 7 000 individuals and located across the foothills and higher elevation areas of the northern Front Range of the Rocky Mountains, Colorado USA (Vieira, 2006). CWD has persisted in the population for at least 40 years. Mule deer share habitats with elk *Cervus elaphus* and white-tailed deer *Odocoileus virginianus* that are also infected with CWD. The mule deer population is partially migratory. Some individuals move up to 70 km between wintering areas north of Fort Collins, Colorado into the headwaters of the Laramie River in southern Wyoming and headwaters of the Poudre River in north-central Colorado. Others remain on wintering areas year-round. Deer occupy lands owned privately for agriculture and livestock industries and publicly by the National Forest Service, Colorado Division of Parks and Wildlife, Larimer County, and the city of Fort Collins. State and national public lands are managed to support sport hunting. County and city areas are largely managed for open-space and recreation. Habitats are characterized by short grass prairie and croplands in the lowest elevation southern and eastern regions. Foothill areas to the north and west include a variety of shrubs (e.g., *Cercocarpus sp.*, *Amelanchier sp.*, *Purshia sp.*) interspersed with ponderosa

pine *Pinus ponderosa*. Higher elevation areas are characterized by ponderosa pine, douglass fir *Psuedotsuga menziesii*, and sub alpine forests. Capture-mark-recapture studies, CWD surveillance efforts, and population monitoring were completed on wintering areas north of Fort Collins, Colorado (Figure 8).

Data Collection

We used capture-mark-recapture methods to estimate survival probability and probability of infection during January, 2010 - 2014. Deer were caught by helicopter net gunning and transferred to nearby processing locations. During the initial year of study, groups of female deer were located by helicopter personnel by randomly searching six areas that were each approximately 75 km². A single female from each group was captured. In subsequent years, deer were also captured from groups that did not include existing study animals. We attempted to capture individuals each year after initial handling. Infection with CWD was determined from immunohistochemistry staining of rectal mucosa associated lymphatic tissue (Wolfe et al., 2007). Age was determined using incisor and molar eruption and wear patterns (Robinette et al., 1957). Deer were fit with very high frequency radio collars (Advanced Telemetry Systems, Isanti, Minnesota, USA). After release, deer were tracked weekly to determine if they were alive and to identify their approximate location. Mortalities were investigated to determine the cause of death. All animals were handled in accordance with IACUC (11-2758A).

The wintering subpopulation has been used effectively to represent the spatial epidemiology of CWD (Conner and Miller, 2004; Farnsworth et al., 2006). Using methods described in detail by Conner and Miller (2004) we used cluster analysis to categorize radio collared deer into four wintering population units. Deer were located every 2 wk to 2 mo during November - February, 2010-13 using aerial telemetry homing techniques. Coordinate medians of winter locations for each individual were used for cluster analysis.

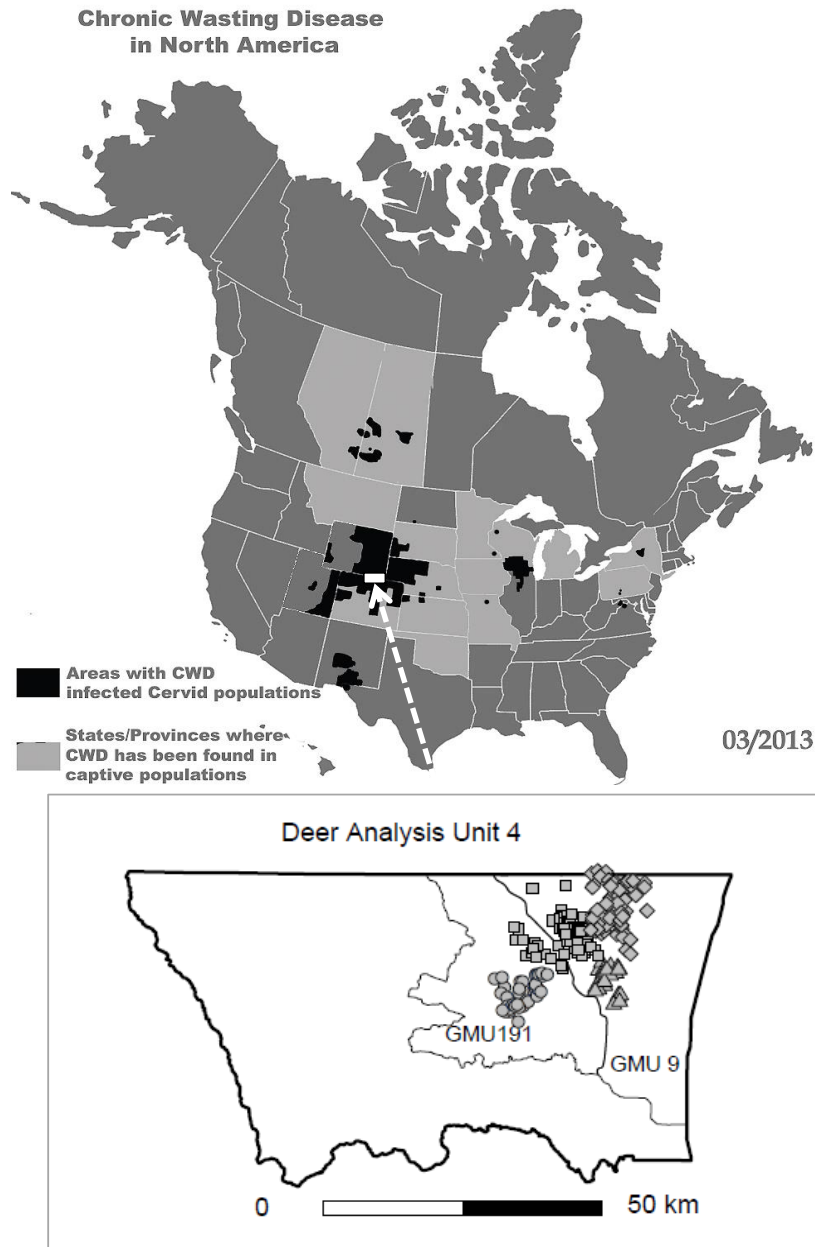


Figure 8: The Red Feather-Poudre River mule deer population is located in the endemic area for CWD. Capture-mark-recapture studies, CWD surveillance efforts, and population monitoring were completed in Colorado Division of Parks and Wildlife Game Management Units (GMU) 9 and 191. Deer Analysis Unit 4 describes the approximate spatial extent of the deer population. Capture-mark-recapture studied deer were further categorized into four population units based on spatial association during winter. Units included Big Hole (diamond), Campbell (triangle), Cherokee (circle), and Red Mountain (square). The map of CWD in North America was provided by the Chronic Wasting Disease Alliance (www.cwd-info.org).

Clusters were identified by unweighted pair-group method using arithmetic averages. We refer to these units as Big Hole, Cherokee, Campbell, and Red Mountain.

Using methods described in detail by Conner and Miller (2004), we delineated the area used by radio collared deer using a bivariate kernel home range estimator. We chose the 80% use contour to represent the area commonly used by deer in winter. This region served as a boundary for helicopter surveys and disease surveillance tests (described below). Therefore, long-term population monitoring data was restricted to a similar geographic area as our capture-mark-recapture study.

Annual helicopter surveys were completed by the Colorado Division of Parks and Wildlife during December-January, 2009-12 to estimate herd composition. Groups were located during systematic searches of areas known to be occupied by deer. Deer in encountered groups were classified as adult females (>12 mo), young of the year (5-6 mo), and males (>12 mo). In total, 184 groups were observed and 1,302 deer were classified. Population density was estimated by counting deer observed on 66 established quarter land section (0.92 km², 0.25 mi²) quadrats. Surveys were completed during 1985-89, 1993, 1996, 1998, 2000-02, and 2009. CWD population prevalence was estimated from disease tests of hunter harvested or culled deer during 1997-2003 (Conner et al., 2007). Four hundred and ten adult female mule deer were determined as CWD positive or negative based on immunohistochemistry exam of retropharyngeal lymph node or tonsil tissue (Miller et al., 2000; Conner et al., 2007)

Population Growth and Disease Trajectory

We aimed to determine the growth rate of a mule deer population infected with CWD and determine if CWD has reached quasi-equilibrium conditions characteristic of an enzootic. We developed a single sex Leslie matrix model that portrayed the deer population in 21 female age and disease stages. The vector \mathbf{n}_t described the number of deer in each of these stages during January of year t . The first element, $n_{1,t}$ was for deer that were 6 months old and CWD susceptible. The next ten elements $n_{2,t}, \dots, n_{11,t}$ represented CWD susceptible deer

from 1.5 to 10.5 years old. The final ten elements $n_{12,t}, \dots, n_{21,t}$ portrayed CWD infected deer from 1.5 to 10.5 years old. The vector $\mathbf{A}n_t$ described the deer population during the subsequent year where \mathbf{A} was a 21×21 projection matrix defined by,

$$\mathbf{A} = \begin{bmatrix} 0 & f_{\text{sus},1.5} & f_{\text{sus},2.5} & \dots & f_{\text{sus},10.5} & f_{\text{inf}} & f_{\text{inf}} & \dots & f_{\text{inf}} \\ s_{\text{sus},0.5}(1 - \psi) & 0 & 0 & \dots & 0 & 0 & 0 & \dots & 0 \\ 0 & s_{\text{sus},1.5}(1 - \psi) & 0 & \dots & 0 & 0 & 0 & \dots & 0 \\ \vdots & \vdots \\ 0 & 0 & 0 & \dots & 0 & 0 & 0 & \dots & 0 \\ s_{\text{inf}}\psi & 0 & 0 & \dots & 0 & 0 & 0 & \dots & 0 \\ 0 & s_{\text{inf}}\psi & 0 & \dots & 0 & s_{\text{inf}} & 0 & \dots & 0 \\ \vdots & \vdots \\ 0 & 0 & 0 & \dots & 0 & 0 & 0 & \dots & 0 \end{bmatrix}$$

We assumed that all deer were born susceptible to CWD and did not develop infection during the first 6 months of life. Deer could develop infection as yearlings or during any subsequent year of life. We treated annual infection probability ψ as constant. Nonlinear infection probability is a hallmark of disease models because the per capita rate of new infections changes with the number of infected and susceptible individuals (McCallum et al., 2001). We realize this is a strong assumption and we addressed the appropriateness of this assumption below (see Data Analysis).

However, CWD has been present in this region for at least 40 years (Miller et al., 2000) providing some support that the disease has reached some form of steady state and the rate of new infections is constant or changing slowly in relation to the lifespan of deer.

We allowed different survival of infected s_{inf} and susceptible deer. For susceptible deer, survival varied with age. Age-specific survival probabilities were $s_{\text{sus},0.5}, \dots, s_{\text{sus},10.5}$. Survival probabilities of deer in the $n_{11,t}$ and $n_{21,t}$ stages representing 10.5 year old animals were fixed

at zero. Elements of the top row of \mathbf{A} are fertilities in a Leslie matrix. To align model updates that occurred in January with the timing of fawning in June, fertility elements were the product of female survival from census to the birth pulse $s_{6,\text{inf}}, s_{6,\text{sus},1.5} \dots, s_{6,\text{sus},10.5}$, birth rate b , and neonate survival to census s_{neo} . CWD infection has small effects on birth rate and neonate survival (Dulberger et al., 2010) and we simplified our model by defining recruitment as $r = bs_{\text{neo}}$. It follows that fertility elements were $f_{\text{inf}} = s_{6,\text{inf}} r$ for infected deer and $f_{\text{sus},j} = s_{6,\text{sus},j} r$ for a susceptible deer of the j^{th} age. Survival and fertility were observed over a four year period without substantial variation in population density and we did not include population density feedbacks.

We evaluated two models, each representing a different spatial scale. The first model represented a single intermixing deer population. Infection probability was constant between individuals. At a finer spatial scale, the second model delineated the population into wintering units and survival, infection, and fertility varied among units.

Data Analysis

Our analysis was divided into three stages. We first developed a hierarchical Bayesian model to estimate the parameters of \mathbf{A} . Next we analyzed \mathbf{A} to determine the population growth rate with and without CWD. We assumed a linear projection model where fertility, survival, and infection probability were constant with time. We concluded by comparing stable prevalence predicted under these assumptions and prevalence from historic CWD surveillance efforts to, in part, validate our assumption.

Infection probability was estimated using an occupancy model (Adams et al., 2010; McClintock et al., 2010) fit to capture-mark-recapture data (Appendix 2). CWD status was treated as a latent binomial random variable where $z_{i,t}$ was the infection status of individual i on the t testing occasion. When an individual was susceptible $z_{i,t} = 0$; when a deer was infected $z_{i,t} = 1$. Infection status followed a first order Markov process. Our model assumed that an infected individual remained infected during the subsequent testing year and a sus-

ceptible individual became infected with probability ψ . Annual infection probability varied among wintering areas and we incorporated these effects using the logistic model. Infection with CWD was determined from immunohistochemistry staining of rectal mucosa associated lymphatic tissue. Tests were imperfect. The presence of infectious agent was indicated by the staining of at least one lymphoid follicle (where infection agent is found) within a tissue sample. Tissue samples contained several lymphoid follicles with $y_{i,t}$ representing the observed number of follicles exhibiting staining and $J_{i,t}$ being the total number of follicles obtained. False positive test results were not believed to occur. Therefore, when $z_{i,t} = 0$ then $y_{i,t} = 0$. However, we may or may not have observed at least one positive follicle when an individual was infected, meaning when $z_{i,t} = 1$ then $y_{i,t} \geq 0$.

Survival probability was estimated using a hazard model fit to capture-mark-recapture data (Appendix 2). Separate hazard functions were used for CWD susceptible and infected deer. The survival function, which is derived from the hazard function gives the probability density that individual i will survive past time t_i (Appendix 2). The survival function for susceptible deer was $\exp(-\lambda_1 t_i^{\alpha_1})^{\exp(\beta \mathbf{x}_i)}$, where λ_1 was the monthly hazard, α_1 described increases in hazards over time, and β were Cox proportional hazard coefficients for age and wintering population unit. For infected deer, the survival function was $\exp(-\lambda_2 t_i^{\alpha_2})$. Annual survival probabilities of our projection matrix were derived using these survival functions (Appendix 2). That is, we set $t_i=12$ (e.g., 12 months) and used posterior estimates of α , λ , and β to estimate the posterior distribution of age- and disease specific annual survival probabilities $s_{\text{inf}}, s_{\text{sus},0.5} \dots, s_{\text{sus},10.5}$.

Several steps were needed to estimate the elements of \mathbf{A} representing fertilities. A Poisson model fit to consecutive annual counts of adult females and fawns was used to estimate recruitment r (Appendix 2). We assumed an equal sex ratio of fawns and only included half of the fawns counted in our analysis. Survival probabilities from census to the birth pulse $s_{6,\text{inf}}, s_{6,\text{sus},1.5} \dots, s_{6,\text{sus},10.5}$ were derived using the above survival functions and setting $t_i=6$

months. In turn, posterior distributions of age- and disease specific fertility elements of \mathbf{A} were approximated as the product of recruitment and survival to the birth pulse.

We estimated the posterior distribution of the dominant eigenvalue of \mathbf{A} (Appendix 2). The eigenvalue provided an estimate of the population rate of growth in the presence of CWD (Caswell, 2001). We repeated this analysis for a population in the absence of CWD by evaluating the upper left 11x11 sub-matrix of \mathbf{A} and fixing annual infection probability at zero. The effect of CWD on population growth was measured as the difference between these two quantities. We also estimated the posterior distribution of the eigenvector of \mathbf{A} associated with the dominant eigenvalue (Appendix 2). These values provided the ergodic composition of age and disease states in the population, assuming a linear projection matrix (Caswell, 2001). Stable CWD prevalence level can be estimated from the ergodic composition. We tested our assumption of linear dynamics by examining predicted stable prevalence and prevalence determined from intense surveillance more than a decade ago (1997-2001). Substantial overlap of these quantities would provide evidence that infection probability was similar during these two points in time.

Results

We monitored survival and CWD infection of 217 female deer with individuals studied for up to four years. Observations totaled 608 animal years. Sixty-seven deer belonged to the Big Hole unit, 30 to Campbell, 39 to Cherokee, 81 to Red Mountain. Twenty-two deer were observed infected with CWD. Seven of these deer entered our research as infected and 15 individuals became infected under study. Ages of conversion from susceptible to infected were 1.5 (1 deer; e.g. 1), 2.5 (1), 3.5 (2), 4.5 (2), 5.5 (2), 6.5 (4), 7.5 (2), and 8.5 (1). New infections were not observed in deer >8.5 years of age. Population prevalence measured as the proportion of CWD positive female deer (>1.5 years of age) during the first year that animals were captured was 0.04 (95% credible interval 0.02 - 0.07).

Annual CWD infection probability averaged across the entire study population was 0.05 (0.02 - 0.08). Spatial differences in infection probability among subpopulations were striking. New infections were spatially localized with all but one case limited to the Red Mountain and Big Hole wintering population units. Nearly 70% (15/22) of new infections occurred within an approximate 50 km² area (Figure 9). New infections were observed in this geographic area each year. Infection probability at the wintering population unit scale varied by nearly an order of magnitude (Table 5). Highest annual infection probability was found in the Red Mountain unit 0.07 (0.03 - 0.12). Therefore, we could not rule out local annual infection probability as high as 0.12 in this unit. Deer in the adjoining Big Hole unit experienced somewhat lower annual infection probability (0.04, 0.01 - 0.10). Deer occupying wintering areas less than 30 km away from this apparent 'hot spot' exhibited annual infection probabilities <0.01 (Figure 10).

After initially being detected as infected with CWD, deer lifetime averaged 410 days (range = 41 - 1,016). Two deer that survived the extent of study lived for more than 700 days. The hazard rate progressively increased after an individual became infected ($\alpha_2=1.67$, 1.07 - 2.53). This equated to annual survival of 0.66 (0.49-0.82) during the first year with infection that declined to 0.42 (0.19 - 0.66) during the second and 0.31 (0.05 - 0.62) during the third year (Figure 11).

Survival of susceptible deer was higher (0.81, 0.76 - 0.86, Figure 11) than survival of infected deer (Table 5). Their hazard rate did not change over time ($\alpha_1=1.09$, 0.91 - 1.28), but hazards were higher for deer that were older at the time of first capture. Susceptible deer survival decreased with age from 0.86 (0.81 - 0.90) in 1.5 year old to 0.65 (0.47 - 0.80) in 10.5 year old animals and varied among wintering areas (Figure 12). Highest survival was found in the Cherokee unit (0.88, 0.79 - 0.94). Survival of susceptible deer was lower in areas with higher CWD prevalence.

One hundred and fourteen deer died due to natural causes. However, 81 (71%) of these deaths were identified resulting from unknown natural cause. Four (4%) deaths were

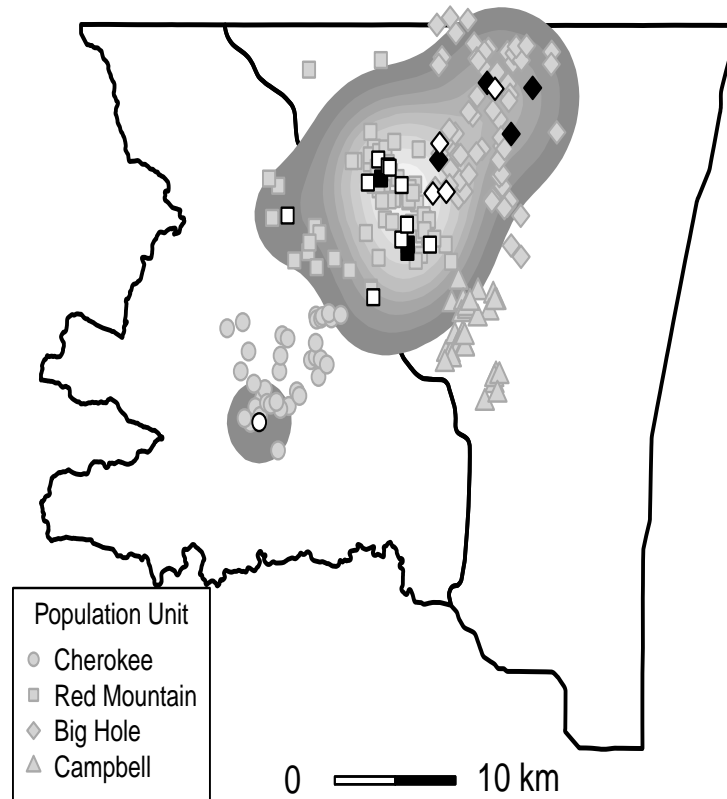


Figure 9: Median winter locations of female mule deer studied during 2010-2014. Deer that entered (black) or converted (white) to CWD positive were mostly located in the central region of the study area. Shaded polygons delineate the area occupied by these infected deer estimated using a bivariate kernel home range estimator.

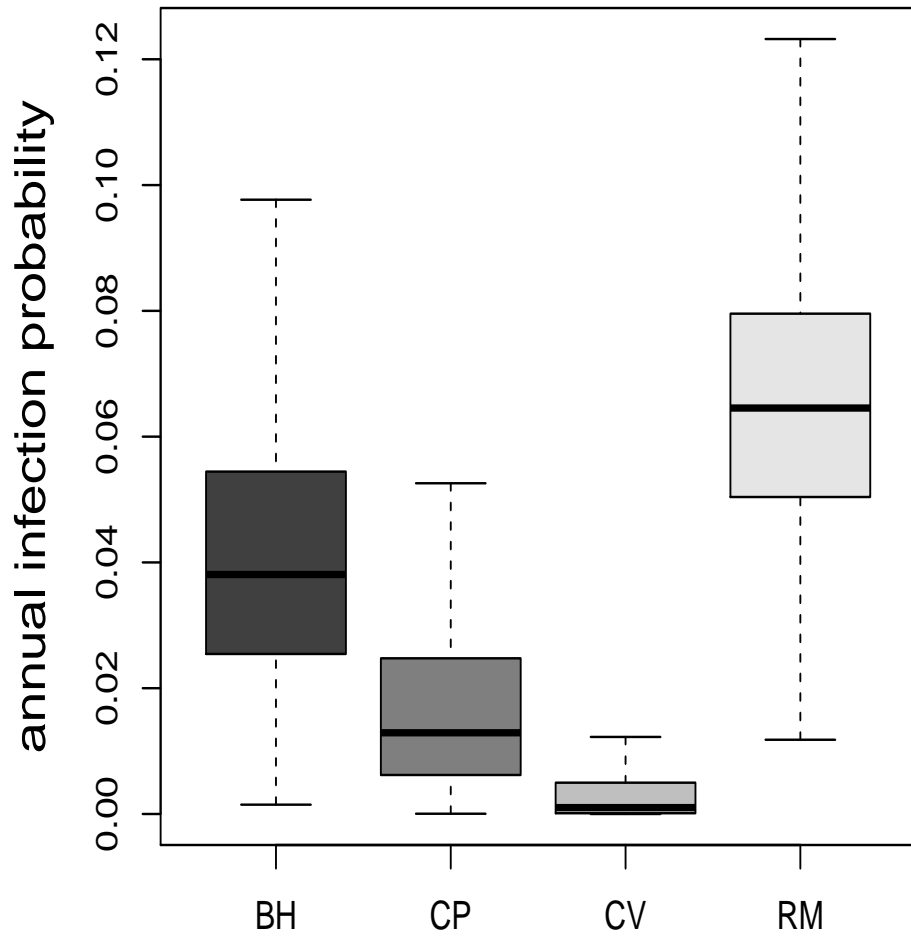


Figure 10: Posterior estimates of annual infection probability for deer of each wintering population unit. Abbreviations are Big Hole (BH), Cherokee (CP), Campbell (CV), and Red Mountain (RM). Boxes show median (dark line), 25%, and 75% quantiles and whiskers show 99% quantiles of posterior distributions.

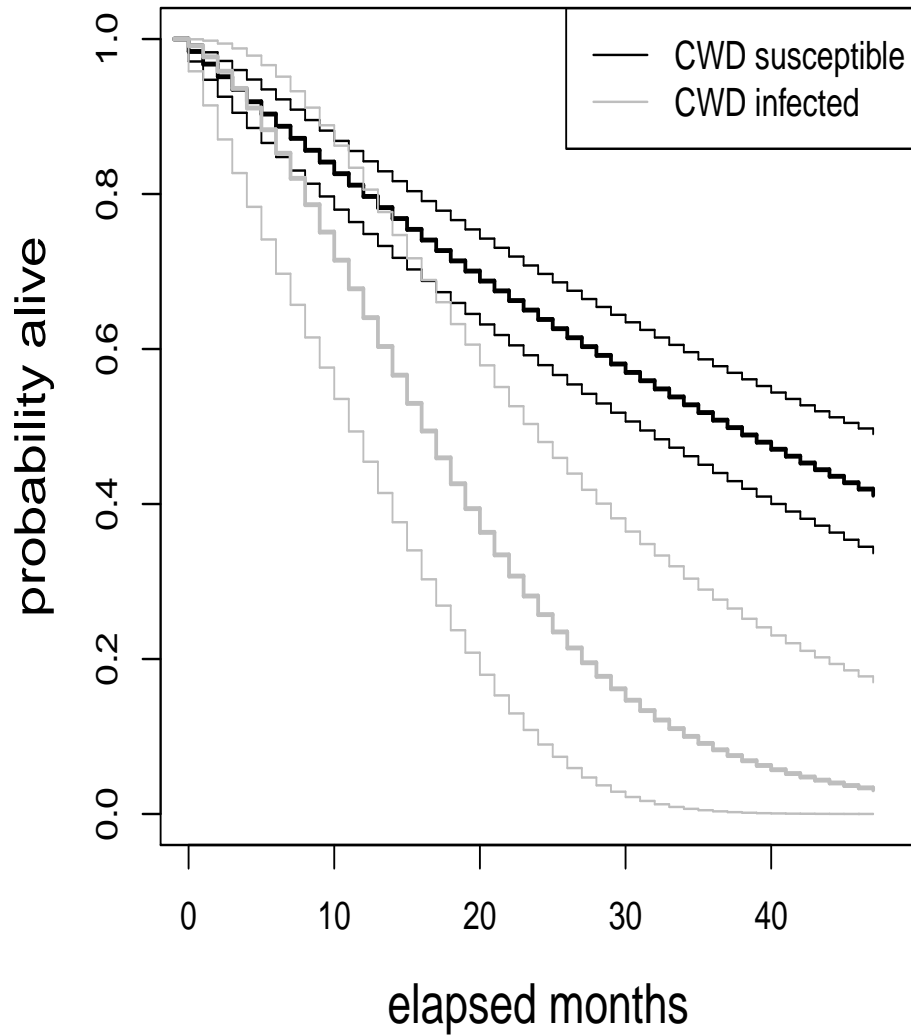


Figure 11: Posterior estimates of survival curves for CWD susceptible and infected adult female mule deer. Curves illustrate the probability of surviving beyond the given month after entry into study for CWD negative animals or after the initial positive test for CWD infected deer.

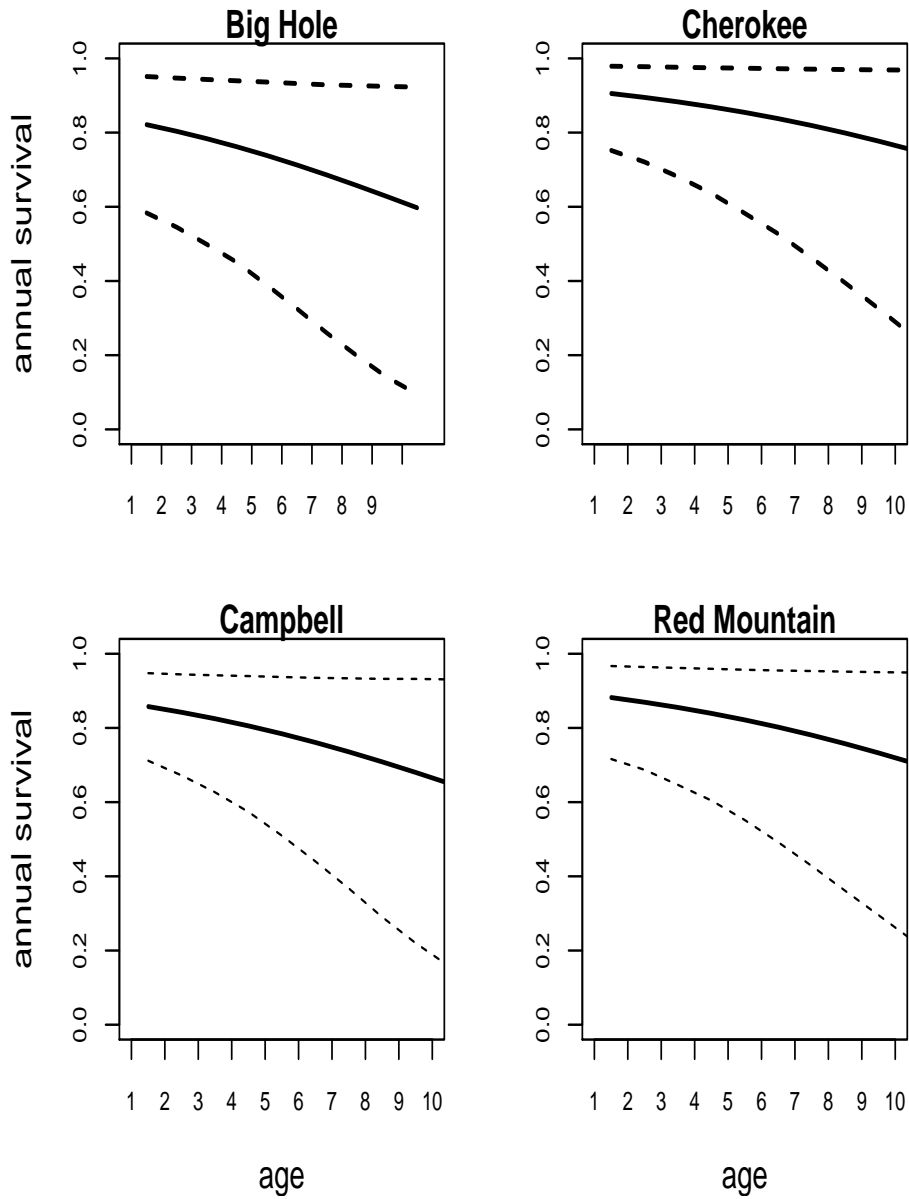


Figure 12: Posterior estimates of adult female survival varied among wintering populations and declined with age. Averaged across these ages, survival was highest in the Cherokee population unit (0.88, 0.79 - 0.94) and progressively lower in the Red Mountain (0.83, 0.76 - 0.89), Campbell (0.80, 0.69 - 0.88) and Big Hole 0.75 (0.66 - 0.83) units. Solid lines show posterior medians and dotted lines show 95% credible intervals.

attributed to CWD. Carcasses from these animals were often found intact. Death was attributed to predation in 23 cases (20%). Field necropsy suggested that nearly all predation events were associated with mountain lion. Additionally, two (1%) deaths were attributed to winter kill and four (4%) to vehicle collision. Two deer were harvested by hunters.

The estimated number of female fawns produced per infected female alive at census that survived until the subsequent census was lower for CWD infected deer. An infected female alive at census produced 0.17 (0.11 - 0.23) female fawns that survived until the next census. Susceptible deer produced fewer female fawns surviving until the next census with age. Averaged among ages, a susceptible female alive at census produced 0.24 (0.20 - 0.28) female fawns that survived until the next census.

At the population scale, there was overlap in the growth rate with CWD ($\lambda_{\text{CWD}} = 0.98$; 0.91 - 1.04) and without CWD ($\lambda = 1.00$; 0.94 - 1.07, Table 5). It is important to note that this overlap does not show that CWD has no impact on the deer population. The posterior distribution of the difference in growth rates averaged -0.03 (-0.11 - 0.06). This equates to a 71% chance that CWD lowered growth. With CWD, the population exhibited a 74% chance of decline (e.g., growth rate <1.0). Removing CWD lowered this chance to 45% and a growing population became the more likely outcome. Stable CWD prevalence predicted by our model was 0.05 (0.01 - 0.15). Observed CWD prevalence recorded from intense surveillance during 1997 - 2003 was 0.08 (0.05 - 0.11). The difference between prevalence estimates was -0.05 (-0.09 - 0.02) suggesting similarities in the CWD epidemic during the two observation periods.

CWD effects on growth rate differed at the wintering population unit scale. Much like at the population scale, we did not detect clear differences between growth with and without CWD. Including CWD increased chances of population decline in units with higher annual infection probability (Figures 10 and 14). Disease effects were strongest in Red Mountain with a 93% chance of local decline ($\lambda_{\text{CWD}}=0.93$, 0.83 - 1.03) and 73% chance that population growth rate was lower with CWD. In Big Hole, local decline was the more likely outcome

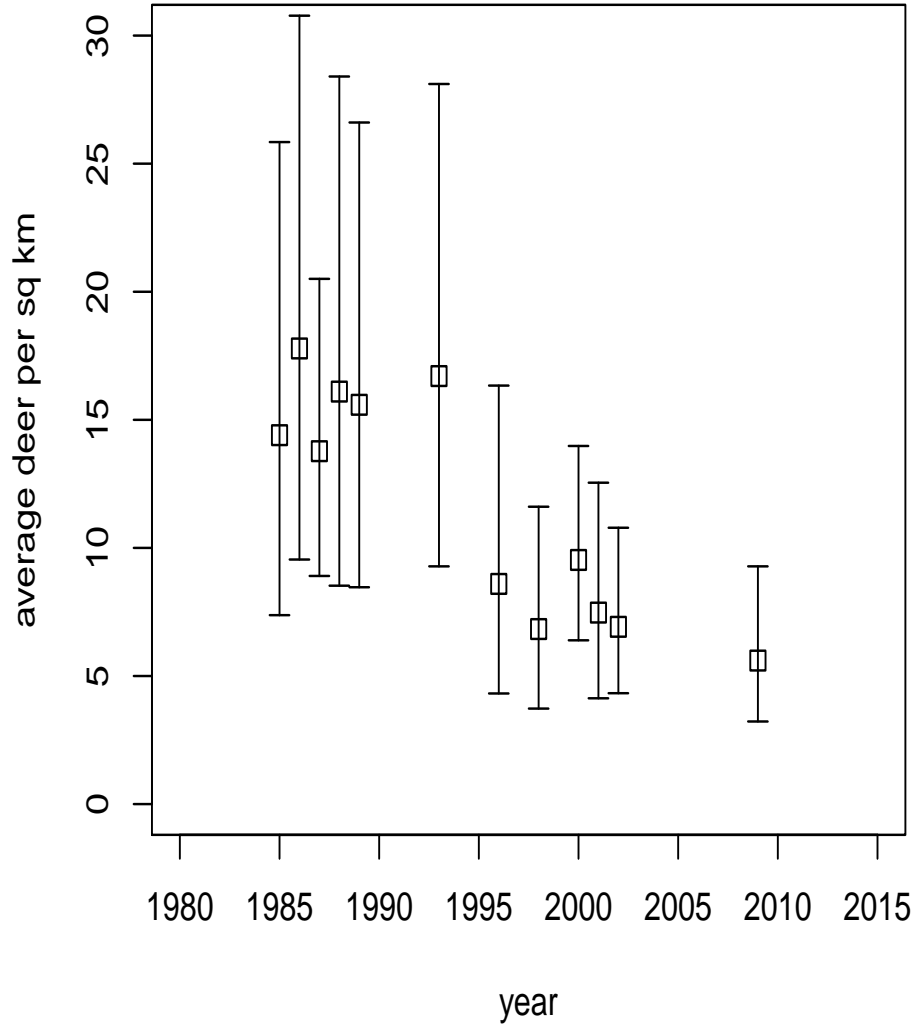


Figure 13: Posterior estimates of deer density km^{-2} estimated from helicopter abundance surveys completed during December, 1985 - 2009. During the middle 1990's the population was managed to maximize hunter opportunity for male harvest. Limited female harvests occurred at that time and male harvests were progressively lower during the middle 1990's suggesting the population decline was unrelated to sport hunting. Management policies were adjusted during 2001 - 2006 to reduce the deer population through liberal female harvest and agency culling in an attempt to suppress CWD prevalence and spread. Since, managers resumed a policy of limited female harvest to support deer population increase.

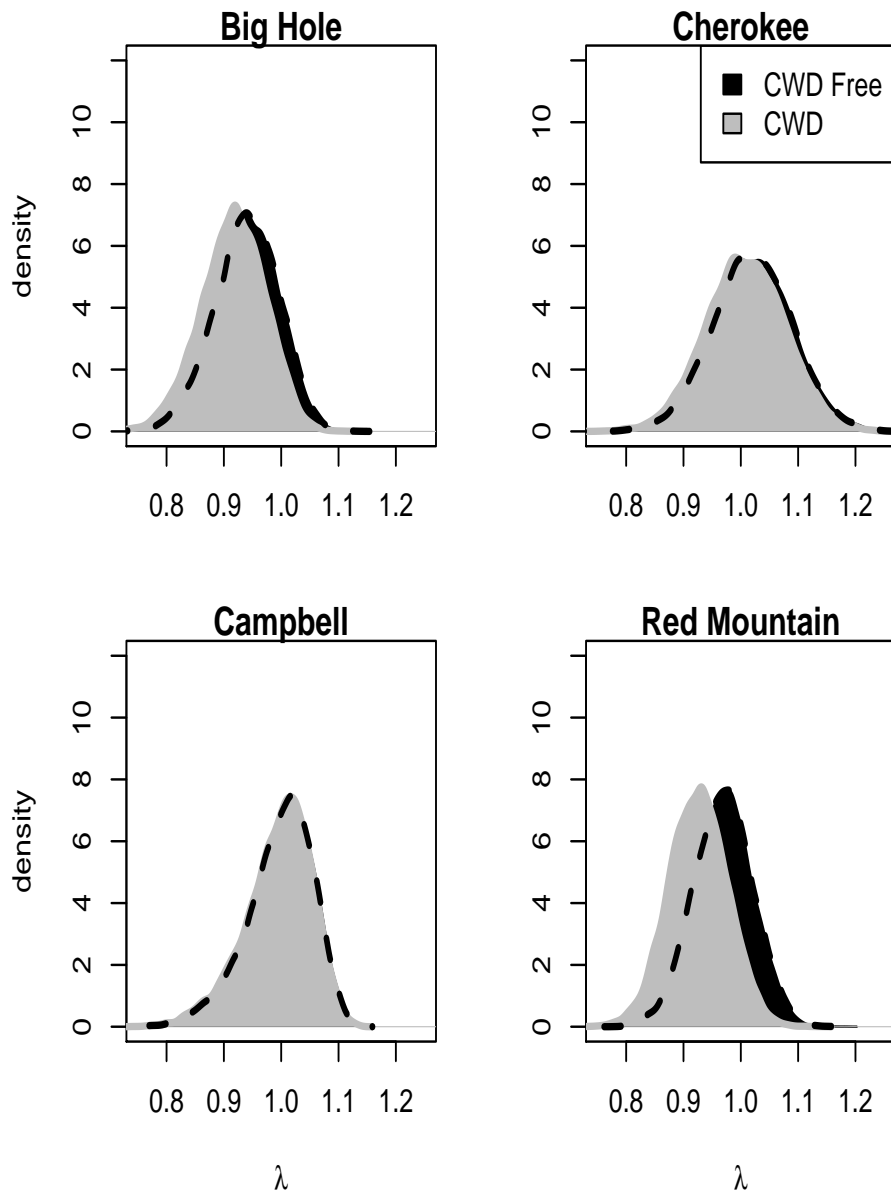


Figure 14: Posterior estimates of population growth rates for wintering mule deer population units with and without CWD.

Table 5: Mean and 95% quantiles of posterior distributions of model parameters and derived quantities.

Description	Quantity	Mean	0.025	0.975
population prevalence	ψ_0	0.04	0.02	0.07
annual infection probability for single population	ψ	0.05	0.02	0.08
annual infection probability population unit coefficients :				
intercept (Red Mountain)	ζ_0	-2.69	-3.48	-2.02
Cherokee	ζ_1	-1.80	-4.56	0.08
Campbell	ζ_2	-4.72	-11.35	-0.49
Big Hole	ζ_3	-0.60	-2.07	0.70
proportion follicles positive in infected deer	π	0.56	0.51	0.60
survival :				
hazard change for susceptible deer	α_1	1.09	0.90	1.30
hazard change for infected deer	α_2	1.88	1.12	2.78
baseline monthly hazard for susceptible deer	λ_1	0.009	0.003	0.023
baseline monthly hazard for infected deer	λ_2	0.0063	0.0002	0.0303
age effect on hazard	β_1	1.20	0.08	2.26
population unit effect on hazard (Cherokee)	β_2	-0.44	-1.33	0.45
population unit effect on hazard (Red Mountain)	β_3	-0.18	-0.88	0.50

Table 5: Mean and 95% quantiles of posterior distributions of model parameters and derived quantities.

Description	Quantity	Mean	0.025	0.975
population unit effect on hazard (Big Hole)	β_4	0.26	-0.43	0.95
recruitment for single population	r	0.26	0.21	0.31
population prevalence 1997-2003	p	0.08	0.06	0.11
population prevalence 1997-2003 by units :				
Cherokee		0.07	0.04	0.11
Red Mountain		0.14	0.08	0.22
Big Hole		0.17	0.07	0.31
Campbell		No Data	No Data	No Data
difference in prevalence over time for single population				
Cherokee		-0.04	-0.09	0.02
Red Mountain		-0.05	-0.10	0.00
Big Hole		-0.06	-0.16	0.07
Big Hole		-0.12	-0.24	0.03
Campbell		NA	NA	NA
growth rate with CWD for single population	λ_{CWD}	0.98	0.91	1.04
growth rate without CWD for single population	λ_{free}	1.00	0.94	1.07

Table 5: Mean and 95% quantiles of posterior distributions of model parameters and derived quantities.

Description	Quantity	Mean	0.025	0.975
difference in growth rate for single population	λ_{diff}	-0.02	-0.11	0.07
Cherokee	λ_{CWD}	1.01	0.87	1.14
	λ_{free}	1.02	0.89	1.16
	λ_{diff}	-0.01	-0.20	0.18
Red Mountain	λ_{CWD}	0.93	0.83	1.03
	λ_{free}	0.97	0.87	1.07
	λ_{diff}	-0.04	-0.18	0.10
Big Hole	λ_{CWD}	0.92	0.80	1.02
	λ_{free}	0.94	0.82	1.04
	λ_{diff}	-0.02	-0.18	0.13
Campbell	λ_{CWD}	1.00	0.86	1.09
	λ_{free}	1.00	0.86	1.09
	λ_{diff}	-0.003	-0.170	0.159

regardless of CWD ($\lambda_{\text{CWD}}=0.92$, 0.80 - 1.02, $\lambda=0.94$, 0.82 - 1.04). Yet, CWD increased the chance of decline from 86% to 94%. Disease effects were less apparent in the Cherokee and Campbell units with virtually no impact of CWD on λ (Figure 14). Growth rates in the absence of disease were higher in Cherokee ($\lambda=1.02$, 0.89 - 1.16) and Campbell ($\lambda=1.00$, 0.86 - 1.09) compared to Red Mountain and Big Hole suggesting important indirect effects of CWD on deer populations.

Modeled stable prevalence was similar to prevalence estimated from earlier surveillance efforts in Red Mountain and Big Hole (Table 5). This was not the case for the Cherokee unit. There, the difference between modeled stable prevalence and surveillance was less than zero (-0.05, -0.10 - 0.00) suggesting a decline in annual infection probability over time.

Discussion

The inevitable consequence of CWD will only begin to play out over our lifetimes. Today's challenge is making decisions about CWD in the face of incomplete understanding. Our research begins to answer important questions about the effect of CWD on deer populations and we offer several clarifying insights.

CWD did not sufficiently lower population growth rate to cause rapid, catastrophic decline and widespread extinction. Instead, effects on growth were more subtle in a population where CWD has been present for at least 40 years. Estimated growth rate with disease centered near one, indicating slow, gradual change in deer abundance. Nonetheless, decline (74%), rather than population increase (26%), was the more likely outcome. On average, deer lived for 17 months after being diagnosed with disease. In terms of understanding CWD population ecology, CWD can be thought of as accelerating the time of demise for infected individuals. Disease moved deer into an equivalent demographic stage as senescent animals, characterized by progressively lower survival and reproduction associated with declines in body condition over time. Moving large numbers of deer early in life into "disease-related

senescence” could have debilitating effects on population growth. However, infection rates were relatively constant between 1.5 and 8.5 years of age with no new infections observed in younger or older deer. Further, the average life expectancy of CWD-free deer was 5.39 (4.23 - 6.91) years and the majority (9 of 15) of new infections were observed in deer that were at least 5.5 years old. Such timing of infection combined with the slow progression of disease offset effects of CWD on population growth. Furthermore, infection was localized with annual infection probability varying by an order of magnitude across relatively fine spatial extents, such that at the population scale insufficient numbers of deer became infected to cause rapid and widespread population collapse.

The Red Feather-Poudre River mule deer population may not be destined to become extinct, but it is clearly less robust today. Deer density has likely declined since the 1980s (Figure 13; Vieira 2006). Although we cannot be sure of the cause of decline, it likely resulted from the interaction of several limiting and regulating pressures, including CWD, other disease outbreaks, habitat fragmentation, a changing climate, and wildlife management practices (Robinson et al., 1992; Daszak et al., 2000; Thomas et al., 2004). We measured the deer population under historically low density and expected to detect higher growth rates. Such discrepancy suggests that we underestimated the CWD effect. Average adult female survival for susceptible deer was 0.81, which is below the range-wide average of 0.85. Because CWD directly lowered population growth by decreasing adult female survival, the difference between susceptible and infected deer survival was less than would be expected if susceptible deer survival was near the range-wide average.

Population growth rates in the absence of CWD were lowest in the Red Mountain and Big Hole. Deer from these units migrated into southern Wyoming where hemorrhagic disease outbreaks were reported during summer 2012. Our data indicated pulses of mortality likely attributable to hemorrhagic disease, which has been associated with local high mortality in deer. Also, apparent competition is an indirect interaction among prey species mediated by a shared predator and has been linked to declines in prey species (Ostfeld and Holt, 2004;

DeCesare et al., 2010). Mountain lions prey selectively on CWD infected deer (Krumm et al., 2010). CWD could be producing an abundance of vulnerable prey, thereby enhancing mountain lion survival and reproduction (Miller et al., 2008). A resulting outcome could be increased predation on susceptible deer and overall depression of the deer population.

The effect of CWD partly depended on the scale of analysis. At the population level, we did not find the remarkably high prevalence observed in two local deer populations (<600 individuals) of the Colorado and Wyoming outbreaks. Mule deer in the Table Mesa population in central Colorado exhibited female prevalence near 20% with annual infection probability of susceptible deer averaging 0.23 (Miller et al., 2008). Similarly, 42% of female white-tailed deer developed CWD during a seven year study of the Deer Creek population in central Wyoming (Edmunds, 2013). The Table Mesa and Deer Creek populations declined and CWD was implicated as an ultimate or contributing cause (Miller et al., 2008; Dulberger et al., 2010; Edmunds, 2013). Annual infection probabilities approached these levels within highly localized areas (<50 km²) of our research (Figure 9) and population decline was the more likely scenario in associated population units (Red Mountain and Big Hole). However, declines were offset by growth in population units with lower infection rates. The emergent pattern was largely unchanging deer abundance at the scale of the entire population (Figure 13).

Long-term outcomes of CWD depend heavily on whether high infection remains a localized phenomenon. To some extent, the causative agent of CWD must rely on the host to be transmitted among individual hosts. Deer show extraordinary fidelity to female structured social groups and home ranges that are established early in life, which may limit the mobility of PrP^{Sc} affording deer some natural resistance against CWD. However, males have larger home ranges and potentially serve as an infection pathway among bands of females through interactions associated with mating. Nonetheless, the role of males in the CWD epidemic was beyond the scope of our research and remains an unanswered question.

CWD prevalence predicted under equilibrium conditions was similar to prevalence estimated from intense surveillance during the preceding decade at both the population and population-unit scales. A variety of dynamics could cause such behavior. Perhaps, the CWD epidemic is playing out as a series of reoccurring epidemics characterized by stable limit cycles or damped or increasing oscillations (Sharp and Pastor, 2011). As a result, numbers of infected and susceptible hosts and infection rates may have varied widely between our two observation periods. Otherwise, the disease may have remained in an approximate steady-state over the past decade. Finally, sufficient time may not have passed to detect whether the CWD epidemic is increasing. If this were the case then the timespan of CWD epidemics is likely that of centuries rather than decades.

As an exception, our findings suggest that the epidemic has decreased in the Cherokee unit. These deer mostly occupy state lands that are heavily hunted. Harvests are predominantly weighted towards males (Vieira, 2006), except during brief periods when deer numbers have been actively reduced through female harvest. In contrast, deer belonging to the other population units occupy private, county, and city lands with limited hunting. A resulting outcome is fewer deer, and lower proportions of males in the Cherokee population units. Male prevalence tends to be nearly twice that of female deer (Miller and Conner, 2005; Osnas et al., 2009), infected deer exhibited higher harvest vulnerability, and more rapid turnover of infected deer could reduce transmission. The state game management agency completed a multi-year effort to reduce deer abundance ending in the early 2000s. At that time, it was determined that reductions in deer density had little impact on CWD prevalence (Conner et al., 2007). Reductions were mostly implemented in the Cherokee unit. Perhaps, these practices augmented with continued male harvests have been more successful than initially reported in affecting the epidemic.

CWD outbreaks suggest average prevalence is highest in mule deer (Colorado and Wyoming 5%, Saskatchewan <2%, Nebraska 1.3%), lower in white-tailed deer (Colorado and Wyoming 2%, Wisconsin 3%, Saskatchewan <1%), and lowest in elk (Colorado and Wyoming 0.5%;

Miller et al. 2000; Joly et al. 2003; Conner and Miller 2004; Miller and Conner 2005; Osnas et al. 2009; Rees et al. 2012). Differences within and among geographic areas have been attributed to time since disease introduction with the Colorado and Wyoming outbreak being the oldest (Conner and Miller, 2004; Miller and Conner, 2005; Heisey et al., 2010). These epidemics show many similarities and our research provides indication of how these other epidemics may progress. We provide compelling evidence that prion epidemics can affect mule deer populations both locally and at coarse spatial scales. Effects were subtle and the protracted time-scale of the epidemic is likely much longer than the thirty year time span of our research. As a result, we could not identify the inevitable fate of deer populations with CWD. Our findings do suggest, in the nearer-term (e.g., decades), mule deer populations persisting at lower levels after disease establishment.

CHAPTER 4: AGE DRIVES CWD ANTE MORTEM TEST SENSITIVITY IN MULE DEER

Developing effective strategies for managing wildlife diseases requires identifying relationships between hosts and pathogens (Dobson and Foufopoulos, 2001; McCallum et al., 2001). Accurate diagnosis of infection status is a necessary first step because imperfect detection can lead to erroneous inferences about disease (McClintock et al., 2010; LaDeau et al., 2011). The veterinary and medical fields have developed statistical techniques for estimating the actual infection status when diagnostic tests are imperfect. Such techniques rarely are applicable to wildlife diseases because little is generally known about the underlying prevalence of disease in the population, and reference tests and repeated independent tests of disease status are not available (Greiner and Gardner, 2000; Toft et al., 2005; Lachish et al., 2012). Also, capture and testing of individuals is inherently difficult and costly, and the information available is often limited to a single test or observation of a sick animal (Morner et al., 2002).

Chronic Wasting Disease (CWD) is a naturally occurring prion disease found in free-ranging elk (*Cervus elaphus*), mule deer (*Odocoileus hemionus*), white-tailed deer (*Odocoileus virginianus*), and moose (*Alces alces*) (Williams and Young, 1992). A malformed variant of native prion protein, PrP^{Sc}, is speculated as the causative agent of disease (Williams et al., 2002). PrP^{Sc} interacts with native prion protein to cause malformation of host PrP and accumulation of the disease-associated variant (Williams et al., 2002). PrP^{Sc} progresses into the lymphatic system early in the infection process where terminal lymphoid follicles serve as a collection center (Fox et al., 2006).

PrP^{Sc} can be identified using live techniques through biopsy of tonsil or rectal tissue and immunohistochemistry staining (Wild et al., 2002; Wolfe et al., 2002; Schuler et al., 2005; Wolfe et al., 2007; Keane et al., 2009; Spraker et al., 2009). Tissue samples typically contain several lymphoid follicles. However, all lymphoid follicles do not necessarily exhibit PrP^{Sc}

presence. The possibility exists that PrP^{Sc} occurs within a tested animal, but is not found during disease testing, particularly if small numbers of follicles are observed. As a result, some researchers proposed that tests are only useful when sufficient numbers of follicles are obtained. For example, Wolfe et al. (2002) recommended that at least nine follicles are necessary to assure an accurate test from tonsil tissue in mule deer. Similar thresholds of six follicles in rectal tissue from white-tailed deer (Keane et al., 2009) and ten follicles from elk (Spraker et al., 2009) have been suggested.

Using such follicle thresholds discards test results that actually provide meaningful information about the infection status of an individual. The probability that a test produces a false negative depends on the true infection status of the animal, the number of follicles tested, and the proportion of follicles that are positive. Tissue samples with large numbers of follicles provide accurate assessment of the infection status of the individual (Wolfe et al., 2002), but samples with fewer follicles contain meaningful information if the uncertainties associated with detection can be quantified. We desired a method to account for this uncertainty. We developed a hierarchical Bayesian occupancy model that simultaneously identified the probability that an individual is infected and probability that a single follicle shows infection in an infected individual. Infection and detection probabilities were determined from numbers of test positive and test negative follicles found in tissue samples collected repeatedly from the same individuals over time. We fit our model to data on free-ranging mule deer in northern Colorado, USA during 2010-14. We identified individual-level effects on test sensitivity. We concluded by estimating chances of false negative diagnosis associated with age and numbers of follicles obtained in tissues.

Materials and Methods

Data Collection

We completed a capture-mark-recapture study of free-ranging mule in northern Colorado. Handling and disease testing occurred during January, 2010 - 2014. Deer were caught by helicopter net gunning and transferred to nearby processing locations. Two hundred and ten adult (≥ 1.5 years) female mule deer were captured by helicopter net gun. Individual deer were captured between one and five times and never more than once during a single year. Five hundred and nineteen disease tests were completed during this research.

Rectal-anal mucosa associated lymphoid tissue (RMALT) was collected using methods described in detail by Wolfe et al. (2007). CWD status was determined through immunohistochemistry (IHC) staining of RMALT using methods described elsewhere (Wild et al., 2002; Wolfe et al., 2002; Thomsen et al., 2012). Briefly, RMALT was embedded in a paraffin block and a 5 μm tissue section was collected from a depth of approximately 250 μm and mounted onto a glass slide for IHC analysis. When fewer than 10 lymphoid follicles were detected in the first section (see Results), a second section was collected from a depth of approximately 350 μm . The second slide enabled us to identify additional lymphoid follicles that were deeper within the biopsy. IHC analyses were completed by the Colorado State University Veterinary Diagnostics Laboratory. We estimated age using tooth wear patterns (Robinette et al., 1957). Genotype of the prion precursor (*Prnp*) gene was determined using the approach of Jewell et al. (2005). Deer were fit with a mortality sensing collar (Advanced Telemetry Systems, Isanti, MN). Field personnel determined weekly survival using standard telemetry techniques. Carcasses were investigated to obtain a post mortem test of CWD infection. The head and spinal column were collected from carcasses whenever possible. Field samples were transported to the Colorado State University Veterinary Diagnostics Laboratory for necropsy and IMH testing of tonsil, retropharyngeal lymph node, dorsal motor nucleus of the vagus nerve, and/or spinal column.

Background and Statistical Analysis Framework

We developed an occupancy model that allowed CWD status (susceptible, infected) to change with test occasion. We assumed that infected animals could be misdiagnosed as susceptible (false negative) and that false positive tests did not occur. Deer were either infected with CWD or susceptible at the time of the first disease test. Deer that entered susceptible could become infected each year and, once infected, animals remained infected for the duration of study.

We assumed that detection varied among individuals. PrP and PrP^{Sc} naturally associate with lymphatic cells. The quantity of lymphoid tissue found within animals decreases with age (Spraker et al., 2009). It follows that these age-related declines diminish our ability to detect PrP^{Sc} in older animals. Other individual-level factors likely influenced our ability to detect CWD such as differences in initial dosing and time since exposure. In addition, PrP^{Sc} does not deposit uniformly in an infected individual. This creates the opportunity to sample areas with local differences in PrP^{Sc} concentration within the same individual. For these reasons, we included age and additional unstructured error in our ability to detect a positive lymphoid follicle in an infected deer.

CWD is affected by various polymorphisms in the gene encoding the hosts cellular prion protein (Prnp) (Ryou, 2007). A non-synonymous substitution of serine (S) for phenylalanine (F) at codon 225 (Jewell et al., 2005) appears to increase the time course of CWD and delay deposition throughout the body (Fox et al., 2006). There is also evidence that deer homozygous for phenylalanine fail to exhibit IMH staining with infection (Wolfe *in preparation*). Consequently, we thought that deer expressing phenylalanine would have lower detection. We initially intended to include an indicator variable for Prnp genotype in our model. However, insufficient numbers of infected deer of different Prnp genotypes were included in our field study to evaluate this hypothesis (see Results).

Detailed Statistical Methods

Next we describe how this conceptual model was represented as a hierarchical Bayesian statistical model. Detailed methods can also be referenced in Chapter 3 and Appendix 3. The observed data \mathbf{Y} , the number of follicles showing PrP^{Sc}, is assumed to depend on the true infection status \mathbf{Z} . The true infection status \mathbf{Z} is latent and therefore not observed.

We define \mathbf{Z} as an infectious status matrix. Elements of \mathbf{Z} are $z_{i,t} = 0$ indicating no infection for the i^{th} deer at the t^{th} testing occasion, 'year' $i = 1, \dots, I$, $t = 1, \dots, T$, and $z_{i,t} = 1$ when a deer was infected. The model for the initial test, $z_{i,1}$, is described below (equation 4.3). After the initial test, infection status at the current time t is conditioned on infections status at the previous time $t - 1$ where

$$[z_{i,t}|\psi] = \begin{cases} 1 & z_{i,t-1} = 1 \\ \text{Bern}(\psi) & z_{i,t-1} = 0 \end{cases}. \quad (4.1)$$

The parameter ψ is the infection probability. Infection probabilities are assumed to be time invariant and similar between individuals. Our model assumes that an infected individual remains infected during the subsequent testing year and a susceptible individual becomes infected with probability ψ .

We define \mathbf{Y} as an observation matrix, where $y_{i,t}$ represents the observed number of follicles exhibiting PrP^{Sc} from individual i during testing occasion t . We define the corresponding matrix, \mathbf{J} , where $J_{i,t}$ is the total number of follicles obtained for individual i at year t . False positive test results were not believed to occur. Therefore, when $z_{i,t} = 0$ then $y_{i,t} = 0$. However, we may or may not have observed at least one positive follicle when an individual was infected, meaning when $z_{i,t} = 1$ then $y_{i,t} \geq 0$. The probability that an

individual follicle is positive is $\pi_{i,t}$, and

$$[y_{i,t} | \pi_{i,t}, J_{i,t}] = \begin{cases} 0 & z_{i,t} = 0 \\ \text{Binom}(J_{i,t}, \pi_{i,t}) & z_{i,t} = 1 \end{cases}. \quad (4.2)$$

The infectious status at time 1 depends on the observed infection value, where a false negative is possible. That is,

$$[z_{i,1} | \psi_0, y_{i,1}] = \begin{cases} 1 & y_{i,1} \geq 1 \\ \text{Bern}(\psi_0) & y_{i,1} = 0 \end{cases}, \quad (4.3)$$

where ψ_0 is the probability that an individual developed disease prior to initial testing. There is an important distinction between ψ and ψ_0 ; ψ only captures infection during a single year, while ψ_0 is the population prevalence.

We incorporated individual effects on detection. We let $\pi_{i,t}$ in equation 4.2 be the detection probability of individual i on occasion t and $\pi_{i,t}$ is related to covariates using the logistic model such that $\text{logit}(\pi_{i,t}) = \mathbf{X}\boldsymbol{\beta} + \epsilon_{i,t}$. The vector $\boldsymbol{\beta} = [\beta_0, \beta_1]^T$ is a 2×1 vector of coefficients representing covariate effects with the first element being the intercept term. The matrix \mathbf{X} represents covariate levels and $\epsilon_{i,t}$ represents additional unstructured error where $\epsilon_{i,t} \sim \text{N}(0, \sigma^2)$. We estimated the parameters of our model using the implementation described in Appendix 3. As a note to readers, we chose to report findings on infection probability in a separate manuscript (Chapters 3 and 5).

Estimating the Chance of a False Negative Test

We estimated the probability of obtaining a false negative diagnosis for deer of different ages. The posterior predictive distribution $\tilde{y}_{i,t}$ was determined for the i^{th} deer at the t^{th} occasion. Posterior predictive distributions were determined for deer between one and ten years old. All deer were assumed infected at the time of testing and we varied the total

number of follicles obtained in tissue sections from one to forty. The proportion of times when $\tilde{y}_{i,t} = 0$, e.g. the times when no positive follicles were observed, provided a probability of obtaining a false negative test for each age and total follicle count level.

Results

At least one lymphoid follicle was obtained from the first tissue section in 482 of 519 (93%) tests (mean = 9 follicles; standard deviation = 9 follicles; range = 0 - 72 follicles). The number of lymphoid follicles obtained during tests decreased with animal age (Figure 15). The mean number of follicles obtained during the initial test year was 12.2 (n=210, SD=10.7), and decreased to 4.8 (n=138, SD=5.9) during the second, 4.9 (n=87, SD=4.4) during the third, 8.5 (n=59, SD=8.1) during the fourth, and 11.5 (n=26, SD=6.5) during the fifth test year. A second tissue section was analyzed when fewer than 10 follicles were detected in the first tissue section. Follicle counts were summed between the first and second tissue sections. Our approach increased the average follicle count across all test years to 13.5 (SD=11.1) and increased the number of tests with at least a single follicle to 506 (97%). All remaining results summarize our findings from the complete data set.

We identified 21 deer that tested CWD positive at some point during our research (Figure 16). Individual deer were tested multiple times and at least one positive lymphoid follicle was detected in 29 tests. Four deer exhibited a negative test finding subsequent to a positive test (Figure 16). Only one of these individuals was tested a third time, when a positive test provided evidence of a false-negative result (Figure 16, deer M).

Carcasses were recovered from 127 previously tested deer. Consumption of carcasses by predators complicated obtaining post mortem samples. Gaining access to privately owned lands also delayed necropsy efforts. Consequently, we secured diagnostic post mortem samples from 31 (24%) carcasses. Post mortem samples from five carcasses tested positive for CWD with these deer also testing RMALT positive. Negative post mortem findings were

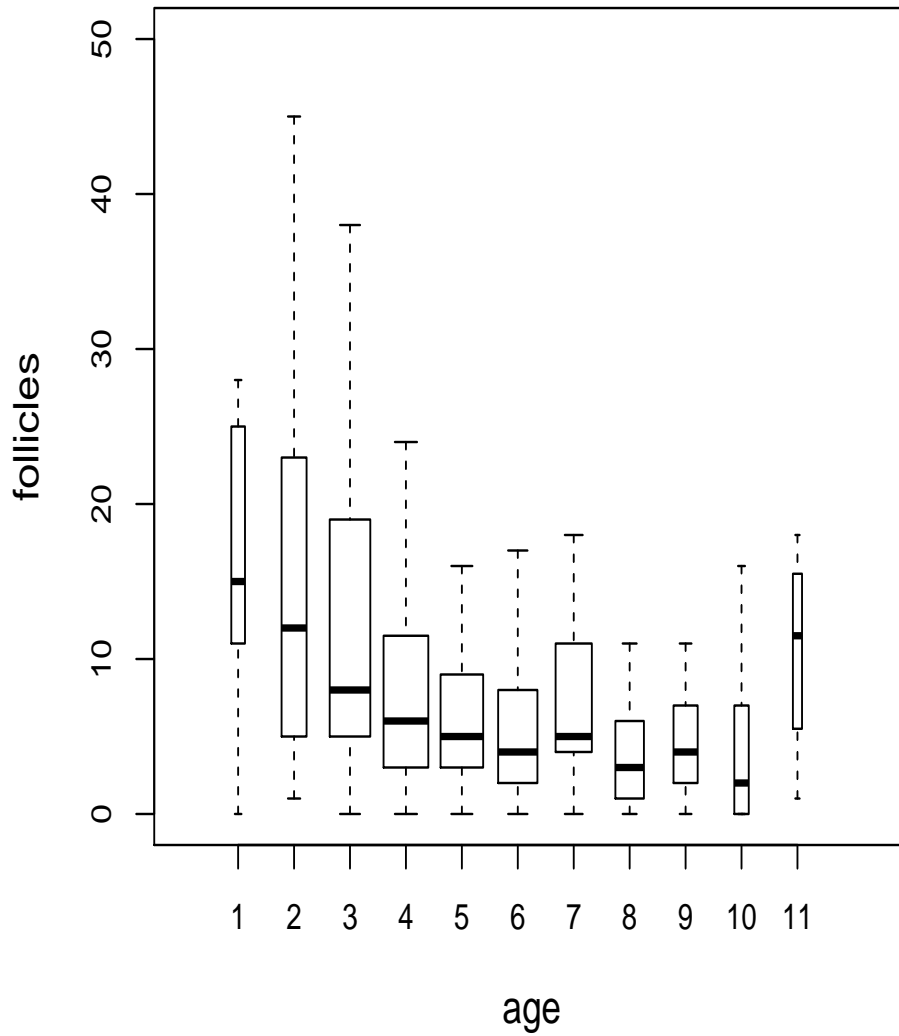


Figure 15: Number of follicles detected in a single rectal-anal mucosa associated lymphoid tissue slide of female deer. Bar widths are proportional to the square root of the number of samples for each age. Bars include multiple tests from the same individual, because deer were tested on more than one occasion.

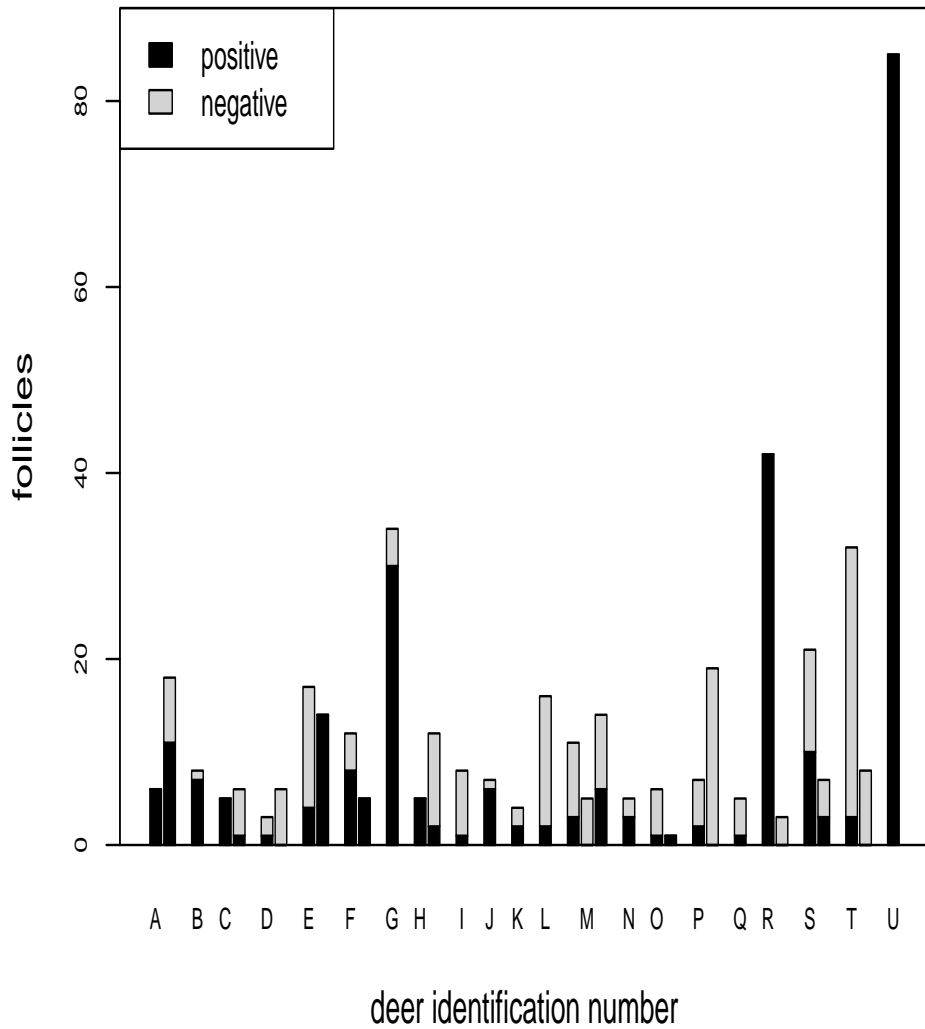


Figure 16: Numbers of positive and negative follicles detected in rectal-anal mucosa associated lymphoid tissue by deer and testing occasion. For each deer, demarcated by capitalized letters, individual bars represent subsequent testing occasions (from left to right) beginning with the first positive test.

confirmed for 25 deer that tested RMALT negative. There was a discrepancy for one deer that tested RMALT and CWD positive in tonsil and retropharyngeal lymph node. This deer was tested by RMALT more than twelve months previous, so it is possible that conversion occurred after RMALT testing.

Monitoring of survival status confirmed RMALT as a good early detection test. Fifteen individuals were observed developing CWD infection based on an initial negative test followed by a positive test during a later year. We were unaware of the exact time of true exposure of these deer. Yet, seven individuals survived at least 365 days (d), five deer survived more than 500 d, and two deer survived more than 700 d (see also Chapter 3) .

Probability that a follicle tested positive in an infected individual declined with age (Figure 17, Table 6). The age coefficient credible interval indicated there was 100% chance that increases in age lowered detection (Table 6). CWD positive deer exhibited additional variation in the chance of detecting a positive follicle than described by age effects alone (Figure 18, Table 6). On average, this probability declined from 88% in 1.5 to 3% in 10.5 year old deer (Figure 19). This does not mean that there was only a 3% chance of correctly identifying an older infected deer. Instead, the probability that a single follicle tests positive in this animal is low requiring more follicles in a test to avoid a false-negative result.

We observed positive tests on nineteen deer that were homozygous for serine (SS) at codon 225. Positive tests were also recorded on two deer that were heterozygous for serine and phenylalanine (SF). FF deer were rare with four individuals in our study and we did not detect infection in these deer. Due to these limited observations, we were unable to evaluate Prnp effects on detection. Yet, we found preliminary evidence that the probability of a follicle testing positive in an infected deer is lower in SF deer (Figure 20). The percentage of follicles testing positive in deer that were known to be positive were 0.52 (sd = 0.38) in SS and 0.16 (sd = 0.15) in SF deer.

Given these findings, we determined the probability of a false negative test associated with ages and follicle counts (Figure 21). In deer less than five years of age, biopsies with

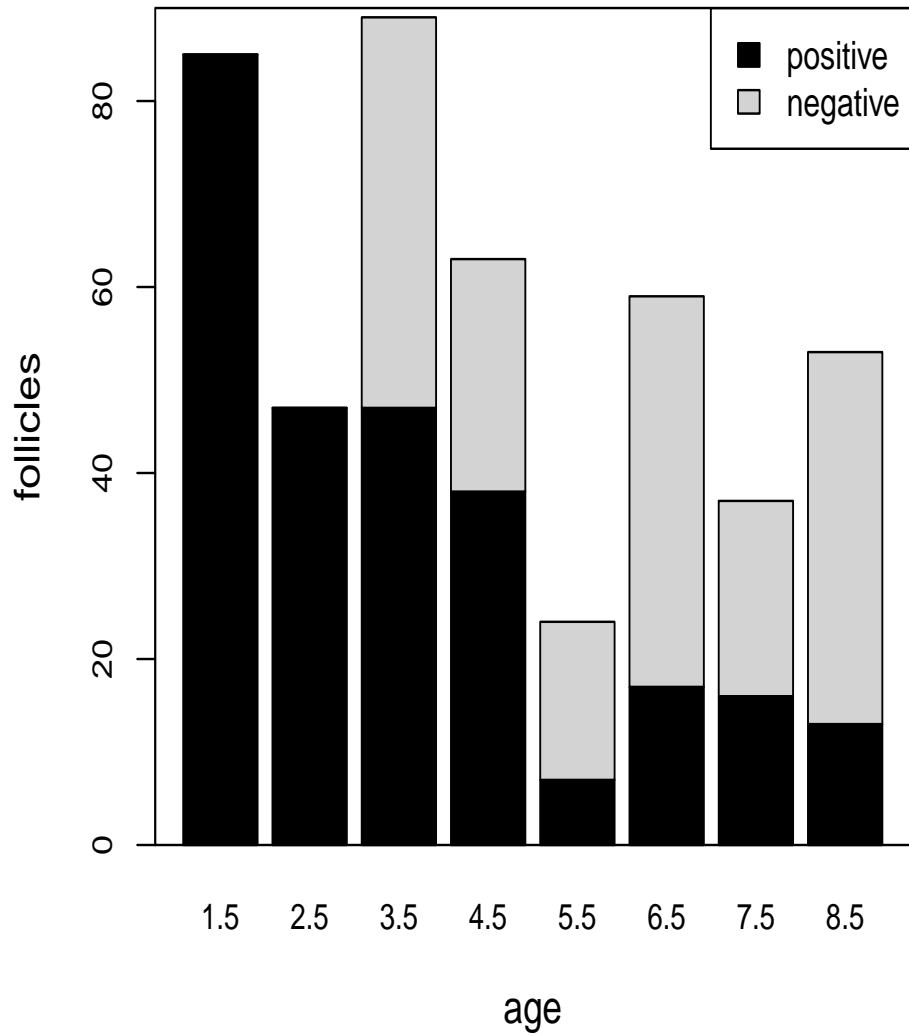


Figure 17: Numbers of positive and negative follicles detected in rectal-anal mucosa associated lymphoid tissue by age in known CWD positive deer.

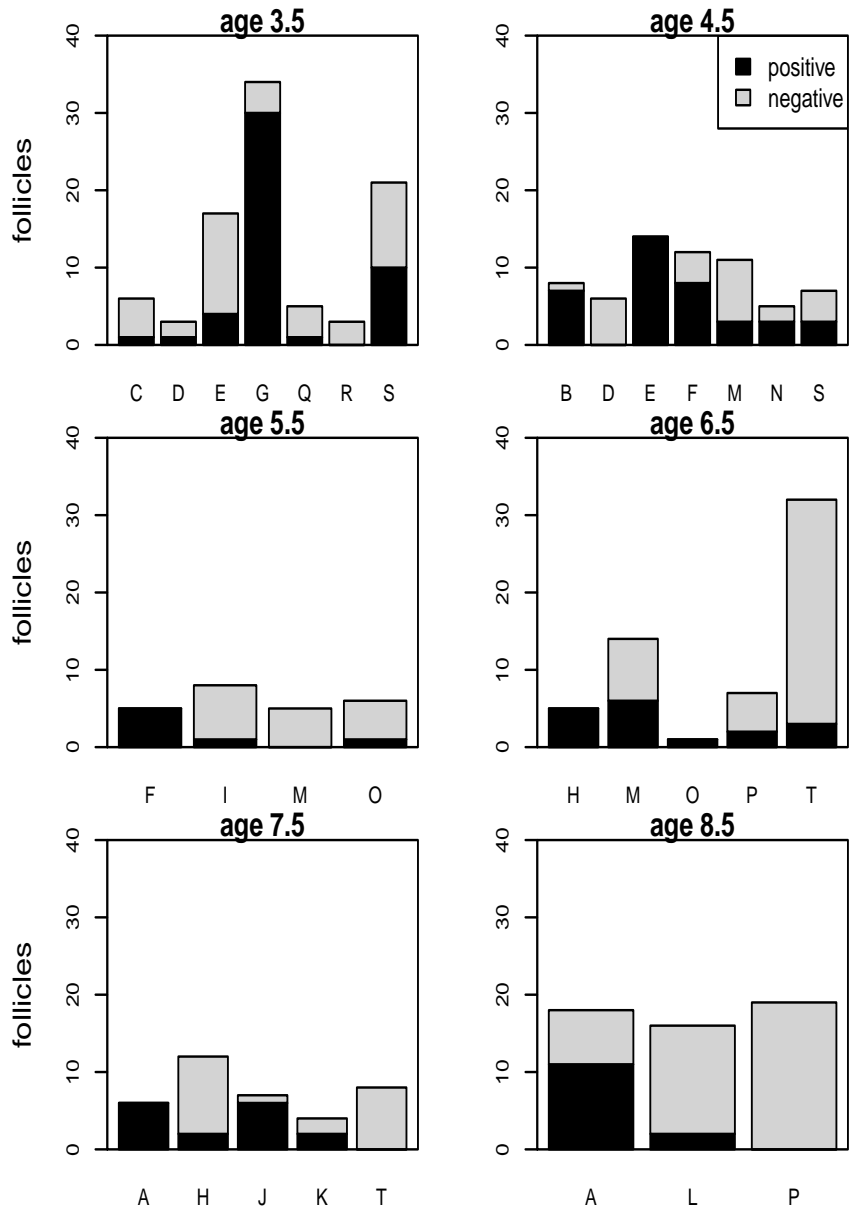


Figure 18: Numbers of positive and negative follicles detected in rectal-anal mucosa associated lymphoid tissue by deer and age in known CWD positive deer. Capitalized letters demarcate individuals.

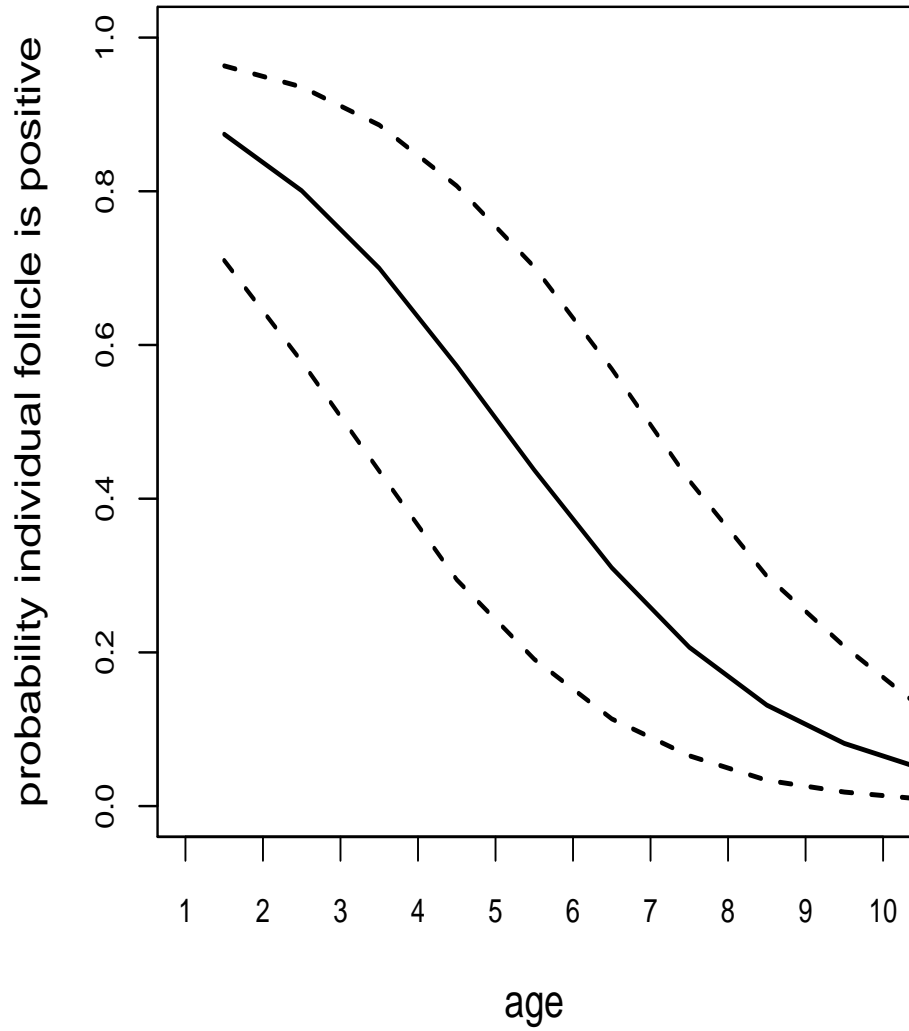


Figure 19: Posterior estimates of age-specific probabilities that a follicle in rectal-anal mucosa associated lymphoid tissue exhibits a positive test (IHC staining) in an infected deer. The solid line shows the mean and dotted lines show 95% credible intervals.

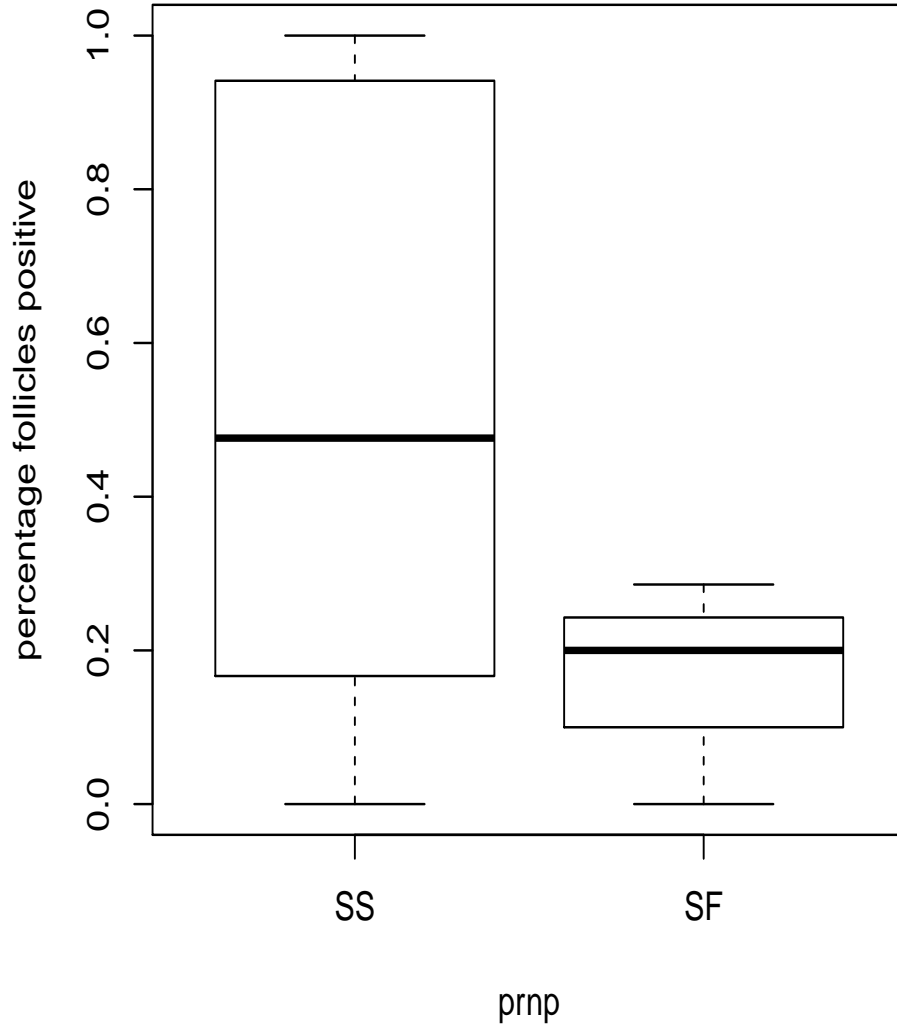


Figure 20: Percentages of positive and negative follicles detected in rectal-anal mucosa associated lymphoid tissue for SS and SF Prnp genotypes in known CWD positive deer.

at least five total follicles had a >95% chance of correctly identifying an infected deer. In older deer, biopsies required greater total follicle counts to provide a similar chance of identifying infected animals. For example, 10 follicles were necessary for 6 year old and 20 follicles for 7 year old deer. Follicle counts of ≥ 40 were needed to reach a 95% chance for deer 8+ years old. However, we aimed to demonstrate that tests with fewer follicles provided meaningful information about the infection status of an individual. On average, we obtained >13 follicles per test in our research. Such follicle counts corresponded a >90% chance of correctly identifying infected deer less than seven years old. This probability declined to a 50% chance in older deer.

Table 6: Posterior estimates of model parameters controlling the probability that an individual follicle tests positive through IHC staining of RMALT in a CWD infected deer.

Definition	Parameter	Median	0.025%	0.975%
Intercept	β_0	-0.73	-1.21	-0.35
Age effect	β_1	-1.94	-2.55	-1.47
Additional individual level variation	σ^2	0.41	0.02	1.42

Discussion

CWD disease surveillance and containment programs benefit from an ability to correctly identify animals using live tests. The model we developed can easily be applied to live surveillance data on mule deer CWD prevalence. Our approach would allow all existing tests regardless of total follicle counts to be used. Our approach would produce probabilistic estimates of the infection status of each tested individual which could then be used to provide 95% credible intervals of population prevalence that account for differences in test quality. Our approach also has application to CWD screening for transport of wild or captive deer or targeted culling efforts. Individuals could be identified that require additional testing to confirm disease status with desired levels of certainty. Others (Wolfe et al., 2002; Espenes et al., 2006; Gonzalez et al., 2006; Keane et al., 2009; Spraker et al., 2009; Thomsen et al., 2012) who have collected similar ante mortem test data on deer and elk with CWD and

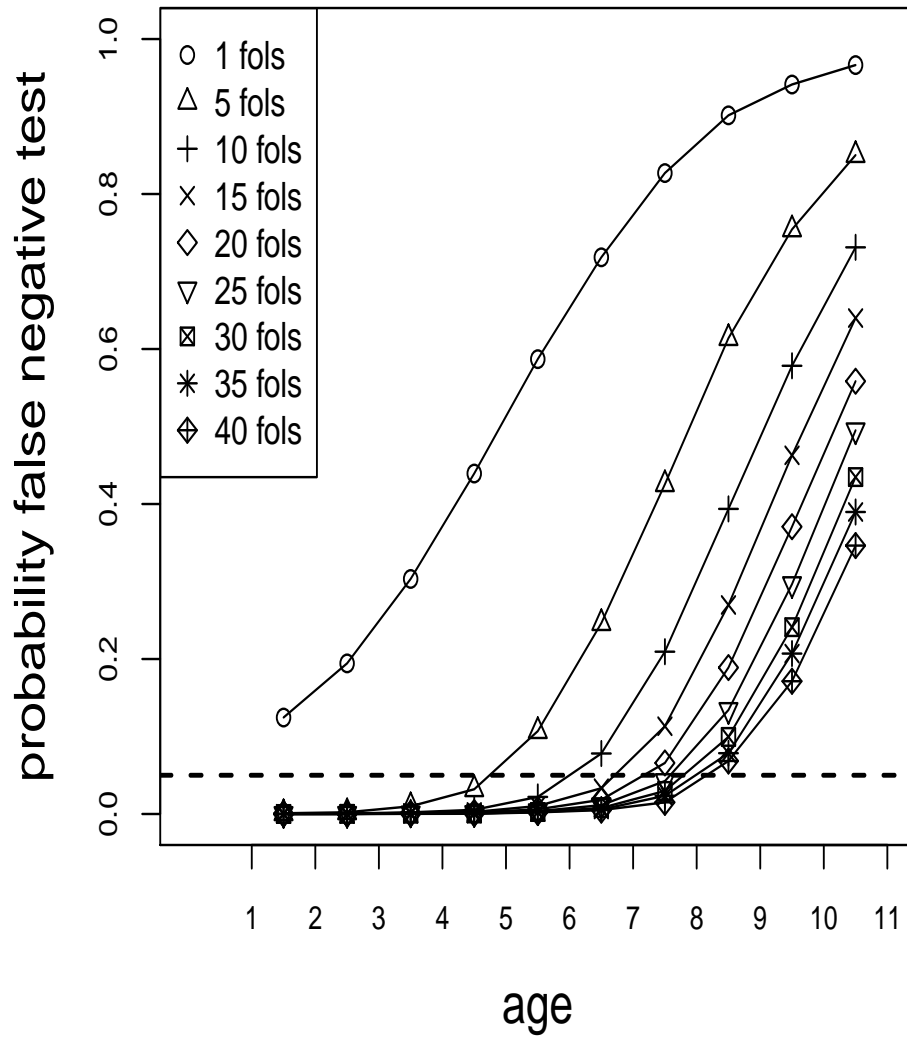


Figure 21: Probabilities of a false negative test by age for total follicles (positive and negative combined) obtained in a rectal-anal mucosa associated lymphoid tissue biopsy.

sheep with scrapie could apply this approach to their data to obtain species specific detection probabilities. Advancement of such multi-species detection probabilities would improve CWD surveillance throughout North America.

Our findings are consistent, in part, with the earlier work of Wolfe et al. (2002) who suggested at least nine follicles were necessary in a tonsil biopsy to accurately determine CWD status in mule deer. Although this was largely the case for young and prime-aged deer, it was not true for older animals. The timing and nature of exposure likely contribute to the age effects we observed. Infection in young deer is in part attributed to a shared neonatal environment with other infected kin (Gear et al., 2010; Cullingham et al., 2011). Deer exhibit extraordinary fidelity to female-structured social groups and home ranges which are established early in life. In turn, deer born into social units with infection may experience repeated exposures early in life (Miller and Conner, 2005). These cumulative exposures likely contributed to the increased deposition of PrP^{Sc} we observed. Adult deer experience similar infection risk each year during the remainder of their life (Miller and Conner, 2005). Adult exposures may result from encountering contaminated environments or unrelated, but infected, deer during courtship and breeding. These exposures likely vary in extent and magnitude. Perhaps, such variation causes the PrP^{Sc} deposition patterns we observed in older deer.

PrP^{Sc} associates with cells of the lymphatic system including follicular dendritic cells, B lymphocytes, and associated macrophages (Sigurdson et al., 2002). Oral exposure to PrP^{Sc} and introduction into the lymphatic tissue of the mouth and esophagus is the likely route of pathogen introduction (Fox et al., 2006). After which, lymphatic cells serve as a vehicle for deposition of PrP^{Sc} in terminal lymphoid follicles of rectal-anal mucosa associated lymphoid tissue (Fox et al., 2006). Declines in immunocompetence with age may hinder proliferation and deposition of PrP^{Sc} in terminal lymphatic tissue, thereby contributing to the PrP^{Sc} patterns we observed. The design of our research precluded us from identifying

the underlying cause of declines of PrP^{Sc} deposition with age. Regardless, our observations suggest slowed CWD progression in older animals.

Every test is not the same and each individual exhibits unique variation. We developed a technique for estimating the state of CWD infection premised on these complications. Disease state becomes a probabilistic statement conditioned on the current test result, previous disease state, and infection and test sensitivity probabilities. Therefore, uncertainty in testing becomes incorporated into the placement of individuals into discrete disease categories. This step forward allows us to make explicit probabilistic statements about whether an individual is infected and the chance that a test result is indeed correct. With CWD, rather than conclude that an individual is infected based on a test result with few follicles or decide that the test was inconclusive, we can now state the probability that an individual is indeed infected. Consequently, we can make statements like "there is a 90% chance that this deer is not infected based on these results."

The model we developed is applicable to other wildlife diseases provided that repeated tests occur. For example, this could include replicate culture plates or serology tests for bacterial microparasite infection, fecal samples for macroparasite infection, or qPCR plates for viral microparasite infection. Furthermore, the infection model we described included two states (susceptible, infected) and a single transition parameter (infection probability). This structure was appropriate for representing CWD. However, our model can be generalized to include additional disease states (exposed, recovered) and transition parameters, such as recovery, recrudescence, and latency.

CHAPTER 5: MOBILITY AND CLAY SOILS UNDERLIE CWD INFECTION IN ADULT FEMALE MULE DEER

Estimation of disease transmission rates is fundamental to understanding host and pathogen dynamics (Anderson et al., 1979; Daszak et al., 2000; McCallum et al., 2001). Accurate estimation of this quantity is essential to evaluating the long term consequence of disease on host populations and implementing meaningful disease containment and eradication efforts (McCallum et al., 2001). Measuring transmission is extremely difficult, because it requires identifying changes in the infection stage of hosts over time. In studying disease in free-ranging wildlife, capture and testing of individuals is inherently difficult and costly, and the information available is often limited to a single test or observation of a sick animal. Furthermore, test results may be imperfect and inaccurate testing results can lead to erroneous inferences about disease (Cooch et al., 2012; LaDeau et al., 2011). The most common type of data collected from disease systems in free-ranging animals is apparent prevalence, defined as the proportion of animals detected in a sample that test positive for disease of interest (Grenfell and Dobson, 1995; Heisey et al., 2006). However, prevalence often provides a less than ideal measure of determining the rate at which animals develop disease (Heisey et al., 2006; Cooch et al., 2012). Estimation from these data is complicated by age and mortality related effects of disease, and inference from apparent prevalence may be strongly influenced by the age-structure of the data sample (Heisey et al., 2006). As a costly and time consuming alternative, infection rate can be explicitly estimated by monitoring the disease status of individual animals over time (Cooch et al., 2012). Such information is obtainable through a capture-mark-recapture study design where the disease status of animals is determined through initial handling and tracked through subsequent handling and testing.

Chronic wasting disease (CWD) of deer (*Odocoileus hemionus*, *Odocoileus virginianus*), elk (*Cervus elaphus*) and moose (*Alces alces*) is a fatal neurodegenerative prion disease that is now found throughout North America (Williams and Young, 1992). CWD has been ob-

served in wild populations in nineteen states and two Canadian provinces and continues to be detected in wild populations across a wider geographic extent (Williams et al., 2002; Miller and Conner, 2005; Saunders et al., 2012a). The long term consequence of CWD on cervid populations is unknown. But, reductions in survival caused by CWD (Miller et al., 2008; Edmunds, 2013) have been implicated in the local decline of mule deer in populations with high disease prevalence. Simulation models predict the potential for population decline and potential extinction (Gross and Miller, 2001; Almberg et al., 2011). Furthermore, management actions have been largely ineffective once disease has established in a population (Conner et al., 2007).

The infectious agent of CWD, PrP^{Sc}, is a malformed variant of host prion protein. PrP^{Sc} appears to replicate by temporarily interacting with normally formed host prion, PrP, to cause mis-folding and new infectious agent (Williams and Young, 1992; Ryou, 2007). Horizontal transmission likely contributes to disease spread (Miller and Williams, 2003) and infectious material can be excreted through feces, saliva, and urine (Mathiason et al., 2006; Tamgüney et al., 2009; Gough and Maddison, 2010; Haley et al., 2011). Indirect transmission through an environmental reservoir plays an important role in infection dynamics (Miller et al., 2004; Mathiason et al., 2009). Direct transmission is also believed to occur (Miller et al., 2000).

Age, population abundance, maternal-relatedness, deer mobility, clay soils, spatial distributions, and variation in the prion precursor gene have been implicated as risk factors for CWD (Miller and Conner, 2005; Farnsworth et al., 2006; Osnas et al., 2009; Gear et al., 2010; Heisey et al., 2010; Cullingham et al., 2011; Walter et al., 2011). To date, findings have been based on inoculation of mice or captive deer with infectious agent or analyses of apparent prevalence. As a result, much remains debated about the factors that contribute to CWD infection in wild deer. To begin clarifying the relative importance of CWD risk factors, we completed a five year capture-mark-recapture study of free-ranging female mule deer in northern Colorado, USA during 2010-14. The same individual deer were captured and

released each winter. Deer were tested for CWD using a live test and fit with a radio collar. We developed a hierarchical Bayesian disease model to portray CWD. Our model treated the true infection status of each individual as a latent (unobserved) variable, which enabled us to estimate infection probability (transitioning from CWD susceptible to infected), effects on infection probability, and allowed for imperfect test detection. Our model is general and our approach can be applied to a variety of wildlife diseases.

Materials and Methods

Data Collection

We completed a capture-mark-recapture study of free-ranging female mule in northern Colorado (Figure 22). Handling and disease testing occurred during January, 2010 - 2014. Two hundred and ten adult (≥ 1.5 years) female mule deer were captured by helicopter net gun. Individual deer were captured between one and five times and never more than once during a single year.

Rectal-anal mucosa associated lymphoid tissue (RMALT) was collected using methods described in detail by Wolfe et al. (2007). CWD status was determined through immunohistochemistry (IHC) staining of RMALT using methods described elsewhere (Wild et al., 2002; Wolfe et al., 2002; Thomsen et al., 2012). Briefly, RMALT was embedded in a paraffin block and a 5 μm tissue section was collected from a depth of approximately 250 μm and mounted onto a glass slide for IHC analysis. When fewer than 10 lymphoid follicles were detected in the first section, a second section was collected from a depth of approximately 350 μm . The second slide enabled us to identify additional lymphoid follicles that were deeper within the biopsy. IHC analyses were completed by the Colorado State University Veterinary Diagnostics Laboratory. We estimated age using tooth wear patterns (Robinette et al., 1957). Genotype of the prion precursor (Prnp) gene was determined using the approach of Jewell et al. (2005).

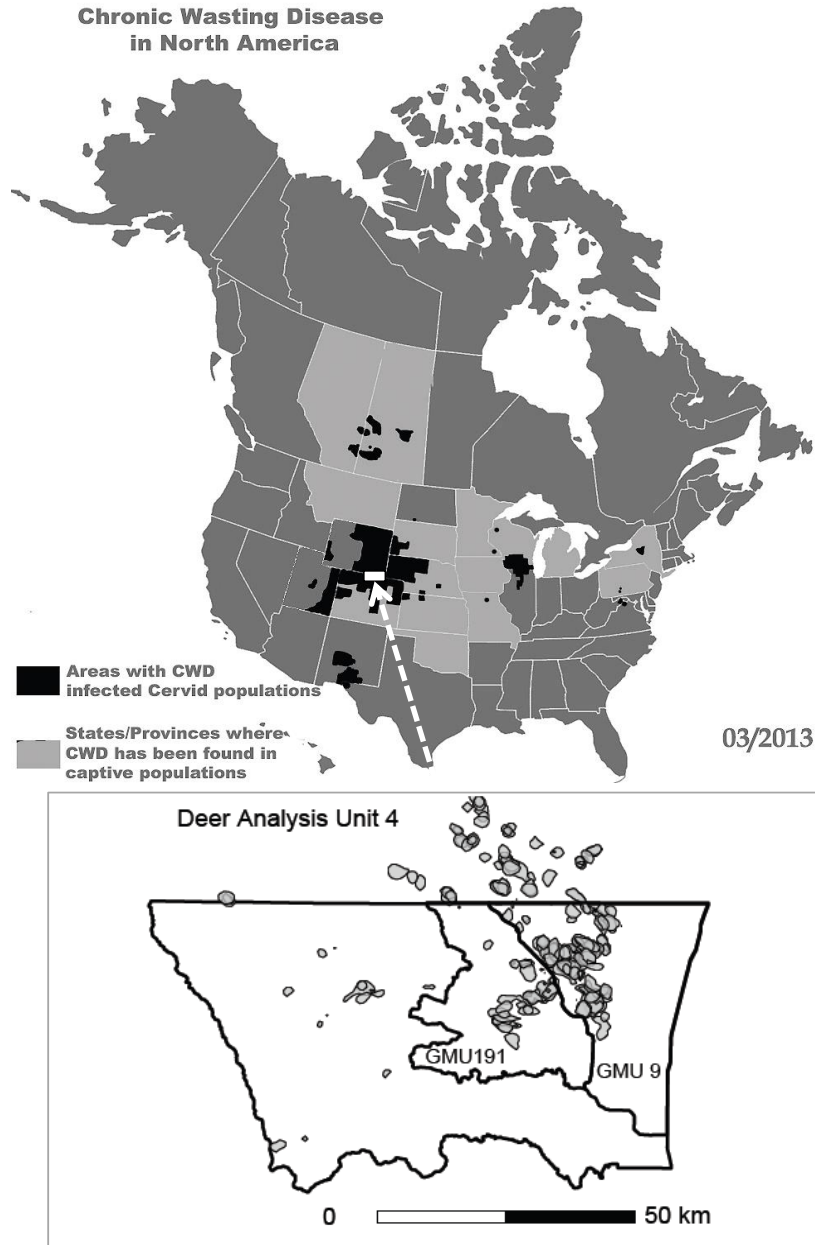


Figure 22: The Red Feather-Poudre River mule deer population is located in the endemic area for CWD. Capture-mark-recapture studies were completed in Colorado Division of Parks and Wildlife Game Management Units (GMU) 9 and 191. Deer Analysis Unit 4 describes the approximate spatial extent of the deer population. Gray polygons show 90% contours of utilization distributions for deer fit with radio collars and GPS devices. The map of CWD in North America was provided by the Chronic Wasting Disease Alliance (www.cwd-info.org).

A set of 105 deer were fit with collars that had an embedded global positioning system (Advanced Telemetry Systems, Isanti, MN). GPS units were programmed to collect one location every 8 hours for one year. The remaining animals were fit with very high frequency radio collars (Advanced Telemetry Systems, Isanti, Minnesota, USA). After release, deer were tracked weekly to determine if they were alive and to identify their approximate location. Deer were located every 2 wk to 2 mo during November - February, 2010-13 using aerial telemetry homing techniques. Deer were again located at least once each year during July and August. All animals were handled in accordance with IACUC protocol 11-2758A, Colorado State University.

Disease Model

The observed data \mathbf{Y} , the number of follicles showing PrP^{Sc}, is assumed to depend on the true infection status \mathbf{Z} . The true infection status \mathbf{Z} is latent and therefore not observed.

We define \mathbf{Z} as an infectious status matrix. Elements of \mathbf{Z} are $z_{i,t} = 0$ indicating no infection for the i^{th} deer at the t^{th} testing occasion, 'year' $i = 1, \dots, I$, $t = 1, \dots, T$, and $z_{i,t} = 1$ when a deer was infected. The model for the initial test, $z_{i,1}$, is described below (equation 5.3). After the initial test, infection status at the current time t is conditioned on infections status at the previous time $t - 1$ where

$$[z_{i,t} | \psi_{i,t}] = \begin{cases} 1 & z_{i,t-1} = 1 \\ \text{Bern}(\psi_{i,t}) & z_{i,t-1} = 0 \end{cases}. \quad (5.1)$$

Infection probability measured over an annual time step is $\psi_{i,t}$ for the i^{th} individual during the t^{th} year. We assumed that infection probability varied among individuals and with time (Figure 23). We used the logistic model to estimate infection probability, where $\text{logit}(\psi_{i,t}) = \mathbf{x}_{i,t}^t \boldsymbol{\beta}$. Here $\mathbf{x}_{i,t}$ is the covariate vector for the i^{th} deer during the t^{th} year and $\boldsymbol{\beta}$ is a vector of logistic model coefficients. Continuous covariates were standardized by subtracting each

value by the mean and dividing the difference by two standard deviations (Gelman, 2008; Schielzeth, 2010). Dividing by two standard deviations, rather than one, allowed direct comparison of coefficient estimates between standardized continuous and unstandardized categorical predictors (Gelman, 2008). Covariates are described in the following subsections.

PrP^{Sc} can be identified using live techniques through biopsy of tonsil or rectal tissue and immunohistochemistry staining (Wild et al., 2002; Wolfe et al., 2002; Schuler et al., 2005; Wolfe et al., 2007; Keane et al., 2009; Spraker et al., 2009). Tissue samples typically contain several lymphoid follicles. However, all lymphoid follicles do not necessarily exhibit PrP^{Sc} presence. We define \mathbf{Y} as an observation matrix, where $y_{i,t}$ represents the observed number of follicles exhibiting PrP^{Sc} from individual i during testing occasion t . We define the corresponding matrix, \mathbf{J} , where $J_{i,t}$ is the total number of follicles obtained for individual i at year t . False positive test results were not believed to occur. Therefore, when $z_{i,t} = 0$ then $y_{i,t} = 0$. However, we may or may not have observed at least one positive follicle when an individual was infected, meaning when $z_{i,t} = 1$ then $y_{i,t} \geq 0$. The probability that an individual follicle is positive is π , and

$$[y_{i,t}|\pi, J_{i,t}] = \begin{cases} 0 & z_{i,t} = 0 \\ \text{Binom}(J_{i,t}, \pi) & z_{i,t} = 1 \end{cases}. \quad (5.2)$$

The infectious status at time 1 depends on the observed infection value, where a false negative is possible. That is,

$$[z_{i,1}|\psi_0, y_{i,1}] = \begin{cases} 1 & y_{i,1} \geq 1 \\ \text{Bern}(\psi_0) & y_{i,1} = 0 \end{cases}, \quad (5.3)$$

where ψ_0 is the probability that an individual developed disease prior to initial testing. We estimated the parameters of our model using the implementation described in Appendix 4. As a note to readers, we chose to report findings on infection probability in a separate manuscript (Chapter4).

Developing Landscape- and Individual- Level Covariates

Disease histories were available from 210 deer, but we chose to fit our model to the subset of 105 animals with GPS devices. This allowed us to include CWD prevalence and percent clay content in areas used by deer as predictors of CWD infection. We began by creating a utilization distribution for each deer. Each utilization distribution was a two dimensional gridded surface of space use generated from a Brownian bridge movement model. The Brownian bridge movement model creates the utilization distribution by estimating the continuous movement path of an individual from successive GPS locations (Horne et al., 2007). Then, we identified the 90% use contour of each utilization distribution as the area commonly used by each deer. Covariate levels for each deer were calculated by averaging spatially explicit covariate values across the 90% use area. Landscape-level covariates were i) CWD prevalence and ii) percent clay content (Figure 23). We also calculated other individual-level covariates, including iii) age, iv) Prnp genotype, v) home range size, and vi) migration behavior.

A. CWD Prevalence and Infection Risk

CWD prevalence varies widely among biologically segregated populations (Miller et al., 2000; Miller and Conner, 2005). Transmission likely occurs within population segments that share wintering areas, because deer aggregate into larger groups, are concentrated into relatively small areas compared to summer, and show strong fidelity to wintering associations (Conner and Miller, 2004). Also, areas with disease likely maintain it over time due to agent persistence in the environment from feces, decaying carcasses, and residue in vegetation and soil (Miller et al., 2004; Miller and Conner, 2005). For these reasons, we believed deer using areas with higher CWD prevalence experienced increased infection risk.

We used a geostatistical model to build a CWD prevalence surface that served as a proxy for the spatial distribution of the magnitude of the CWD epidemic. The complete set of 210 adult female deer were used to generate the prevalence surface. Each deer was assigned a

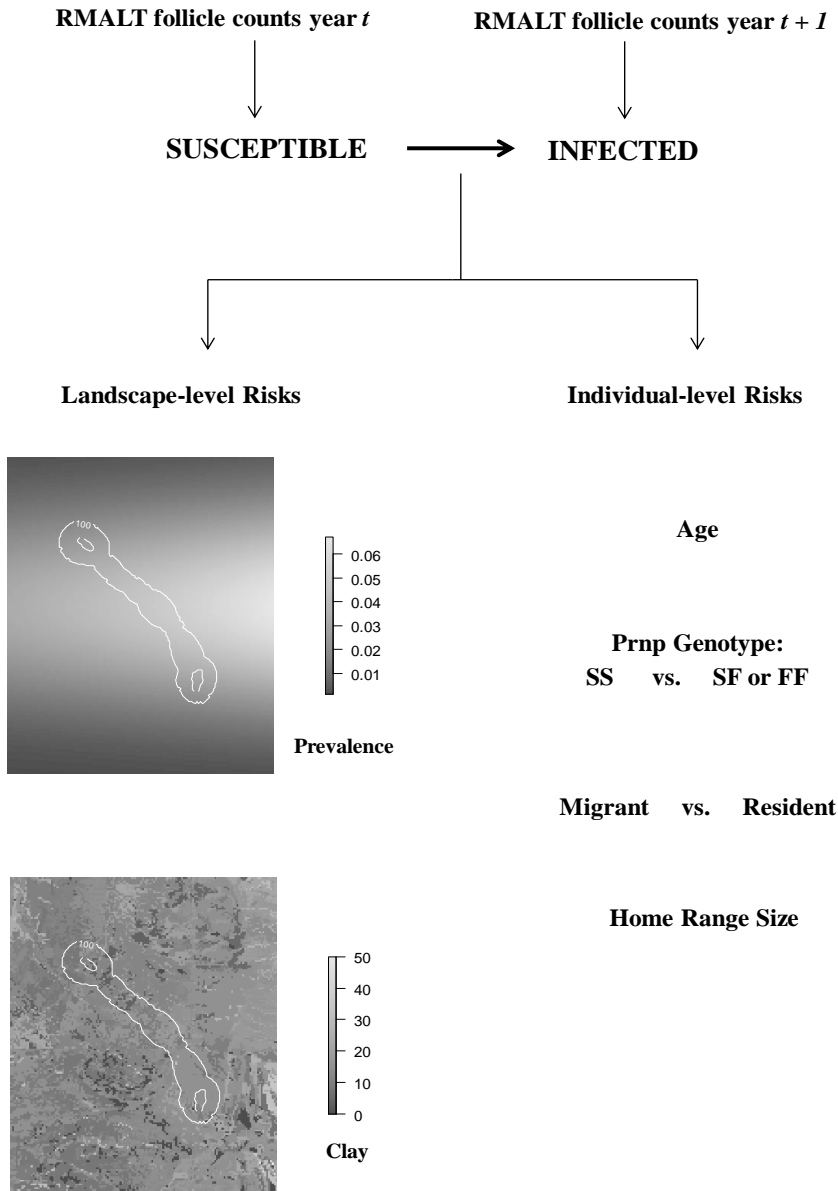


Figure 23: One hundred and five adult female mule deer were captured each year to identify animals that converted from susceptible to infected with CWD. We identified landscape- and individual- level factors contributing to annual infection probability: i) deer utilization distributions were estimated from GPS locations; ii) landscape-level covariate levels were determined by averaging clay and prevalence data across utilization distributions; and iii) other individual-level covariates were measured by identifying age, Prnp genotype, migration status, and home range size.

winter location \mathbf{w}_i and a summer location \mathbf{s}_i that was the median of aerial telemetry locations recorded during each season. Disease status (infected or susceptible) was determined by the first disease test for each deer. Therefore, the disease status of the i^{th} deer during winter $y(\mathbf{w}_i)$ and summer $y(\mathbf{s}_i)$ was the same. Elements of the infection status vector $\mathbf{y} = (y(\mathbf{s}_1), y(\mathbf{w}_1), y(\mathbf{s}_2), y(\mathbf{w}_2), \dots, y(\mathbf{s}_n), y(\mathbf{w}_n))^T$ were $y(\mathbf{w}_i), y(\mathbf{s}_i)=1$ when the i^{th} deer tested CWD positive during the first test and $y(\mathbf{w}_i), y(\mathbf{s}_i)=0$ when the i^{th} deer tested CWD negative. We assumed $y(\mathbf{l}_i)$ followed a Bernoulli distribution with probability $p(\mathbf{l}_i)$. Bernoulli probabilities were related to covariates using the logistic model $\text{logit}(p(\mathbf{l}_i)) = \mathbf{x}_{l_i}\boldsymbol{\zeta}$ where \mathbf{x}_{l_i} are the covariate data for the i^{th} deer and $\boldsymbol{\zeta}$ is a vector of spatial regression coefficients. Locations $y(\mathbf{l}_i)$ were recorded in Universe Transverse Mercator, a projected coordinate system. We included northing as a covariate, because disease flow of CWD into our study area was likely from north to south (Conner and Miller, 2004). A quadratic term was included in representing northing effects. We also included easting as a covariate, because CWD prevalence historically increased from west to east in this area (Farnsworth et al., 2006). Moran's I calculated using Pearson's residuals of our model confirmed that errors were spatially uncorrelated. We generated posterior predictive mean values for each 310×310 m grid cell that overlapped deer utilization distributions. CWD Prevalence values for each deer were the mean of all grid cells within the individual's 90% use contour.

B. Clay Soils and Infection Risk

Inoculation studies in mice have shown that PrP^{Sc} binds to clay minerals and clay-laden whole soils with dramatic increases on infectivity (Johnson et al., 2006b, 2007). Ruminants ingest soil both deliberately and inadvertently during foraging and grooming. PrP^{Sc} proliferated in lymphoid tissue of the mouth, esophagus and gut may bind to ingested soil particles enhancing infectivity within the host. Rumination may extend exposure within the host, as ingested infectious material repeatedly comes into contact with these lymphoid tissues through regurgitation of food (Fox et al., 2006). Furthermore, ruminants rely on mi-

crobes within the rumen for digestion of highly fibrous materials. Bypass protein describes dietary protein that by some means or alteration is resistant to degradation by rumen microbes and is potentially available to the host through digestion in the small intestine (Leng and Nolan, 1984). Small amounts of clay within ruminant diets has been shown to increase bypass protein. Thus, clay soils may also extend exposure within the host by facilitating transport of infectious material to the lower gut where it may come into contact with distal lymphatic tissue. Outside the host, excretion of soil-bound complexes into the environment may provide a reservoir for future infection (Walter et al., 2011). Likely owing to these reasons, a 1% increase in clay sizes particle content in soils of deer home ranges has been related to increases in infection odds of nearly 9% (Walter et al., 2011) in wild mule deer.

Clay-laden soils in our study area were derived from Cretaceous shale and the clay sized particles include high smectite content (Walter et al., 2011). A variety of clay minerals have been shown to adsorb PrP^{Sc} and enhance infectivity (Johnson et al., 2007), including montmorillonite which comprises 26-40% of clay content in our study area (Schmehl and Jackson, 1957). We used a soil data mapping tool to determine the weighted average of percent clay in the surface layer of the Soil Survey Geographic (SSURGO) database. Clay consisted of mineral soil particles that are less than 0.002 millimeter in diameter. The estimated clay content of each soil layer was given as a percentage, by weight, of the soil material that was less than 2 millimeters in diameter. SSURGO data was converted into a 310 × 310 m gridded surface and clay values for each deer were the mean of all grid cells within the individual's 90% use contour.

C. Migration and Infection Risk

Animals that migrate from wintering areas may experience decreased infection rate, because individuals are spending time on areas with comparatively less disease associated residue (Conner and Miller, 2004). Female mule deer were partially migratory. Some individuals moved up to 70 km between wintering areas north of Fort Collins, Colorado into

the headwaters of the Laramie River in southern Wyoming and headwaters of the Poudre River in north-central Colorado. Others remained on wintering areas year-round. Migrations began during late March and early April. Some migrants were located on transitional ranges before being found on final summer ranges in July-August. Most migrants returned to wintering areas between October and November. Earlier studies established that Euclidean distances of ≥ 6 km between seasonal use areas differentiated migratory from resident deer (Conner and Miller, 2004). Utilization distributions were inspected to identify the spatial extent of deer home ranges. We defined migration as a categorical covariate with migrants being deer with 90% use areas that were more than 6 km apart.

We also considered home range size as a predictor of infection probability. Resident deer had smaller home ranges and we believed an inverse relationship between infection probability and home range size. Covariate levels for each deer were the size of 90% use areas.

D. Age and Infection Risk

Infection risk appears to increase in early adulthood resulting in relatively high prevalence in mule deer >2 years of age compared to younger animals (Miller and Conner, 2005). Increases likely result from cumulative exposures early in life combined with slow progression of disease and potential changes in susceptibility with reproductive maturity. After, risk of infection seems to be similar across prime reproductive ages with some decline in senescent individuals (Miller and Conner, 2005). Deer exhibit extraordinary fidelity to female structured social groups and home ranges which are established early in life. There is strong influence of infected female kin on infection risk compared to less-related kin in close geographic proximity (Greear et al., 2010; Cullingham et al., 2011). Also, spatially distant kin show correlated infection risk (Greear et al., 2010). Therefore, age effects on infection may arise from a shared neonatal environment, after which, animals experience similar lifetime risk due to chances of encountering contaminated environments or unrelated deer during

courtship and breeding. For these reasons, we considered age as a continuous covariate and believed infection risk would decline with age.

E. Prnp Genotype and Infection Risk

Disruption of the protein replication process and reduced accumulation of the malformed variant provide a mechanism for disease resistance (Caughey, 2003; Caughey and Baron, 2006). A nucleotide substitution in the 225th codon of mule deer leads to an amino acid change of serine for phenylalanine (Jewell et al., 2005). It is unknown whether this amino acid change disrupts the protein replication process. But, substitution of phenylalanine for serine has been associated with slower disease progression in mule deer (Fox et al., 2006). Similar non-synonymous nucleotide substitutions in white-tailed deer (O'Rourke et al., 2004; Johnson et al., 2006a) and elk (Green et al., 2008) indicate reduced prevalence in individuals exhibiting the rare allele. Therefore, we included genotype as a categorical covariate. Too few deer were detected that were homozygous for phenylalanine and we did not distinguish between heterozygous and homozygous deer.

Model Selection

We thought the strength and direction of covariate effects would depend on the magnitude of the CWD epidemic in areas used by deer. Our modeled disease prevalence surface served as a proxy for the magnitude of the epidemic. We considered ten models. The first five models included the additive effects of prevalence and a single main effect term and included 1) prevalence + clay; 2) prevalence + home range size; 3) prevalence + migration; 4) prevalence + age; and 5) prevalence + Prnp. The remaining five models included the interaction between prevalence and a single main effect term and were 6) prevalence \times clay; 7) prevalence \times home range size; 8) prevalence \times migration; 9) prevalence \times age; and 10) prevalence \times Prnp.

In our hierarchical framework, a logistic model was used to estimate effects on infection probability. Identifying covariate effects is complicated when logistic models contain interac-

tions particularly when interactions are among continuous covariates. However, only a single model with an interaction was supported by our data (see Results). The posterior predictive distribution was used to compare covariate effects (Gelman and Hill, 2007). For models with only additive effects, we estimated posterior predictive distributions of log odds. Odds are defined as the ratio of the probability of success (becoming infected) over the probability of failure (remaining susceptible) (Gelman and Hill, 2007). Models contained more than one covariate and we estimated log odds ratios as the log of ratio of odds when a single predictor variable was varied and the others were held at a certain value. Because log odds ratios also followed a probability distribution, we were able to identify the area of the posterior predictive distribution that was greater than zero. This area indicated the probability, or chance, that a covariate increased CWD infection.

The posterior predictive distribution was also used to compare covariate effects for models with interactions between continuous covariates. We generated posterior predictive distributions of annual infection probability by holding a single predictor at a fixed value and varying the other.

We used the Deviance Information Criterion (DIC) to select among models. Due to the missing data structure, we used a modified form of the DIC statistic, DIC_4 , introduced by Celeux et al. (2006). Let $\theta = (\psi_0, \psi, \pi)$ be the vector of unknown parameters. Then formula for DIC_4 for the model proposed above is given by

$$DIC_4 = -4E_{\theta, \mathbf{Z}} (\log[\mathbf{Y}, \mathbf{Z}|\theta]|\mathbf{Y}) + 2E_{\mathbf{Z}} (\log [\mathbf{Y}, \mathbf{Z}|E_{\theta}(\theta|\mathbf{Y}, \mathbf{Z})]|\mathbf{Y})$$

The above equation can be estimated using MCMC for B iterations after burn-in. The first term is approximated by

$$E_{\theta, \mathbf{Z}} \left(\log [\mathbf{Y}, \mathbf{Z} | \theta] \mid \mathbf{Y} \right) \approx \frac{1}{B} \sum_{b=1}^B \sum_{i=1}^m z_{i,1}^{(b)} \log ([y_{i,1} | \pi^{(b)}]) + \log \left([z_{i,1}^{(b)} | \psi_0^{(b)}] \right) + \frac{1}{B} \sum_{t=2}^T \sum_{i=1}^m \left\{ \left(z_{i,t}^{(b)} \right) V_{i,t} \log [y_{i,t} | \pi^{(b)}] + \left((1 - z_{i,t-1}^{(b)}) U_{i,t} \right) \log [z_{i,t}^{(b)} | \boldsymbol{\beta}^{(b)}] \right\},$$

where $z_{i,1}^{(b)}$ denotes the value of $z_{i,1}$ at the b th MCMC iteration and the other parameters are defined similarly. The second term is given by

$$E_{\mathbf{Z}} \left(\log [\mathbf{Y}, \mathbf{Z} | E_{\theta}(\theta | \mathbf{Y}, \mathbf{Z})] \mid \mathbf{Y} \right) \approx \sum_{i=1}^m \hat{z}_{i,1} \log ([y_{i,1} | \hat{\pi}]) + \log \left([\hat{z}_{i,1} | \hat{\psi}_0] \right) + \sum_{t=2}^T \sum_{i=1}^m \left\{ \left(\hat{z}_{i,t} \right) V_{i,t} \log [y_{i,t} | \hat{\pi}] + \left((1 - \hat{z}_{i,t-1}) U_{i,t} \right) \log [\hat{z}_{i,t} | \hat{\boldsymbol{\beta}}] \right\}$$

where $\hat{\pi}$ is the posterior estimate of π , i.e., $\hat{\pi} = (1/B) \sum_{b=1}^B \pi^{(b)}$ and the parameters $\boldsymbol{\beta}$ and ψ_0 are estimated similarly. For all $\hat{z}_{i,t}$ quantities, estimation is based on the mode of the posterior distribution. For example, $\hat{z}_{i,1} = \text{mode of } \left\{ \hat{z}_{i,1}^{(1)}, \dots, \hat{z}_{i,1}^{(B)} \right\}$. This allows the \hat{z} values to be equal to 0 or 1.

Results

We monitored CWD infection of 95 female deer with individuals studied for up to four years. Observations totaled 322 animal years. Two hundred eighty-four disease tests were completed on these deer. Ten deer (9.5%) were observed infected with CWD by the end of our research. One deer was infected when first tested and nine deer became infected during the study. Deer that developed infection were concentrated in the central regions of the

wintering area (Figure 27). All but a single infected deer migrated to summering areas in southern Wyoming (Figures 25 - 28). The resident animal remained on the central portions of the wintering area year round.

The model representing the effects of the interaction between clay and prevalence on infection probability was most supported by our data (Table 7). DIC_4 for this model was nearly three units lower than any other model. DIC_4 and posterior distributions of the interaction term in all remaining models (Tables 8 and 9) suggested that additive models were more appropriate for representing age, Prnp, migration, and home range size effects. Therefore, we do not discuss these interaction models further. Models portraying effects of deer mobility on infection probability were also supported by our data. There was noticeably less support for models including age or Prnp genotype.

Table 7: Deviance information criteria (DIC_4) for disease models fit to capture-mark-recapture data on adult female mule deer. Models varied in their representation of annual infection probability.

Model	DIC_4	ΔDIC_4
prevalence \times clay	317.0	0.0
prevalence + home range size	319.7	2.7
prevalence \times home range size	319.8	2.8
prevalence + migration	319.8	2.8
prevalence + Prnp	322.8	5.8
prevalence \times migration	322.9	5.9
prevalence + clay	323.7	6.7
prevalence \times age	325.2	8.2
prevalence + age	325.4	8.4
prevalence \times Prnp	326.3	9.3

Table 8: Posterior distributions of logistic model parameters of annual infection probability. Capture-mark-recapture data were fit to hierarchical disease models that included the additive effects of CWD prevalence, and clay content, age, migration, or Prnp genotype effects.

Model	Parameter Description	Parameter	Mean	Standard Deviation
prevalence + clay	intercept	β_0	-3.36	0.40
	prevalence	β_1	1.07	0.76
	clay	β_2	0.30	0.63
prevalence + home range size	intercept	β_0	-3.64	0.47
	prevalence	β_1	1.09	0.70
	home range size	β_2	-2.17	1.14
prevalence + migration	intercept	β_0	-2.53	0.65
	prevalence	β_1	1.52	0.70
	migration	β_2	-1.20	0.80
prevalence + age	intercept	β_0	-3.39	0.41
	prevalence	β_1	1.21	0.74
	age	β_2	-0.33	1.05
prevalence + Prnp	intercept	β_0	-3.00	0.44
	prevalence	β_1	1.06	0.74
	Prnp	β_2	-1.74	1.20

Table 9: Posterior distributions of logistic model parameters of annual infection probability. Capture-mark-recapture data were fit to hierarchical disease models that included the interaction between CWD prevalence, and clay content, age, migration, or Prnp genotype effects.

Model	Parameter Description	Parameter	Mean	Standard Deviation
prevalence \times clay	intercept	β_0	-3.64	0.48
	prevalence	β_1	1.96	0.93
	clay	β_2	1.24	0.89
	prevalence \times clay	β_3	-2.43	1.47
prevalence \times home range size	intercept	β_0	-3.68	0.48
	prevalence	β_1	1.01	0.89
	home range size	β_2	-2.21	1.22
	prevalence \times home range size	β_3	-0.33	1.83
prevalence \times migration	intercept	β_0	-2.66	0.68
	prevalence	β_1	0.82	0.98
	migration	β_2	-1.51	0.96
	prevalence \times migration	β_3	1.71	1.51
prevalence \times age	intercept	β_0	-3.45	0.42
	prevalence	β_1	1.25	0.75
	age	β_2	-0.28	1.14
	prevalence \times age	β_3	-0.23	1.94
prevalence \times Prnp	intercept	β_0	-3.01	0.44
	prevalence	β_1	1.03	0.79
	Prnp	β_2	-2.12	1.39
	prevalence \times Prnp	β_3	0.61	2.18

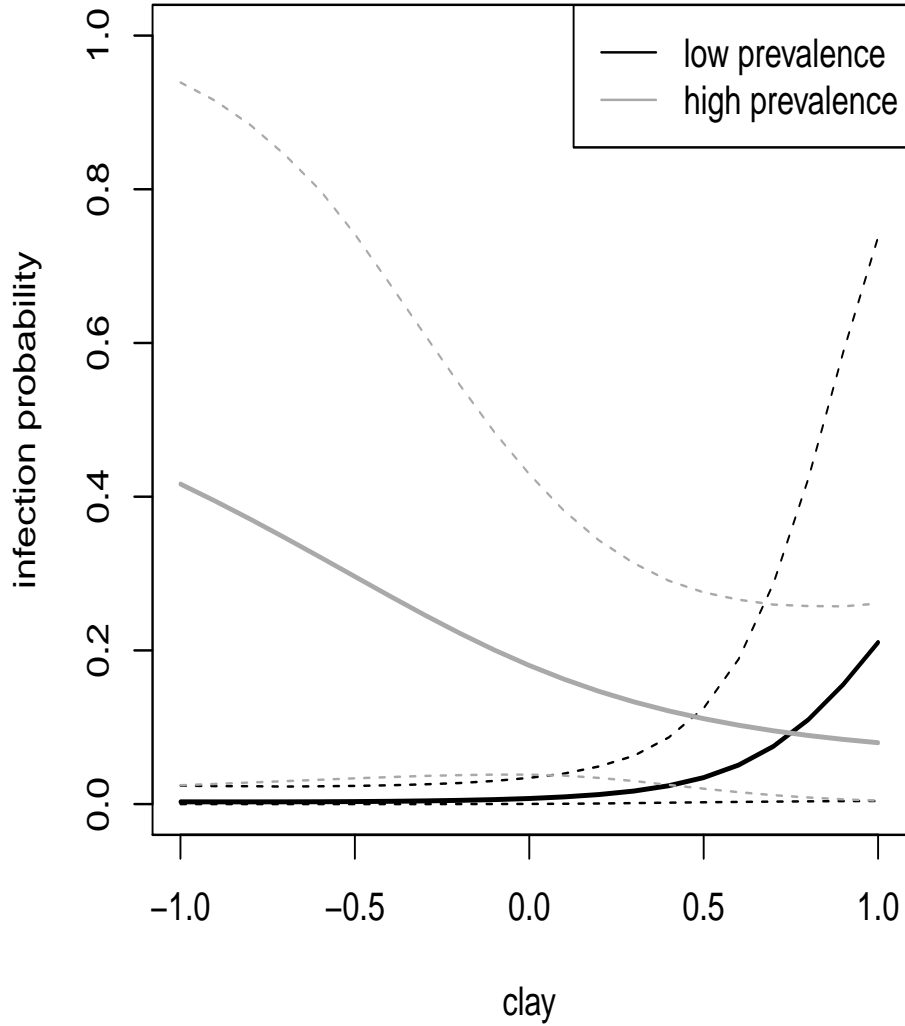


Figure 24: Posterior predictive means (emphasized) and 95% quantiles of infection probability generated for clay values ranging from one standardized unit below average to one standardized unit above average. The black lines show posterior predictions when CWD prevalence is one standardized unit below average and the gray lines show posterior predictions when CWD prevalence is one standardized unit above average.

Clay effects on infection probability varied with disease prevalence (Figure 24). Enhancing effects of clay on infection probability were stronger for deer using areas with lower prevalence. As prevalence increased, enhancing effects of clay lessened. Percent clay content averaged across 90% deer utilization distributions ranged from 10.1% to 20.2%. Clay values were standardized and a value one standardized unit above average equated to 15.7% and a value one standardized unit below average was 12.2%. Small differences in clay content existed among deer, yet, these differences resulted in important effects on infection probability. Clay increased infection probability when deer used areas with low CWD prevalence, which we defined as 1% (one standardized unit below average prevalence; Figure 24 and Table 9). The mean posterior predictive log odds ratio of infection under low prevalence was 3.68 (SD = 2.12) and we found 96% probability that increases in clay resulted in higher infection probability. However, the mean posterior predictive log odds ratio of infection under high prevalence (5%; one standardized unit above average prevalence) was -1.19 (SD = 1.18) and there was only 15% probability that increases in clay resulted in higher infection probability (Figure 29).

Migration reduced infection probability. Seventy-seven deer were categorized as migrants and eighteen deer were resident on wintering areas year round. The mean posterior predictive log odds ratio of migration was -1.20 (SD = 0.80). This equated to 94% probability that migration lowered infection probability. Furthermore, migration effects were unrelated to CWD prevalence in areas used by deer (Table 9). We considered home range size as an alternate measure of deer mobility. Because home range size was calculated as the extent of 90% use areas, smaller home range sizes did not necessarily indicate resident deer. But, home range size of resident deer (mean = 726 km², sd = 432) was smaller (Two sample T-test, p-value = 0.04) than migrants (mean = 947 km², sd = 435). Overall, home range sizes varied from 192 km² to 3391 km². The mean posterior predictive log odds ratio of home range size was -2.18 (SD = 1.14) which meant a decrease in one standardized unit of home range size equated to 98% probability of an increase in annual infection probability.

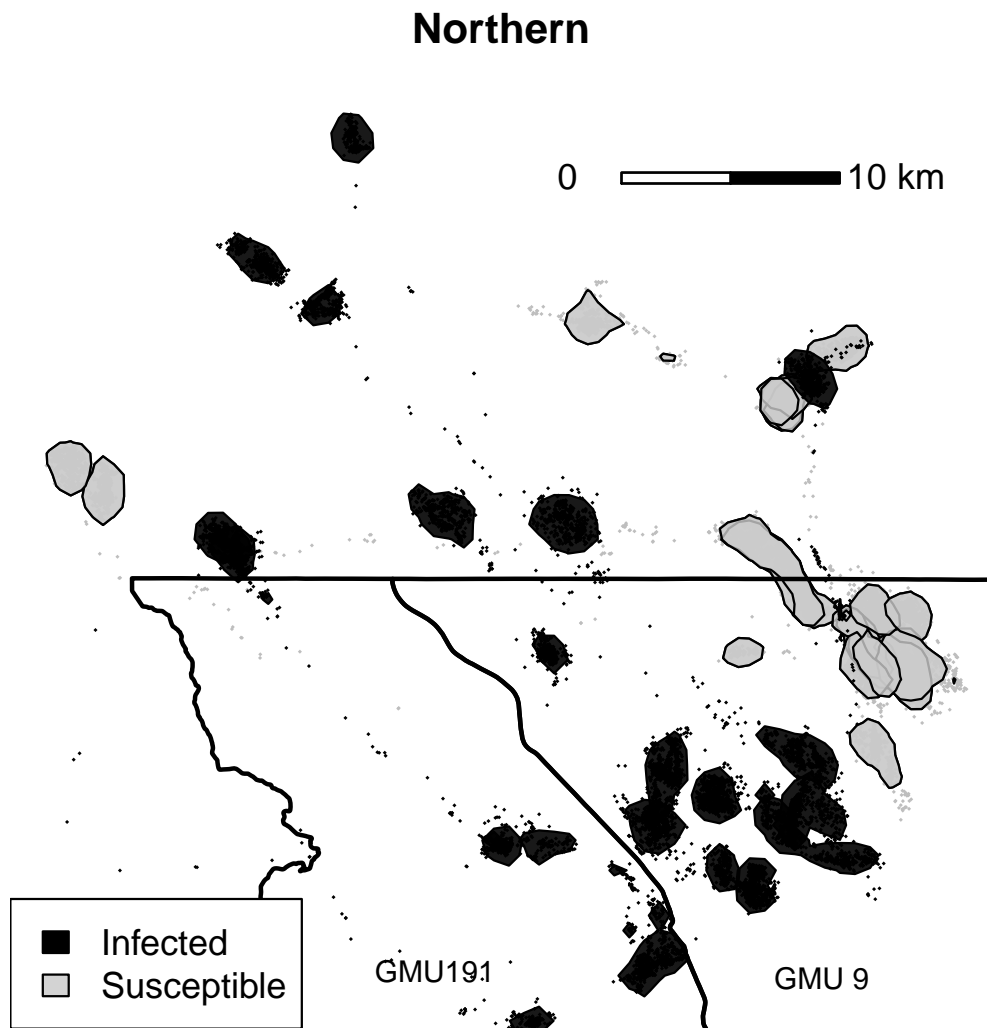


Figure 25: Ninety percent use areas of adult female mule deer that were susceptible throughout or developed CWD during January 2010-14. Contours were derived from Brownian bridge movement models fit to GPS histories. Individual dots show GPS locations outside 90% use areas and indicate approximate migration paths. Use areas and migration routes are displayed for deer that developed CWD or concentrated in northern portions of the wintering area.

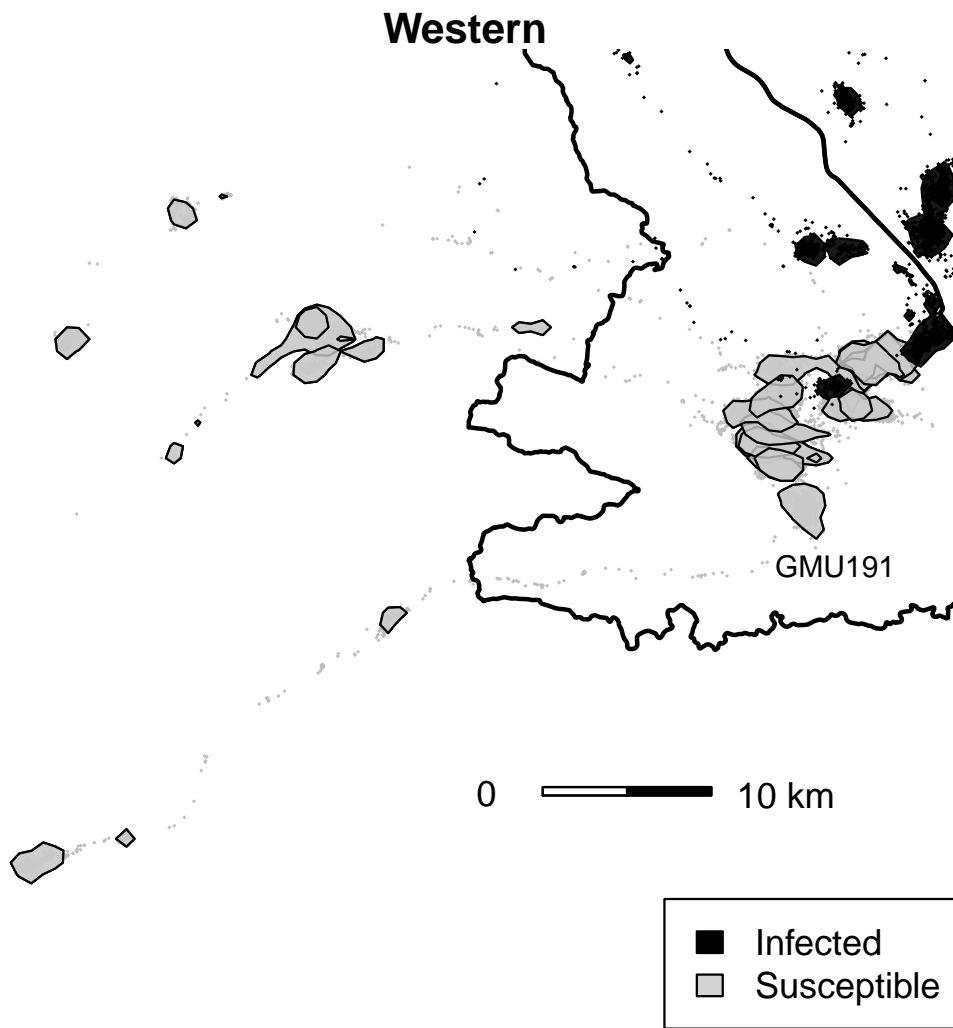


Figure 26: Ninety percent use areas of adult female mule deer that were susceptible throughout or developed CWD during January 2010-14. Contours were derived from Brownian bridge movement models fit to GPS histories. Individual dots show GPS locations outside 90% use areas and indicate approximate migration paths. Use areas and migration routes are displayed for deer that developed CWD or concentrated in western portions of the wintering area.

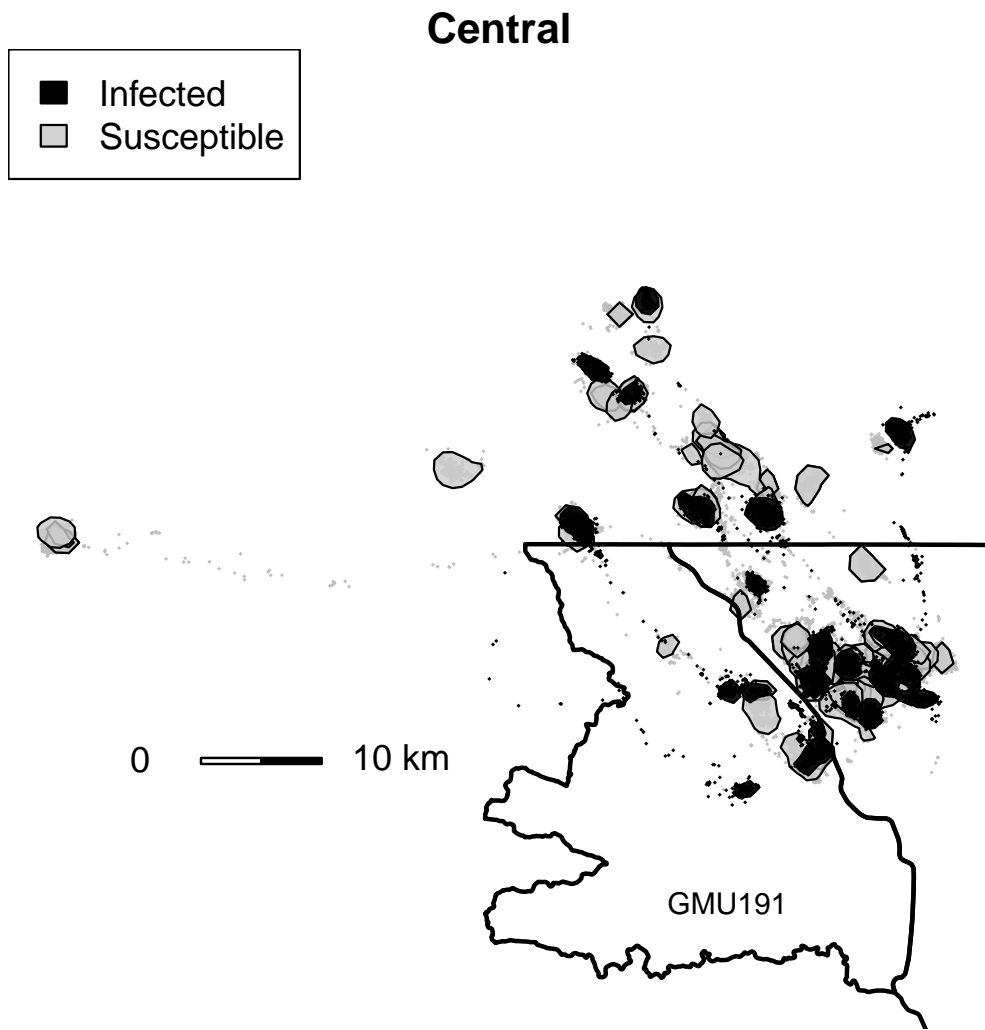


Figure 27: Ninety percent use areas of adult female mule deer that were susceptible throughout or developed CWD during January 2010-14. Contours were derived from Brownian bridge movement models fit to GPS histories. Individual dots show GPS locations outside 90% use areas and indicate approximate migration paths. Use areas and migration routes are displayed for deer that developed CWD or concentrated in central portions of the wintering area.

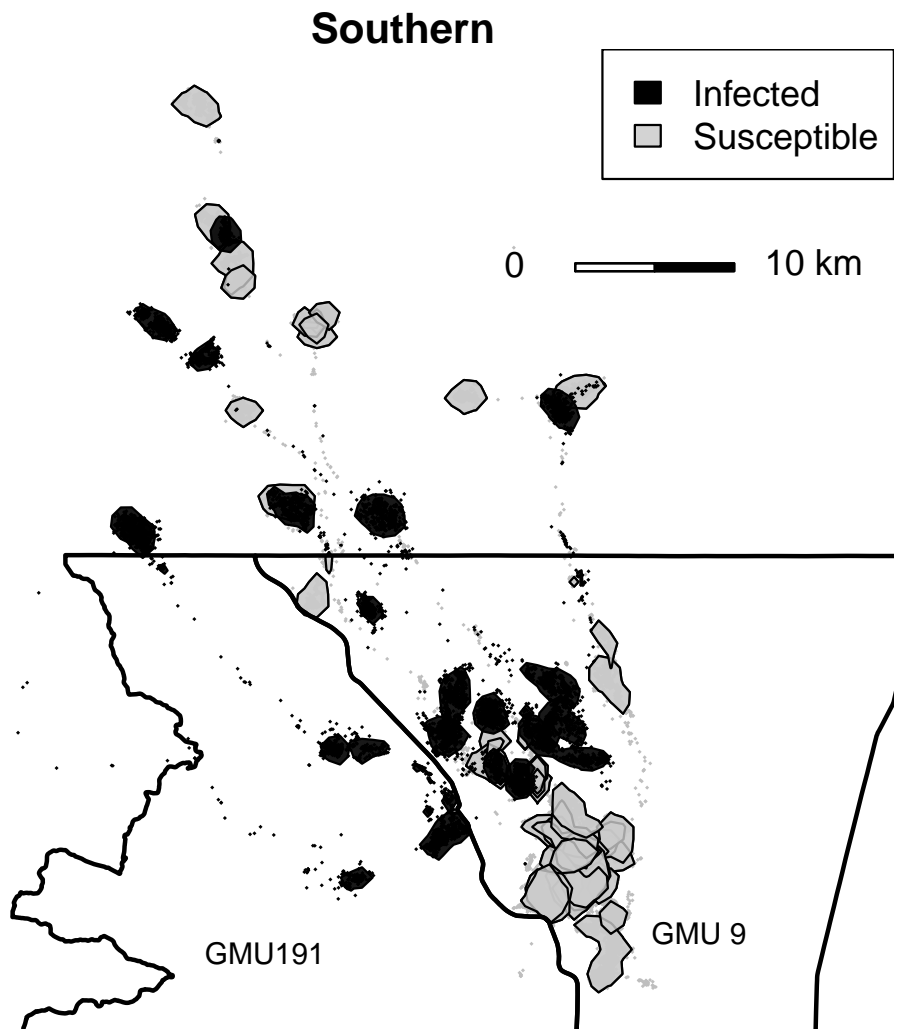


Figure 28: Ninety percent use areas of adult female mule deer that were susceptible throughout or developed CWD during January 2010-14. Contours were derived from Brownian bridge movement models fit to GPS histories. Individual dots show GPS locations outside 90% use areas and indicate approximate migration paths. Use areas and migration routes are displayed for deer that developed CWD or concentrated in southern portions of the wintering area.

Utilization distributions showed that deer segregated into four spatially segregated population segments on the wintering area (Figure 25 - 28). However, some deer from wintering population segments overlapped use areas during migration.

Deer expressing phenylalanine experienced lower infection probability. We tracked the disease status of 68 deer that were homozygous for serine, 35 heterozygous for serine and phenylalanine, and 2 homozygous for phenylalanine. A single heterozygous deer was observed becoming infected and the remaining eight converting deer were homozygous for serine. We found 95% probability that deer expressing phenylalanine experienced lower infection probability and effects did not vary with CWD prevalence in areas used by deer. The mean posterior predictive log odds ratio of phenylalanine was -1.74 (SD = 1.20).

Deer developed CWD between 1.5 and 8.5 years old. Deer younger than one year of age were not tested for CWD. The posterior predictive log odds ratio of age broadly spanned zero (mean = -0.33; SD = 1.05), which equated to 62% probability that age lowered infection risk. Similarly, there was 48% probability that age increased infection risk. Our findings suggest infection probability is relatively constant among adult aged deer.

Discussion

Soil characteristics have been linked to patterns of prion disease occurrence at broad geographical scales (Walter et al., 2011). Whether soils play an important role in facilitating indirect transmission of CWD remains an unresolved issue (Imrie et al., 2009; Saunders et al., 2012b; Storm et al., 2013). Evaluation of fine-scale data can reveal the importance of soils in CWD transmission.

Previous research on mule and white-tailed deer related spatially referenced disease tests of deer harvested by hunters or sharp shooters to soil attributes. We built on these studies by tracking individual adult female deer both before and after CWD exposure and collecting detailed mobility data using global positioning devices. We demonstrated that a meaningful

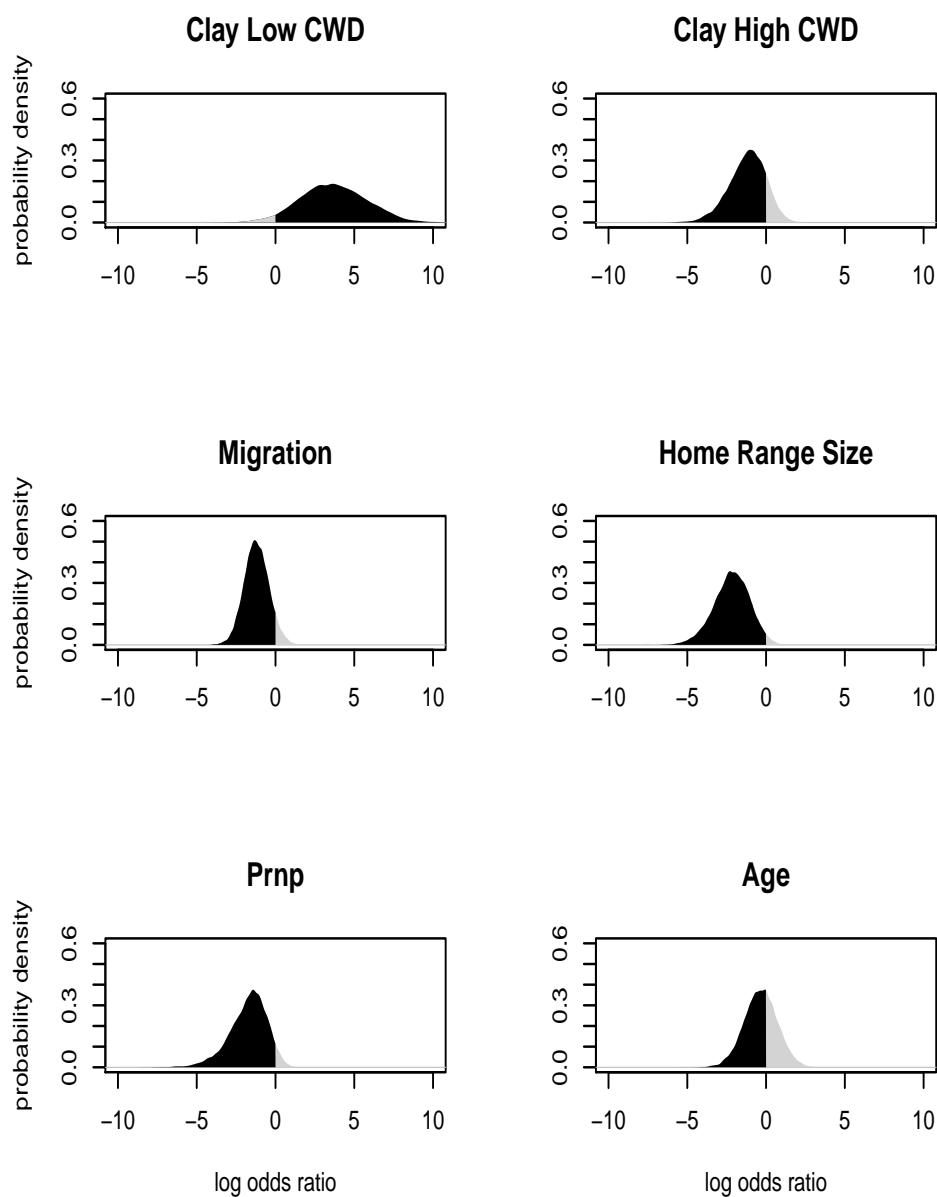


Figure 29: Posterior predictive log odds ratios for models showing the direction and relative magnitude of covariate effects of clay (top row), migration and home range size (middle row), and Prnp and age (bottom row). Regions shaded in black show the probability that the covariate increased or lowered infection probability.

index (percent clay) shown to experimentally enhance oral prion transmission experimentally in mice has an important effect on infection probability. When prevalence in areas used by deer was near 1%, we found that increases in clay content from 12 to 16% increased infection odds by nearly 45%. However, as CWD prevalence increased in areas, the enhancing effect of clay declined, such that increases in clay soils were more likely associated with declines in infection probability. Our findings provide evidence that clay soils may be a particularly important component of the transmission process during the early and late stages of epidemics. When prevalence is low, such as during the early stages of an epidemic, clays provide a means for increasing infection risk by enhancing infectivity. As CWD prevalence increases, infection spreads throughout entire wintering areas leading to more uniform distribution of infected hosts (Figure 27). As a result, all deer within the wintering area experience increased infection probability regardless of fine scale changes in clay soils.

An increasing number of studies have concluded that silent and non-synonymous nucleotide substitutions in white tailed deer (O'Rourke et al., 2004; Johnson et al., 2006a; Kelly et al., 2008; Blanchong et al., 2009; Wilson et al., 2009), elk (Green et al., 2008), and mule deer (Jewell et al., 2005; Wilson et al., 2009) correlate reduced prevalence in individuals expressing the rare allele. Current evidence is based on hunter or sharp shooter harvested deer and these findings could be confounded by allele-specific differences in survival of susceptible and infected individuals and familial associations. Inoculation studies have shown that deer expressing the rare allele uniformly develop disease (Jewell et al., 2005; Fox et al., 2006; Johnson et al., 2011). Therefore, the contribution of polymorphism of the Prnp gene to infection risk remains an unanswered question.

Our capture-mark-recapture study design controls for some of these confounding sources. We showed that deer expressing phenylalanine experience lower annual infection probability. PrP^{Sc}, the infectious agent of CWD, replicates through the protein only hypothesis. PrP^{Sc} temporarily interacts with normally formed host prion, PrP, to cause mis-folding and new infectious agent (Williams and Young, 1992; Ryou, 2007). This change is thought to be a two

step process of aggregation and temporary binding (Ryou, 2007) followed by conversion to the malformed variant (Cohen and Prusiner, 1998; Prusiner, 1998). Amino acid substitutions that contribute to the efficiency of the aggregation step provide a plausible mechanism for changes in host susceptibility. Alternatively, our findings may in part be due to the methods of CWD testing. There is evidence that deer expressing phenylalanine fail to exhibit IMH staining with infection (Wolfe *in preparation*).

CWD has existed in wild deer in our study area for at least four decades (Spraker et al., 1997; Miller et al., 2000). However, the spatial distribution of new infections appeared to be a localized phenomenon. Deer that became infected spent winter concentrated in the central portion of the wintering area (Figure 25). Otherwise, wintering contours of deer using the northern (Figure 25), western (Figure 26), and southern (Figure 28) portions of the wintering area overlapped only a single deer that became infected. Deer show extraordinary fidelity to female structured social groups and home ranges that are established early in life (Garrott et al., 1987). These movement tendencies appear to provide some natural containment of the CWD epidemic. Even though deer were concentrated during winter, individuals in relatively close proximity, such as deer found within a single hunting district or game management unit, did not use shared areas. Consequently, infection remained in a relative 'hot spot' in the central portion of the entire wintering area (Figure 27). Furthermore, spatial structuring of disease did not appear to be a phenomenon limited to the timespan of our research. CWD prevalence was previously estimated using disease tests of hunter harvested or culled deer during 1997-2003 (Farnsworth et al., 2006; Conner et al., 2007). Historic prevalence (Farnsworth et al., 2006) resembled the prevalence surface we developed as part of our research (Figure 30).

Migration was a plausible mechanism of disease spread. Migratory deer from the northern, western, and southern portions of the wintering area shared migration routes, stop-over sites, and summering areas with infected deer. A single individual became infected that wintered outside of the central portions of the wintering area (Figure 26). This deer shared

CWD Prevalence

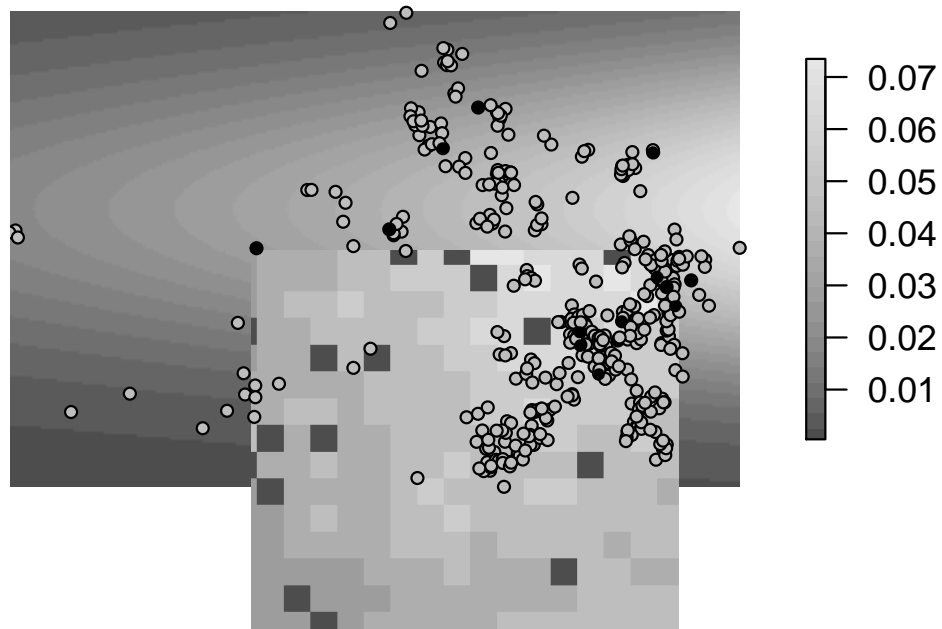


Figure 30: The bottom layer are posterior predictive mean values of CWD prevalence in adult female mule deer generated using a geostatistical model fit to the disease tests on 210 adult female. Black circles show infected and gray circles show susceptible deer. There are two locations for each individual, a winter and summer. A gridded CWD prevalence surface developed by (Farnsworth et al., 2006) fit to disease tests from hunter harvested or culled deer during 1997-2003 is overlaid to show consistency in prevalence over time.

a summering area with other deer that developed infection and spent winters in the relative 'hot spot' for disease. Pathogens that are highly virulent threaten their own existence through demise of the host and reductions in transmission opportunities. In turn, highly virulent pathogens have developed strategies to persist, such as remaining infectious in a free-stage in the environment and delaying progression of the pathological effects of disease (Ewald, 1994). Host migration serves as an eloquent mechanism of the spread of CWD. Delays in the onset of clinical effects of CWD allow newly infected individuals to spread infectious agent to new areas. Once there, PrP^{Sc} has the ability to remain in the environment for years.

The spatial structuring we observed among deer suggests that CWD epidemics may best be conceptualized as several, largely independent epidemics that are occurring simultaneously. Our findings suggest a continuing epidemic in the central portions of the deer wintering area that is at a different point in the epidemic wave compared to nearby areas. We are left to reconcile why. Some have theorized that CWD epidemics cannot establish when host populations are below critical densities (Sharp and Pastor, 2011) and deer densities are highest in the central portions of the study area (Vieira, 2006). Deer from the central area share migration routes and summering areas with some individuals from the other wintering areas. Therefore, it is likely that diseased deer from the central area have come into contact with deer from adjoining wintering areas during summer. Deer densities in the alternative areas may be below levels necessary to allow for epidemic dynamics. Particularly, deer occupying western areas use state lands that allow hunting and deer densities are lowest there (Vieira, 2006).

Furthermore, clay soils in areas used by deer from the central portions of the wintering area averaged higher than areas used by deer from any of the remaining areas. These soil attributes may have promoted earlier establishment, proliferation, or maintenance of the epidemic.

Our findings were also limited to adult female mule deer. CWD prevalence is approximately twice as high in male deer (Miller and Conner, 2005). Male deer are believed to use larger areas during breeding when searching and competing for mates. Male deer densities are highest in the central portions of the wintering area, because these areas are largely protected from sport hunting practices. Consequently, males may play an important role in CWD transmission, which was hidden from our research.

LITERATURE CITED

- Adams, M. J., N. D. Chelgren, D. Reinitz, R. A. Cole, L. J. Rachowicz, S. Galvan, B. McCreary, C. A. Pearl, L. L. Bailey, J. Battaso, E. L. Bull, and M. Leu, 2010. Using occupancy models to understand the distribution of an amphibian pathogen, *Batrachochytrium dendrobatidis*. *Ecological Applications* **20**:289–302.
- Albon, S. and R. Langvatn, 1992. Plant phenology and the benefits of migration in a temperate ungulate. *Oikos* **65**:502–513.
- Almberg, E. S., P. C. Cross, C. J. Johnson, D. M. Heisey, and B. J. Richards, 2011. Modeling routes of chronic wasting disease transmission: environmental prion persistence promotes deer population decline and extinction. *PloS one* **6**:e19896.
- Anderson, R. M., R. M. May, et al., 1979. Population biology of infectious diseases: part i. *Nature* **280**:361–367.
- Bailey, D., J. Gross, E. Laca, L. Rittenhouse, M. Coughenour, D. Swift, and P. Sims, 1996. Mechanisms that result in large herbivore grazing distribution patterns. *Journal of Range Management* **49**:386–400.
- Ball, J., C. Nordengren, and K. Wallin, 2001. Partial migration by large ungulates: characteristics of seasonal moose *Alces alces* ranges in northern Sweden. *Wildlife Biology* **7**:39–47.
- Bartlam-Brooks, H. L. A., M. C. Bonyongo, and S. Harris, 2011. Will reconnecting ecosystems allow long-distance mammal migrations to resume? A case study of a zebra *Equus burchelli* migration in Botswana. *Oryx* **45**:210–216.

- Berger, J., 2004. The last mile: how to sustain long-distance migration in mammals. *Conservation Biology* **18**:320–331.
- Berliner, L., 1996. Hierarchical Bayesian time series models. In Hanson, KM and Silver, RN, editor, *Maximum entropy and Bayesian methods*, volume 79 of *Fundamental theories of physics*, pages 15–22. Los Alamos Natl Lab, Ctr Nonlinear Studies; Los Alamos Natl Lab, Radiog Diagnost Program; Santa Fe Inst. 15th International Workshop on Maximum Entropy and Bayesian Methods, ST JOHNS COLL, SANTA FE, NM, JUL 31-AUG 04, 1995.
- Blanchong, J. A., D. M. Heisey, K. T. Scribner, S. V. Libants, C. Johnson, J. M. Aiken, J. A. Langenberg, and M. D. Samuel, 2009. Genetic susceptibility to chronic wasting disease in free-ranging white-tailed deer: complement component c1q and prnp polymorphisms. *Infection, Genetics and Evolution* **9**:1329–1335.
- Bruggeman, J. E., P. J. White, R. A. Garrott, and F. G. R. Watson, 2009. The ecology of large mammals in central Yellowstones sixteen years of integrated field studies, chapter 12: Partial migration in central Yellowstone bison, pages 217–235. Academic Press.
- Bruno, J. F., L. E. Petes, C. Drew Harvell, and A. Hettinger, 2003. Nutrient enrichment can increase the severity of coral diseases. *Ecology Letters* **6**:1056–1061.
- Caswell, H., 2001. Matrix population models construction, analysis, and interpretation. Sinauer Associates Inc. Publishers.
- Caughey, B., 2003. Prion protein conversions: insight into mechanisms, tse transmission barriers and strains. *British Medical Bulletin* **66**:109–120.
- Caughey, B. and G. S. Baron, 2006. Prions and their partners in crime. *Nature* **443**:803–810.
- Celeux, G., F. Forbes, C. P. Robert, D. M. Titterington, et al., 2006. Deviance information criteria for missing data models. *Bayesian Analysis* **1**:651–673.

- Clark, J. S., 2007. Models for ecological data an introduction. Princeton University Press.
- Cohen, F. E. and S. B. Prusiner, 1998. Pathologic conformations of prion proteins. *Annual Review of Biochemistry* **67**:793–819.
- Conner, M. M. and M. W. Miller, 2004. Movement patterns and spatial epidemiology of a prion disease in mule deer population units. *Ecological Applications* **14**:1870–1881.
- Conner, M. M., M. W. Miller, M. R. Ebinger, and K. P. Burnham, 2007. A meta-bac approach for evaluating management intervention on chronic wasting disease in mule deer. *Ecological Applications* **17**:140–153.
- Cooch, E. G., P. B. Conn, S. P. Ellner, A. P. Dobson, and K. H. Pollock, 2012. Disease dynamics in wild populations: modeling and estimation: a review. *Journal of Ornithology* **152**:485–509.
- Crabtree, R., C. Potter, R. Mullen, J. Sheldon, S. Huang, J. Harmsen, A. Rodman, and C. Jean, 2009. A modeling and spatio-temporal analysis framework for monitoring environmental change using NPP as an ecosystem indicator. *Remote Sensing of the Environment* **113**:1486–1496.
- Cullingham, C. I., E. H. Merrill, M. J. Pybus, T. K. Bollinger, G. A. Wilson, and D. W. Coltman, 2011. Broad and fine-scale genetic analysis of white-tailed deer populations: estimating the relative risk of chronic wasting disease spread. *Evolutionary Applications* **4**:116–131.
- Daszak, P., A. A. Cunningham, and A. D. Hyatt, 2000. Emerging infectious diseases of wildlife—threats to biodiversity and human health. *Science* **287**:443–449.
- Daszak, P., A. A. Cunningham, and A. D. Hyatt, 2003. Infectious disease and amphibian population declines. *Diversity and Distributions* **9**:141–150.

- DeCesare, N., M. Hebblewhite, H. Robinson, and M. Musiani, 2010. Endangered, apparently: the role of apparent competition in endangered species conservation. *Animal Conservation* **13**:353–362.
- D'Eon, R. and R. Serrouya, 2005. Mule deer seasonal movements and multiscale resource selection using global positioning system radiotelemetry. *Journal of Mammology* **86**:736–744.
- Dobson, A. and J. Foufopoulos, 2001. Emerging infectious pathogens of wildlife. *Philosophical Transactions of the Royal Society of London Series B-Biological Sciences* **356**:1001–1012.
- Doerr, J., E. DeGayner, and G. Ith, 2005. Winter habitat selection by Sitka black-tailed deer. *Journal of Wildlife Management* **69**:322–331.
- Dulberger, J., N. T. Hobbs, H. M. Swanson, C. J. Bishop, and M. W. Miller, 2010. Estimating chronic wasting disease effects on mule deer recruitment and population growth. *Journal of Wildlife Diseases* **46**:1086–1095.
- Edmunds, D. R., 2013. Chronic wasting disease ecology and epidemiology of white-tailed deer in Wyoming. Ph.D. thesis, University of Wyoming.
- Espenes, A., C. M. Press, T. Landsverk, M. Tranulis, M. Aleksandersen, G. Gunnes, S. Benestad, R. Fuglestad, and M. Ulvund, 2006. Detection of prpsc in rectal biopsy and necropsy samples from sheep with experimental scrapie. *Journal of Comparative Pathology* **134**:115–125.
- Ewald, P. W., 1994. Evolution of infectious disease. Oxford University Press.
- Farnsworth, M., J. Hoeting, N. Hobbs, and M. Miller, 2006. Linking chronic wasting disease to mule deer movement scales: a hierarchical Bayesian approach. *Ecological Applications* **16**:1026–1036.

- Fortin, D., M. Boyce, E. Merrill, and J. Fryxell, 2004. Foraging costs of vigilance in large mammalian herbivores. *Oikos* **107**:172–180.
- Fortin, D., M.-E. Fortin, H. L. Beyer, T. Duchesne, S. Courant, and K. Dancose, 2009. Group-size-mediated habitat selection and group fusion-fission dynamics of bison under predation risk. *Ecology* **90**:2480–2490.
- Fox, J. L., K. Dhondup, and T. Dorji, 2009. Tibetan antelope *Pantholops hodgsonii* conservation and new rangeland management policies in the western Chang Tang Nature Reserve, Tibet: is fencing creating an impasse? *Oryx* **43**:183–190.
- Fox, K. A., J. E. Jewell, E. S. Williams, and M. W. Miller, 2006. Patterns of prp(cwd) accumulation during the course of chronic wasting disease infection in orally inoculated mule deer (*Odocoileus hemionus*). *Journal of General Virology* **87**:3451–3461.
- Fryxell, J. and A. Sinclair, 1988. Causes and consequences of migration by large herbivores. *Trends in Ecology & Evolution* **3**:237–241.
- Fryxell, J., J. Wilmshurst, and A. Sinclair, 2004. Predictive models of movement by Serengeti grazers. *Ecology* **85**:2429–2435.
- Fuller, J. A., R. A. Garrott, P. J. White, K. E. Aune, T. J. Roffe, and J. C. Rhyan, 2007. Reproduction and survival of Yellowstone bison. *Journal of Wildlife Management* **71**:2365–2372.
- Galvin, K., R. Behnke, N. Hobbs, and R. Reid, editors, 2008. Fragmentation in semi-arid and arid Landscapes: consequences for human and natural systems. Springer.
- Garrott, R. A., G. C. White, R. M. Bartmann, L. H. Carpenter, and A. W. Alldredge, 1987. Movements of female mule deer in northwest colorado. *The Journal of Wildlife Management* pages 634–643.

- Gates, C. C., B. Stelfox, T. Muhley, T. Chowns, and R. J. Hudson, 2005. The ecology of bison movements and distribution in and beyond yellowstone national park. Technical report, University of Calgary.
- Gelman, A., 2008. Scaling regression inputs by dividing by two standard deviations. *Statistics in medicine* **27**:2865–2873.
- Gelman, A. and J. Hill, 2007. Data analysis using regression and multilevel/hierarchical models. Cambridge University Press.
- Gelman, A., X. Meng, and H. Stern, 1996. Posterior predictive assessment of model fitness via realized discrepancies. *Statistica Sinica* **6**:733–760.
- Gelman, A. and D. B. Rubin, 1992. Inference from iterative simulation using multiple sequences. *Statistical Science* **7**:457–511.
- Geremia, C., P. White, R. Garrott, W. RL, K. Aune, J. Treanor, and J. Fuller, 2009. The ecology of large mammals in central Yellowstones sixteen years of integrated field studies, chapter 14: Demography of central Yellowstone bison: effects of climate, density, and disease, pages 255–280. Elsevier.
- Geremia, C., P. J. White, R. L. Wallen, F. G. R. Watson, J. J. Treanor, J. Borkowski, C. S. Potter, and R. L. Crabtree, 2011. Predicting bison migration out of Yellowstone National Park using bayesian models. *PLoS one* **6**.
- Gonzalez, L., M. Dagleish, S. Bellworthy, S. Siso, M. Stack, M. Chaplin, L. Davis, S. Hawkins, J. Hughes, M. Jeffrey, et al., 2006. Postmortem diagnosis of preclinical and clinical scrapie in sheep by the detection of disease-associated prp in their rectal mucosa. *Veterinary Record* **158**:325.
- Gough, K. C. and B. C. Maddison, 2010. Prion transmission: Prion excretion and occurrence in the environment. *Prion* **4**:275–282.

- Greear, D. A., M. D. Samuel, K. T. Scribner, B. V. Weckworth, and J. A. Langenberg, 2010. Influence of genetic relatedness and spatial proximity on chronic wasting disease infection among female white-tailed deer. *Journal of Applied Ecology* **47**:532–540.
- Green, K. M., S. R. Browning, T. S. Seward, J. E. Jewell, D. L. Ross, M. A. Green, E. S. Williams, E. A. Hoover, and G. C. Telling, 2008. The elk prnp codon 132 polymorphism controls cervid and scrapie prion propagation. *Journal of General Virology* **89**:598–608.
- Greiner, M. and I. A. Gardner, 2000. Application of diagnostic tests in veterinary epidemiologic studies. *Preventative Veterinary Medicine* **45**:43–59.
- Grenfell, B. T. and A. P. Dobson, 1995. Ecology of infectious diseases in natural populations, volume 7. Cambridge University Press.
- Gross, J. E. and M. W. Miller, 2001. Chronic wasting disease in mule deer: disease dynamics and control. *The Journal of Wildlife Management* pages 205–215.
- Haley, N. J., C. K. Mathiason, S. Carver, M. Zabel, G. C. Telling, and E. A. Hoover, 2011. Detection of chronic wasting disease prions in salivary, urinary, and intestinal tissues of deer: potential mechanisms of prion shedding and transmission. *Journal of virology* **85**:6309–6318.
- Hansen, A. J. and R. DeFries, 2007. Ecological mechanisms linking protected areas to surrounding lands. *Ecological Applications* **17**:974–988.
- Harrison, P. J., S. T. Buckland, L. Thomas, R. Harris, P. P. Pomeroy, and J. Harwood, 2006. Incorporating movement into models of grey seal population dynamics. *Journal of Animal Ecology* **75**:634–645.
- Harvell, C., K. Kim, J. Burkholder, R. Colwell, P. R. Epstein, D. Grimes, E. Hofmann, E. Lipp, A. Osterhaus, R. M. Overstreet, et al., 1999. Emerging marine diseases—climate links and anthropogenic factors. *Science* **285**:1505–1510.

- Harvell, C. D., C. E. Mitchell, J. R. Ward, S. Altizer, A. P. Dobson, R. S. Ostfeld, and M. D. Samuel, 2002. Climate warming and disease risks for terrestrial and marine biota. *Science* **296**:2158–2162.
- Hebblewhite, M., E. Merrill, and G. McDermid, 2008. A multi-scale test of the forage maturation hypothesis in a partially migratory ungulate population. *Ecological Monographs* **78**:141–166.
- Hebblewhite, M. and E. H. Merrill, 2007. Multiscale wolf predation risk for elk: does migration reduce risk? *Oecologia* **152**:377–387.
- Heisey, D. M., D. O. Joly, and F. Messier, 2006. The fitting of general force-of-infection models to wildlife disease prevalence data. *Ecology* **87**:2356–2365.
- Heisey, D. M., E. E. Osnas, P. C. Cross, D. O. Joly, J. A. Langenberg, and M. W. Miller, 2010. Linking process to pattern: estimating spatiotemporal dynamics of a wildlife epidemic from cross-sectional data. *Ecological Monographs* **80**:221–240.
- Hess, S., 2002. Aerial survey methodology for bison population estimation in Yellowstone National Park. Ph.D. thesis, Montana State University.
- Hobbs, N., K. Galvin, C. Stokes, J. Lockett, A. Ash, R. Boone, R. Reid, and P. Thornton., 2008. Fragmentation of rangelands: implications for humans, animals, and landscapes. *Global Environmental Change-Human and Policy Dimensions* **18**:776–785.
- Holdo, R. M., J. M. Fryxell, A. R. E. Sinclair, A. Dobson, and R. D. Holt, 2011. Predicted impact of barriers to migration on the Serengeti wildebeest population. *PLoS one* **6**.
- Holdo, R. M., R. D. Holt, and J. M. Fryxell, 2009. Opposing rainfall and plant nutritional gradients best explain the wildebeest migration in the Serengeti. *American Naturalist* **173**:431–445.

- Horne, J. S., E. O. Garton, S. M. Krone, and J. S. Lewis, 2007. Analyzing animal movements using Brownian bridges. *Ecology* **88**:2354–2363.
- Huang, S., C. S. Potter, R. L. Crabtree, S. Hager, and P. Gross, 2010. Fusing optical and radar data to estimate grass and sagebrush percent cover in non-forested areas of Yellowstone. *Remote Sensing of the Environment* **2**:251–264.
- Imrie, C., A. Korre, and G. Munoz-Melendez, 2009. Spatial correlation between the prevalence of transmissible spongiform diseases and british soil geochemistry. *Environmental geochemistry and health* **31**:133–145.
- Ito, T., N. Miura, B. Lhagvasuren, D. Enkhbileg, S. Takatsuki, A. Tsunekawa, and Z. Jiang, 2005. Preliminary evidence of a barrier effect of a railroad on the migration of Mongolian gazelles. *Conservation Biology* **19**:945–948.
- Jewell, J. E., M. M. Conner, L. L. Wolfe, M. W. Miller, and E. S. Williams, 2005. Low frequency of prp genotype 225sf among free-ranging mule deer (*Odocoileus hemionus*) with chronic wasting disease. *Journal of General Virology* **86**:2127–2134.
- Johnson, C., J. Johnson, J. P. Vanderloo, D. Keane, J. M. Aiken, and D. McKenzie, 2006a. Prion protein polymorphisms in white-tailed deer influence susceptibility to chronic wasting disease. *Journal of General Virology* **87**:2109–2114.
- Johnson, C. J., A. Herbst, C. Duque-Velasquez, J. P. Vanderloo, P. Bochsler, R. Chappell, and D. McKenzie, 2011. Prion protein polymorphisms affect chronic wasting disease progression. *PLoS one* **6**:e17450.
- Johnson, C. J., J. A. Pedersen, R. J. Chappell, D. McKenzie, and J. M. Aiken, 2007. Oral transmissibility of prion disease is enhanced by binding to soil particles. *PLoS Pathogens* **3**:e93.

- Johnson, C. J., K. E. Phillips, P. T. Schramm, D. McKenzie, J. M. Aiken, and J. A. Pedersen, 2006b. Prions adhere to soil minerals and remain infectious. *PLoS Pathogens* **2**:e32.
- Joly, D. O., C. A. Ribic, J. A. Langenberg, K. Beheler, C. A. Batha, B. J. Dhuey, R. E. Rolley, G. Bartelt, T. R. Van Deelen, and M. D. Samuel, 2003. Chronic wasting disease in free-ranging wisconsin white-tailed deer. *Emerging Infectious Diseases* **9**:599.
- Keane, D., D. Barr, R. Osborn, J. Langenberg, K. O'Rourke, D. Schneider, and P. Bochsler, 2009. Validation of use of rectoanal mucosa-associated lymphoid tissue for immunohistochemical diagnosis of chronic wasting disease in white-tailed deer (*Odocoileus virginianus*). *Journal of Clinical Microbiology* **47**:1412–1417.
- Kelly, A. C., N. E. Mateus-Pinilla, J. Diffendorfer, E. Jewell, M. O. Ruiz, J. Killefer, P. Shelton, T. Beissel, and J. Novakofski, 2008. Prion sequence polymorphisms and chronic wasting disease resistance in illinois white-tailed deer (*Odocoileus virginianus*). *Prion* **2**:28–36.
- Kilpatrick, A. M., C. M. Gillin, and P. Daszak, 2009. Wildlife-livestock conflict: the risk of pathogen transmission from bison to cattle outside Yellowstone National Park. *Journal of Applied Ecology* **46**:476–485.
- Krumm, C. E., M. M. Conner, N. T. Hobbs, D. O. Hunter, and M. W. Miller, 2010. Mountain lions prey selectively on prion-infected mule deer. *Biology Letters* **6**:209–211.
- Lachish, S., A. M. Gopaldaswamy, S. C. L. Knowles, and B. C. Sheldon, 2012. Site-occupancy modelling as a novel framework for assessing test sensitivity and estimating wildlife disease prevalence from imperfect diagnostic tests. *Methods in Ecology and Evolution* **3**:339–348.
- LaDeau, S. L., G. E. Glass, N. T. Hobbs, A. Latimer, and R. S. Ostfeld, 2011. Data-model fusion to better understand emerging pathogens and improve infectious disease forecasting. *Ecological Applications* **21**:1443–1460.

- Larter, N. and C. Gates, 1991. Diet and habitat selection of wood bison in relation to seasonal-changes in forage quantify and quality. *Canadian Journal of Zoology-Revue Canadienne de Zoologie* **69**:2677–2685.
- Laundre, J., L. Hernandez, and K. Altendorf, 2001. Wolves, elk, and bison: reestablishing the “landscape of fear” in Yellowstone National Park, USA. *Canadian Journal of Zoology-Revue Canadienne de Zoologie* **79**:1401–1409.
- Leng, R. and J. Nolan, 1984. Nitrogen metabolism in the rumen. *Journal of Dairy Science* **67**:1072–1089.
- Li, C., Z. Jiang, X. Ping, J. Cai, Z. You, C. Li, and Y. Wu, 2012. Current status and conservation of the endangered Przewalski’s gazelle *Procapra przewalskii*, endemic to the Qinghai-Tibetan Plateau, China. *Oryx* **46**:145–153.
- Mathiason, C. K., S. A. Hays, J. Powers, J. Hayes-Klug, J. Langenberg, S. J. Dahmes, D. A. Osborn, K. V. Miller, R. J. Warren, G. L. Mason, et al., 2009. Infectious prions in pre-clinical deer and transmission of chronic wasting disease solely by environmental exposure. *PLoS one* **4**:e5916.
- Mathiason, C. K., J. G. Powers, S. J. Dahmes, D. A. Osborn, K. V. Miller, R. J. Warren, G. L. Mason, S. A. Hays, J. Hayes-Klug, D. M. Seelig, et al., 2006. Infectious prions in the saliva and blood of deer with chronic wasting disease. *Science* **314**:133–136.
- McCallum, H., N. Barlow, and J. Hone, 2001. How should pathogen transmission be modelled? *Trends in Ecology & Evolution* **16**:295–300.
- McCallum, H. and A. Dobson, 1995. Detecting disease and parasite threats to endangered species and ecosystems. *Trends in Ecology & Evolution* **10**:190–194.
- McClintock, B. T., J. D. Nichols, L. L. Bailey, D. I. MacKenzie, W. L. Kendall, and A. B.

- Franklin, 2010. Seeking a second opinion: uncertainty in disease ecology. *Ecology Letters* **13**:659–674.
- Meagher, M., 1973. The bison of Yellowstone National Park. National Park Service Scientific Monograph Series No. 1.
- Meagher, M., 1989. Range expansion by bison of Yellowstone National Park. *Journal of Mammology* **70**:670–675.
- Meagher, M., 1998. Recent changes in Yellowstone bison numbers and distributions. In *International Symposium on Bison Ecology and Management in North America*.
- Metzger, K. L., A. R. E. Sinclair, R. Hilborn, J. G. C. Hopcraft, and S. A. R. Mduma, 2010. Evaluating the protection of wildlife in parks: the case of African buffalo in Serengeti. *Biodiversity and Conservation* **19**:3431–3444.
- Miller, M. and M. Conner, 2005. Epidemiology of chronic wasting disease in free-ranging mule deer: spatial, temporal, and demographic influences on observed prevalence patterns. *Journal of Wildlife Diseases* **41**:275–290.
- Miller, M. W., H. M. Swanson, L. L. Wolfe, F. G. Quartarone, S. L. Huwer, C. H. Southwick, and P. M. Lukacs, 2008. Lions and prions and deer demise. *PLoS one* **3**:e4019.
- Miller, M. W. and E. S. Williams, 2003. Prion disease: horizontal prion transmission in mule deer. *Nature* **425**:35–36.
- Miller, M. W., E. S. Williams, N. T. Hobbs, L. L. Wolfe, et al., 2004. Environmental sources of prion transmission in mule deer. *Emerging Infectious Diseases* **10**:1003.
- Miller, M. W., E. S. Williams, C. W. McCarty, T. R. Spraker, T. J. Kreeger, C. T. Larsen, and E. T. Thorne, 2000. Epizootiology of chronic wasting disease in free-ranging cervids in colorado and wyoming. *Journal of Wildlife Diseases* **36**:676–690.

- Morgantini, T. and R. J. Hudson, 1988. Migratory patterns of the wapiti *Cervus elaphus* in Banff National Park, Alberta. *Canadian Field-Naturalist* **102**:12–19.
- Morner, T., D. L. Obendorf, M. Artois, and M. H. Woodford, 2002. Surveillance and monitoring of wildlife diseases. *Revue Scientifique et Technique-Office International des Epizooties* **21**:67–76.
- Morrison, T. A. and D. T. Bolger, 2012. Wet season range fidelity in a tropical migratory ungulate. *Journal of Animal Ecology* **81**:543–552.
- Mueller, T. and W. F. Fagan, 2008. Search and navigation in dynamic environments - from individual behaviors to population distributions. *Oikos* **117**:654–664.
- Mueller, T., K. A. Olson, G. Dressler, P. Leimgruber, T. K. Fuller, C. Nicolson, A. J. Novaro, M. J. Bolgeri, D. Wattles, S. DeStefano, J. M. Calabrese, and W. F. Fagan, 2011. How landscape dynamics link individual- to population-level movement patterns: a multispecies comparison of ungulate relocation data. *Global Ecology and Biogeography* **20**:683–694.
- Mysterud, A., R. Langvatn, N. Yoccoz, and N. Stenseth, 2001. Plant phenology, migration and geographical variation in body weight of a large herbivore: the effect of a variable topography. *Journal of Animal Ecology* **70**:915–923.
- Nellemann, C., I. Vistnes, P. Jordhoy, and O. Strand, 2001. Winter distribution of wild reindeer in relation to power lines, roads and resorts. *Biological Conservation* **101**:351–360.
- Nelson, M. E. and L. D. Mech, 1991. White-tailed deer movements and wolf predation risk. *Canadian Journal of Zoology* **69**:2696–2699.
- Nicholson, M. C., R. T. Bowyer, and J. G. Kie, 1997. Habitat selection and survival of mule deer: tradeoffs associated with migration. *Journal of Mammology* **78**:483–504.

- Olexa, E. M. and P. J. Gogan, 2007. Spatial population structure of yellowstone bison. *The Journal of Wildlife Management* **71**:1531–1538.
- O'Rourke, K. I., T. R. Spraker, L. K. Hamburg, T. E. Besser, K. A. Brayton, and D. P. Knowles, 2004. Polymorphisms in the prion precursor functional gene but not the pseudogene are associated with susceptibility to chronic wasting disease in white-tailed deer. *Journal of General Virology* **85**:1339–1346.
- Osnas, E. E., D. M. Heisey, R. E. Rolley, and M. D. Samuel, 2009. Spatial and temporal patterns of chronic wasting disease: fine-scale mapping of a wildlife epidemic in wisconsin. *Ecological Applications* **19**:1311–1322.
- Ostfeld, R. S. and R. D. Holt, 2004. Are predators good for your health? evaluating evidence for top-down regulation of zoonotic disease reservoirs. *Frontiers in Ecology and the Environment* **2**:13–20.
- Parker, K., C. Robbins, and T. Hanley, 1984. Energy expenditures for locomotion by mule deer and elk:. *Journal of Wildlife Management* **48**:474–488.
- Patterson, T. A., L. Thomas, C. Wilcox, O. Ovaskainen, and J. Matthiopoulos, 2008. State-space models of individual animal movement. *Trends in Ecology & Evolution* **23**:87–94.
- Plumb, G. E., P. J. White, M. B. Coughenour, and R. L. Wallen, 2009. Carrying capacity, migration, and dispersal in Yellowstone bison. *Biological Conservation* **142**:2377–2387.
- Potter, C., S. Klooster, A. Huete, and V. Genovese, 2007. Terrestrial carbon sinks for the United States predicted from MODIS satellite data and ecosystem modeling. *Earth Interactions* **11**:1–21.
- Potter, C. S. and S. A. Klooster, 1999. Dynamic global vegetation modeling (DGVM) for prediction of plant functional types and biogenic trace gas fluxes. *Global Ecology and Biogeography Letters* **8**:473–488.

- Prusiner, S. B., 1998. Prions. *Proceedings of the National Academy of Sciences* **95**:13363–13383.
- Rees, E. E., E. H. Merrill, T. K. Bollinger, Y. T. Hwang, M. J. Pybus, and D. W. Coltman, 2012. Targeting the detection of chronic wasting disease using the hunter harvest during early phases of an outbreak in saskatchewan, canada. *Preventive Veterinary Medicine* **104**:149–159.
- Rhyan, J. C., K. Aune, T. Roffe, D. Ewalt, S. Hennager, T. Gidlewski, S. Olsen, and R. Clarke, 2009. Pathogenesis and epidemiology of brucellosis in Yellowstone bison: serologic and culture results from adult females and their progeny. *Journal of Wildlife Diseases* **45**:729–739.
- Robinette, W. L., D. A. Jones, G. Rogers, and J. S. Gashwiler, 1957. Notes on tooth development and wear for rocky mountain mule deer. *The Journal of Wildlife Management* **21**:134–153.
- Robinson, G. R., R. D. Holt, M. S. Gaines, S. P. Hamburg, M. L. Johnson, H. S. Fitch, E. A. Martinko, et al., 1992. Diverse and contrasting effects of habitat fragmentation. *Science(Washington)* **257**:524–526.
- Ryou, C., 2007. Prions and prion diseases: fundamentals and mechanistic details. *Journal of Microbiology and Biotechnology* **17**:1059–1070.
- Saunders, S. E., S. L. Bartelt-Hunt, J. C. Bartz, et al., 2012a. Occurrence, transmission, and zoonotic potential of chronic wasting disease. *Emerging Infectious Diseases* **18**:369.
- Saunders, S. E., J. C. Bartz, and S. L. Bartelt-Hunt, 2012b. Soil-mediated prion transmission: is local soil-type a key determinant of prion disease incidence? *Chemosphere* **87**:661–667.
- Sawyer, H., M. J. Kauffman, R. M. Nielson, and J. S. Horne, 2009. Identifying and priori-

- tizing ungulate migration routes for landscape-level conservation. *Ecological Applications* **19**:2016–2025.
- Schaefer, J. and F. Messier, 1995. Habitat selection as a hierarchy: the spatial scales of winter foraging by muskoxen. *Ecography* **18**:333–344.
- Schick, R. S., S. R. Loarie, F. Colchero, B. D. Best, A. Boustany, D. A. Conde, P. N. Halpin, L. N. Joppa, C. M. McClellan, and J. S. Clark, 2008. Understanding movement data and movement processes: current and emerging directions. *Ecology Letters* **11**:1338–1350.
- Schielzeth, H., 2010. Simple means to improve the interpretability of regression coefficients. *Methods in Ecology and Evolution* **1**:103–113.
- Schmehl, W. and M. Jackson, 1957. Mineralogical analyses of soil clays from colorado surface soils. *Soil Science Society of America Journal* **21**:373–380.
- Schuler, K., J. Jenks, C. DePerno, M. Wild, and C. Swanson, 2005. Tonsillar biopsy test for chronic wasting disease: two sampling approaches in mule deer and white-tailed deer. *Journal of Wildlife Diseases* **41**:820–824.
- Senft, R., M. Coughenour, D. Bailey, L. Rittenhouse, O. Sala, and D. M. Swift, 1987. Large herbivore foraging and ecological hierarchies. *Bioscience* **37**:789–&.
- Sharp, A. and J. Pastor, 2011. Stable limit cycles and the paradox of enrichment in a model of chronic wasting disease. *Ecological Applications* **21**:1024–1030.
- Sigurdson, C. J., C. Barillas-Mury, M. W. Miller, B. Oesch, L. J. van Keulen, J. P. Langeveld, and E. A. Hoover, 2002. Prpcwd lymphoid cell targets in early and advanced chronic wasting disease of mule deer. *Journal of General Virology* **83**:2617–2628.
- Sinclair, A. R. E. and P. Arcese, 1995. Serengeti II: dynamics, management, and conservation of an ecosystem, volume 2. University of Chicago Press.

- Spraker, T., M. Miller, E. Williams, D. Getzy, W. Adrian, G. Schoonveld, R. Spowart, K. I. O'Rourke, J. Miller, and P. Merz, 1997. Spongiform encephalopathy in free-ranging mule deer (*Odocoileus hemionus*), white-tailed deer (*Odocoileus virginianus*) and rocky mountain elk (*Cervus elaphus nelsoni*) in northcentral colorado. *Journal of Wildlife Diseases* **33**:1–6.
- Spraker, T. R., K. C. VerCauteren, T. L. Gidlewski, R. D. Munger, W. D. Walter, and A. Balachandran, 2009. Impact of age and sex of rocky mountain elk (*Cervus elaphus nelsoni*) on follicle counts from rectal mucosal biopsies for preclinical detection of chronic wasting disease. *Journal of Veterinary Diagnostic Investigation* **21**:868–870.
- Storm, D. J., M. D. Samuel, R. E. Rolley, P. Shelton, N. S. Keuler, B. J. Richards, and T. R. Van Deelen, 2013. Deer density and disease prevalence influence transmission of chronic wasting disease in white-tailed deer. *Ecosphere* **4**:art10.
- Tamgüney, G., M. W. Miller, L. L. Wolfe, T. M. Sirochman, D. V. Glidden, C. Palmer, A. Lemus, S. J. DeArmond, and S. B. Prusiner, 2009. Asymptomatic deer excrete infectious prions in faeces. *Nature* **461**:529–532.
- Thomas, C. D., A. Cameron, R. E. Green, M. Bakkenes, L. J. Beaumont, Y. C. Collingham, B. F. Erasmus, M. F. De Siqueira, A. Grainger, L. Hannah, et al., 2004. Extinction risk from climate change. *Nature* **427**:145–148.
- Thomsen, B. V., D. A. Schneider, K. I. O'Rourke, T. Gidlewski, J. McLane, R. W. Allen, A. A. McIsaac, G. B. Mitchell, D. P. Keane, T. R. Spraker, et al., 2012. Diagnostic accuracy of rectal mucosa biopsy testing for chronic wasting disease within white-tailed deer (*Odocoileus virginianus*) herds in north america effects of age, sex, polymorphism at prnp codon 96, and disease progression. *Journal of Veterinary Diagnostic Investigation* **24**:878–887.

- Thouless, C., 1995. Long distance movements of elephants in northern Kenya. *African Journal of Ecology* **33**:321–334.
- Toft, N., E. Jorgensen, and S. Hojsgaard, 2005. Diagnosing diagnostic tests: evaluating the assumptions underlying the estimation of sensitivity and specificity in the absence of a gold standard. *Preventative Veterinary Medicine* **68**:19–33.
- Treanor, J. J., C. Geremia, P. Crowley, J. J. Cox, P. J. White, R. L. Wallen, and D. W. Blanton, 2011. Estimating probabilities of active brucellosis infection in Yellowstone bison through quantitative serology and tissue culture. *Journal of Applied Ecology* **48**:1324–1332.
- Urban, D. and T. Keitt, 2001. Landscape connectivity: a graph-theoretic perspective. *Ecology* **82**:1205–1218.
- USDI and USDA, 2000a. Final environmental impact statement for the interagency bison management plan for the state of Montana and Yellowstone National Park. Technical report, National Park Service.
- USDI and USDA, 2000b. Record of decision for final environmental impact statement and bison management plan for the state of Montana and Yellowstone National Park. Technical report, National Park Service.
- Vieira, M., 2006. Red Feather-Poudre Canyon deer herd management plan data analysis unit D04. Technical report, Colorado Division of Wildlife.
- Vistnes, I., C. Nellemann, P. Jordhoy, and O. Strand, 2004. Effects of infrastructure on migration and range use of wild reindeer. *Journal of Wildlife Management* **68**:101–108.
- Walter, W. D., D. P. Walsh, M. L. Farnsworth, D. L. Winkelman, and M. W. Miller, 2011. Soil clay content underlies prion infection odds. *Nature Communications* **2**:200.

- Walters, C. and C. Holling, 1990. Large-scale management experiments and learning by doing. *Ecology* **71**:2060–2068.
- Wasserberg, G., E. E. Osnas, R. E. Rolley, and M. D. Samuel, 2009. Host culling as an adaptive management tool for chronic wasting disease in white-tailed deer: a modelling study. *Journal of Applied Ecology* **46**:457–466.
- Watson, F., W. Newman, J. Coughlan, and R. Garrott, 2006. Testing a distributed snowpack simulation model against diverse observations. *Journal of Hydrology* **328**:453–466.
- White, P., T. L. Davis, K. K. Barnowe-Meyer, and R. L. Crabtree, 2007. Partial migration and philopatry of Yellowstone pronghorn. *Biological Conservation* **135**:502–210.
- White, P. J., R. L. Wallen, C. Geremia, J. J. Treanor, and D. W. Blanton, 2011. Management of Yellowstone bison and brucellosis transmission risk - implications for conservation and restoration. *Biological Conservation* **144**:1322–1334.
- Wild, M., T. Spraker, C. Sigurdson, K. O'Rourke, and M. Miller, 2002. Preclinical diagnosis of chronic wasting disease in captive mule deer (*Odocoileus hemionus*) and white-tailed deer (*Odocoileus virginianus*) using tonsillar biopsy. *Journal of General Virology* **83**:2629–2634.
- Williams, B., R. Szaro, and S. CD, 2007. Adaptive management the U. S. Department of Interior technical guide. Technical report, U.S. Department of the Interior.
- Williams, E., 2005. Chronic wasting disease. *Veterinary Pathology* **42**:530–549.
- Williams, E. and S. Young, 1992. Spongiform encephalopathies in *Cervidae*. *Revue Scientifique et Technique (International Office of Epizootics)* **11**:551.
- Williams, E. S., M. W. Miller, T. J. Kreeger, R. H. Kahn, and E. T. Thorne, 2002. Chronic wasting disease of deer and elk: a review with recommendations for management. *The Journal of Wildlife Management* pages 551–563.

- Wilmshurst, J., J. Fryxell, and R. Hudson, 1995. Forage quality and patch choice by wapiti (*Cervus-Elaphus*). *Behavioral Ecology* **6**:209–217.
- Wilson, G. A., S. M. Nakada, T. K. Bollinger, M. J. Pybus, E. H. Merrill, and D. W. Coltman, 2009. Polymorphisms at the prnp gene influence susceptibility to chronic wasting disease in two species of deer (*Odocoileus Spp.*) in western Canada. *Journal of Toxicology and Environmental Health, Part A* **72**:1025–1029.
- Wittmer, H. U., B. N. McLellan, R. Serrouya, and C. D. Apps, 2007. Changes in landscape composition influence the decline of a threatened woodland caribou population. *Journal of Animal Ecology* **76**:568–579.
- Wolfe, L., M. Conner, T. Baker, V. Dreitz, K. Burnham, E. Williams, N. Hobbs, and M. Miller, 2002. Evaluation of antemortem sampling to estimate chronic wasting disease prevalence in free-ranging mule deer. *Journal of Wildlife Management* **66**:564–573.
- Wolfe, L. L., T. R. Spraker, L. Gonzalez, M. P. Dagleish, T. M. Sirochman, J. C. Brown, M. Jeffrey, and M. W. Miller, 2007. PrPCWD in rectal lymphoid tissue of deer (*Odocoileus spp.*). *Journal of General Virology* **88**:2078–2082.
- Zweifel-Schielly, B., M. Kreuzer, K. C. Ewald, and W. Suter, 2009. Habitat selection by an alpine ungulate: the significance of forage characteristics varies with scale and season. *Ecography* **32**:103–113.

APPENDIX 1: SUPPLEMENTARY MATERIAL

Here we describe the model described in the Statistical Analysis section in more detail and provide the details of the Markov chain Monte Carlo algorithm (steps 1-8).

The latent variable for the true number of bison in each wintering area during month t and year j is a 10×1 column vector assumed to follow a gamma distribution $\mathbf{z}_{t,j} \sim \text{Gamma}(\beta, \mathbf{A}\mathbf{z}_{t-1,j}\beta)$ where β is the rate parameter and \mathbf{A} is a transition matrix for movement γ and survival ϕ . Note that $\mathbf{z}_{t,j} = \mathbf{A}\mathbf{z}_{t-1,j}$ and are given by Figure 1.

$$\mathbf{z}_{t,j} = \begin{bmatrix} \text{Hayden} \\ \text{Firehole} \\ \text{Gibbon} \\ \text{Hebgen} \\ \text{Blacktail(central)} \\ \text{Gardiner(central)} \\ \text{Lamar} \\ \text{Lower Yellowstone} \\ \text{Blacktail(northern)} \\ \text{Gardiner(northern)} \end{bmatrix}$$

$$\mathbf{A} = \phi \begin{bmatrix} (1 - \gamma_1^*)(1 - \gamma_5^*) & 0 & 0 & 0 & 0 & 0 & 0 & 0 & 0 & 0 & 0 \\ \gamma_1^* & (1 - \gamma_2^*) & 0 & 0 & 0 & 0 & 0 & 0 & 0 & 0 & 0 \\ \gamma_5^* & \gamma_2^* & (1 - \gamma_3^*)(1 - \gamma_4^*) & 0 & 0 & 0 & 0 & 0 & 0 & 0 & 0 \\ 0 & 0 & \gamma_4^* & 1 & 0 & 0 & 0 & 0 & 0 & 0 & 0 \\ 0 & 0 & \gamma_3^* & 0 & (1 - \gamma_6^*) & 0 & 0 & 0 & 0 & 0 & 0 \\ 0 & 0 & 0 & 0 & \gamma_6^* & 1 & 0 & 0 & 0 & 0 & 0 \\ 0 & 0 & 0 & 0 & 0 & 0 & (1 - \gamma_7^*) & 0 & 0 & 0 & 0 \\ 0 & 0 & 0 & 0 & 0 & 0 & \gamma_7^* & (1 - \gamma_8^*) & 0 & 0 & 0 \\ 0 & 0 & 0 & 0 & 0 & 0 & 0 & \gamma_8^* & (1 - \gamma_6^*) & 0 & 0 \\ 0 & 0 & 0 & 0 & 0 & 0 & 0 & 0 & \gamma_6^* & 1 & 0 \end{bmatrix}$$

The matrix \mathbf{A} varies with each month and year because movement probabilities are affected by time-varying covariates. Rather than subscript \mathbf{A} and each movement probability with time, we generalize our notation where $\gamma_1^*, \gamma_2^*, \dots, \gamma_8^*$ refer to the eight movement probabilities at a given time. We model movement probabilities via a logistic model, so, for example, the movement probability along the first migration path is given by $\text{logit}(\gamma_1^*) = \boldsymbol{\gamma}_1 \boldsymbol{\mu}_{x_j}$, where $\boldsymbol{\gamma}_1$ is a column vector of logistic model coefficients and $\boldsymbol{\mu}_{x_j}$ is a corresponding row in a covariate matrix. The other movement probabilities are defined similarly.

The observed aerial count during month t and year j is a 8×1 column vector assumed to follow a Poisson-gamma mixture distribution (e.g., Negative binomial) with intensity $\boldsymbol{\lambda}_{t,j}$. Note that $\mathbf{y}_{1_{t,j}} \sim \text{Poisson}(\boldsymbol{\lambda}_{t,j})$ and $\boldsymbol{\lambda}_{t,j} \sim \text{Gamma}(\alpha, \mathbf{B}\mathbf{z}_{t,j}\alpha)$ where α is the rate parameter for gamma and \mathbf{B} is an alignment matrix to align wintering areas and aerial counts described below in step 7. Also observed are individual animal GPS locations \mathbf{y}_2 which follow multinomial distributions with multinomial probabilities equal to the proportion of bison in the i^{th} wintering area $\mathbf{z}_{m,j,i} / \sum_i \mathbf{z}_{m,j,i}$.

Covariates are assumed to be measured with error as described below in step 2. A normal model was assumed for each covariate. For example, if annual snow pack is considered to be the first covariate, then observed annual snow pack in the j^{th} year is modeled as $\log(x_{j1}) \sim N(\mu_{xj1}, \sigma_{x1})$.

Parameter prior distributions are as follows: $\log(\mathbf{z}_{1,j}) \sim N(\log(\mathbf{y}_{1,j}), .5)$, $\phi \sim \text{Beta}(1,1)$, $\gamma \sim N(0,1000)$, $\log(\sigma_{x1}) \sim N(1.6,.1)$ for snow conditions, $\log(\sigma_{x2}) \sim N(1,.1)$ for standing crop, and the log of all remaining parameters were $N(0,100)$. Additional model subscripts are the subset of months when aerial counting occurred T_j , l , the subset of months when GPS locations were collected m , and the number of years of study N .

The joint posterior distribution of the unknown parameters of interest and the latent variables given the observed data can be factored and written as

$$\begin{aligned}
[\mathbf{z}, \gamma, \phi, \boldsymbol{\mu}_x, \boldsymbol{\sigma}_x, \alpha, \beta | \mathbf{y}_1, \mathbf{y}_2, \mathbf{x}] &\propto \prod_{j=1}^N \prod_{t=2}^{T_j} [\mathbf{z}_{t,j} | \mathbf{z}_{t-1,j}, \boldsymbol{\mu}_{x_j}, \gamma, \phi, \beta] \prod_{j=1}^N \prod_l [\boldsymbol{\lambda}_{l,j} | \mathbf{z}_{l,j}, \alpha] [\mathbf{y}_{1,j} | \boldsymbol{\lambda}_{l,j}] \\
&\times \prod_{j=1}^N \prod_m [\mathbf{y}_{2,m,j} | \mathbf{z}_{m,j}] \prod_{j=1}^N [\mathbf{z}_{1,j}] \prod_{j=1}^N [\mathbf{x}_j | \boldsymbol{\mu}_{x_j}, \boldsymbol{\sigma}_x] [\gamma] [\phi] [\boldsymbol{\mu}_x] [\boldsymbol{\sigma}_x] [\alpha] [\beta].
\end{aligned}$$

The joint posterior distribution is not available in closed form. We use a Markov chain Monte Carlo (MCMC) algorithm to simulate from the posterior distribution and to estimate the parameters of the of the unknown parameters of interest and the latent variables. The MCMC algorithm proceeds as follows:

1. Initialize each parameter $\mathbf{z}, \boldsymbol{\lambda}, \gamma, \phi, \boldsymbol{\sigma}_x, \alpha, \beta, \boldsymbol{\mu}_x$ with a starting value.
2. The matrix $\boldsymbol{\mu}_x$ are covariate conditions with rows representing years and columns as covariate types. For the j^{th} year, $\boldsymbol{\mu}_{x_j} = [\mu_{xj1}, \mu_{xj2}, \dots, \mu_{xjn}]$ is a vector of covariate conditions where elements are snow, standing crop, and herd size conditions. Note that snow, standing crop, and herd size conditions are treated as latent variables and \mathbf{x}_j are observed covariate conditions. Update each element of $\boldsymbol{\mu}_{x_j}$ from its complete

conditional distribution given by

$$[\boldsymbol{\mu}_{x_j}|\cdot] \propto \prod_{t=2}^{T_j} [\mathbf{z}_{t,j}|\mathbf{z}_{t-1,j}, \boldsymbol{\mu}_{x_j}, \boldsymbol{\gamma}, \phi, \beta][\mathbf{x}_j|\boldsymbol{\mu}_{x_j}, \boldsymbol{\sigma}_x][\boldsymbol{\mu}_{x_j}].$$

3. The vector $\boldsymbol{\sigma}_x = [\sigma_{x1}, \sigma_{x2}, \dots, \sigma_{xn}]^T$ has one element for each latent covariate type, e.g., snow, standing crop, and herd sizes. Sequentially update each element of $\boldsymbol{\sigma}_x$ from its complete conditional distribution. The first element is given by

$$[\sigma_{x1}|\cdot] \propto \prod_{j=1}^N [x_{j1}|\mu_{x_{j1}}, \sigma_{x1}][\sigma_{x1}]$$

and the others are defined similarly.

4. Update the survival parameter ϕ from its full conditional distribution given by

$$[\phi|\cdot] \propto \prod_{j=1}^N \prod_{t=2}^{T_j} [\mathbf{z}_{t,j}|\mathbf{z}_{t-1,j}, \boldsymbol{\mu}_{x_j}, \boldsymbol{\gamma}, \phi, \beta][\phi].$$

5. Movement parameters are given by the matrix $\boldsymbol{\gamma}$ with rows corresponding to logistic regression coefficients of covariate effects and columns as each migration route. The i^{th} migration route is given by the seven element vector $\boldsymbol{\gamma}_i = [\gamma_{i1}, \gamma_{i2}, \dots, \gamma_{i7}]^T$ where elements are the intercept term, months since snow as a second order polynomial, snow, herd size, standing crop, and year of study. At this point, the matrix $\boldsymbol{\mu}_x$ consists only of latent covariate conditions. Additional columns are added to the matrix $\boldsymbol{\mu}_x$ that correspond covariate conditions that are measured without error including months since snow and year of study. Batch update each vector $\boldsymbol{\gamma}_i$ sequentially beginning with $\boldsymbol{\gamma}_1$ from their full conditional distributions. New values are proposed for elements of each vector simultaneously. The full conditional distribution of the i th vector $\boldsymbol{\gamma}_i$ is

$$[\boldsymbol{\gamma}_i|\cdot] \propto \prod_{j=1}^N \prod_{t=2}^{T_j} [\mathbf{z}_{t,j}|\mathbf{z}_{t-1,j}, \boldsymbol{\mu}_{x_j}, \boldsymbol{\gamma}_i, \phi, \beta][\boldsymbol{\gamma}_i].$$

6. Process variance enters the model through the parameter β . Update β from its complete conditional distribution given by

$$[\beta|\cdot] \propto \prod_{j=1}^N \prod_{t=2}^{T_j} [z_{t,j} | z_{t-1,j}, \boldsymbol{\mu}_{x_j}, \boldsymbol{\gamma}, \phi, \beta][\beta].$$

7. Aerial count \mathbf{y}_1 are assumed to follow a Poisson-gamma mixture distribution based on observed and unobserved data on average abundance in count areas $\boldsymbol{\lambda}$ and numbers of bison in wintering areas \mathbf{z} . The values \mathbf{y}_1 and \mathbf{z} differ for three reasons: sampling error, count and wintering areas do not completely overlap, and some counts of wintering areas were incomplete. Both $\boldsymbol{\lambda}$ and \mathbf{z} are latent gamma variables.

Several steps are necessary to handle this hierarchically.

- (a) The 10×1 column vector $\mathbf{z}_{t,j}$ is the number of bison in each of 10 wintering areas during year j and month t . The 8×1 column vector $\boldsymbol{\lambda}_{t,j}$ is the average number of bison in each of 8 count areas during year j and month t . The 8×10 relation matrix \mathbf{B} aligns count and wintering areas and is given by,

$$\mathbf{B} = \begin{bmatrix} 1 & 0 & 0 & 0 & 0 & 0 & 0 & 0 & 0 & 0 \\ 0 & 1 & 0 & 0 & 0 & 0 & 0 & 0 & 0 & 0 \\ 0 & 0 & 1 & 0 & 0 & 0 & 0 & 0 & 0 & 0 \\ 0 & 0 & 0 & 1 & 0 & 0 & 0 & 0 & 0 & 0 \\ 0 & 0 & 0 & 0 & 1 & 0 & 0 & 0 & 1 & 0 \\ 0 & 0 & 0 & 0 & 0 & 1 & 0 & 0 & 0 & 1 \\ 0 & 0 & 0 & 0 & 0 & 0 & 1 & 0 & 0 & 0 \\ 0 & 0 & 0 & 0 & 0 & 0 & 0 & 1 & 0 & 0 \end{bmatrix}.$$

Numbers of bison in each wintering area were estimated during each month of the year and are referenced by the subscript t . Counts did not occur during each

month and the subscript l references the subset of months when counts occurred.

- (b) Counting variance enters the model through the parameter α . Update α from its complete conditional distribution given by

$$[\alpha|\cdot] \propto \prod_{j=1}^N \prod_l [\lambda_{l,j} | \mathbf{B}z_{l,j}, \alpha] [\alpha].$$

- (c) Update λ from their complete conditional distribution given by

$$[\lambda|\cdot] \propto \prod_{j=1}^N \prod_l [\lambda_{l,j} | \mathbf{B}z_{l,j}, \alpha] [\mathbf{y}_{1,l,j} | \lambda_{l,j}].$$

8. \mathbf{y}_2 are individual animal GPS locations and follow multinomial distributions with multinomial probabilities equal to the proportion of bison in the i^{th} wintering area $\mathbf{z}_{m,j,i} / \sum_i \mathbf{z}_{m,j,i}$. The full conditional distribution of \mathbf{z} depends on the timing of the model update. During the first time step of each year,

$$[\mathbf{z}_{1,j}|\cdot] \propto \prod_{j=1}^N [\mathbf{z}_{2,j} | \mathbf{z}_{1,j}, \boldsymbol{\mu}_{x_j}, \boldsymbol{\gamma}, \phi, \beta] \prod_{j=1}^N [\lambda_{1,j} | \mathbf{B}z_{1,j}, \alpha] \prod_{j=1}^N [\mathbf{z}_{1,j}] [\mathbf{y}_{2,1,j} | \mathbf{z}_{1,j}].$$

Between the first and final time steps,

$$\begin{aligned} [\mathbf{z}_{t,j}|\cdot] &\propto \prod_{j=1}^N \prod_{t=2}^{T_j} [\mathbf{z}_{t,j} | \mathbf{z}_{t-1,j}, \boldsymbol{\mu}_{x_j}, \boldsymbol{\gamma}, \phi, \beta] \prod_{j=1}^N \prod_{t=1}^{T_j-1} [\mathbf{z}_{t+1,j} | \mathbf{z}_{t,j}, \boldsymbol{\mu}_{x_j}, \boldsymbol{\gamma}, \phi, \beta] \\ &\times \prod_{j=1}^N \prod_l [\lambda_{l,j} | \mathbf{B}z_{l,j}, \alpha] \prod_{j=1}^N \prod_m \mathbf{y}_{2m,j} | \mathbf{z}_{m,j}. \end{aligned}$$

During the final time step,

$$[\mathbf{z}_{T_j,j}|\cdot] \propto \prod_{j=1}^N [\mathbf{z}_{T_j,j} | \mathbf{z}_{T_j-1,j}, \boldsymbol{\mu}_{x_j}, \boldsymbol{\gamma}, \phi, \beta] \prod_{j=1}^N [\lambda_{T_j,j} | \mathbf{B}z_{T_j,j}, \alpha] \prod_{j=1}^N [\mathbf{y}_{2T_j,j} | \mathbf{z}_{T_j,j}].$$

9. Repeat steps 2 through 8 many times.

This completes the MCMC algorithm.

APPENDIX 2: SUPPLEMENTARY MATERIAL

We proceed by developing each component of the model, specifying the posterior distribution, and outlining the Markov chain Monte Carlo algorithm. Within the MCMC algorithm we also describe the estimation process for derived quantities including elements of the projection matrix \mathbf{A} , population growth, and the stable stage structure.

We evaluated two models, each representing a different spatial scale. The first model represented a single intermixing deer population. Infection probability was constant between individuals. At a finer spatial scale, the second model delineated the population into wintering units. Differences among winter units were reflected in estimates of survival, annual infection probability, and fertility. Here, we describe the subpopulation model.

CWD Infection: CWD infection status was estimated using an occupancy model. We define \mathbf{Z} as an infectious status matrix, $\mathbf{Z} = [z_{i,t}]$ for the i th deer $i = 1, \dots, I$ and the t th the testing occasion (year) $t = 1, \dots, T$. When an individual is infected in the t th year, $z_{i,t} = 1$; $z_{i,t} = 0$ otherwise. Infection status was treated as a first order Markov process. The model for the initial test, $z_{i,1}$, is described below. After the initial test, infection status at the current time t is conditioned on infection status at the previous time $t - 1$ where

$$[z_{i,t}|z_{i,t-1}, \psi_i] = \begin{cases} 1 & z_{i,t-1} = 1 \\ \text{Bern}(\psi_i) & z_{i,t-1} = 0 \end{cases}.$$

The parameter ψ_i is the infection probability for the i th deer. Our model assumes that an infected individual remains infected during the subsequent testing year and a susceptible individual becomes infected with probability ψ_i . Infection probability is assumed to be time invariant but may vary between individuals based on wintering population unit membership. We use the logistic model to estimate the probability of infection, where $\text{logit}(\psi)_i = \mathbf{x}_i^t \boldsymbol{\zeta}$.

Here \mathbf{x}_i is the covariate vector for the i th deer with columns representing wintering population unit membership and $\boldsymbol{\zeta}$ is a vector of logistic model coefficients.

We define \mathbf{Y} as an observation matrix, where $y_{i,t}$ represents the observed number of follicles exhibiting PrP^{Sc} from individual i during testing occasion t . We define the corresponding matrix, \mathbf{J} , where $J_{i,t}$ is the total number of follicles obtained for individual i at year t . False positive test results were not believed to occur. Therefore, when $z_{i,t} = 0$ then $y_{i,t} = 0$. However, we may or may not have observed at least one positive follicle when an individual was infected, meaning when $z_{i,t} = 1$ then $y_{i,t} \geq 0$. The probability that an individual test is positive is π , and

$$[y_{i,t} | \pi, J_{i,t}, z_{i,t}] = \begin{cases} 0 & z_{i,t} = 0 \\ \text{Binom}(J_{i,t}, \pi) & z_{i,t} = 1 \end{cases}.$$

The infectious status at time 1, ψ_0 , depends on the observed infection value, where a false negative is possible. That is,

$$[z_{i,1} | \psi_0, y_{i,1}] = \begin{cases} 1 & y_{i,1} \geq 1 \\ \text{Bern}(\psi_0) & y_{i,1} = 0 \end{cases},$$

where ψ_0 is the probability that an individual developed disease prior to initial testing. There is an important distinction between ψ_i and ψ_0 ; ψ_i only captures infection during a single year, while ψ_0 is the population prevalence.

We specify diffuse Beta(1,1) prior distributions for ψ_0 and π and slightly informative N(0,5) prior distributions for elements of $\boldsymbol{\psi}$. There are I total individuals which were in the study for a variable number of years. We define the indicator variable $U_{i,t}$ coded using the reference value of 0 when an individual i was no longer in the study on occasion t and with the value of 1 when individual i was in the study. Similarly, we define the indicator variable $V_{i,t}$ coded as 0 when individual i was not tested and 1 when individual i was tested.

Survival: A Bayesian hazard model was used to estimate survival. The response variable t_i is the final time that an individual is observed. We were unable to observe the time of death for each individual because deer died unnaturally due to hunter harvest or capture related cause, telemetry devices failed, or animals survived the extent of the study. The indicator variable δ_i identifies animals that were censored. We set $\delta_i = 1$ when the death of the i^{th} deer is observed; $\delta_i = 0$ when the i^{th} deer exits the study prior to death. From established results in hazard modeling, survival and hazard functions provide different but equivalent characterizations of the distribution of \mathbf{t} . The hazard function $h(t_i)$ gives the instantaneous rate of death. Integrating the hazard function over a duration provides the cumulative hazard $\Lambda(t_i)$ which can be thought of as the sum of risks during this interval. The survival function $S(t_i)$ is the reciprocal of the cumulative hazard and gives the probability density that individual i will survive past time t , so

$$h(t_i) = -\frac{\partial \log(S(t_i))}{\partial t}.$$

Only the survival function contributes to the likelihood expression when $\delta_i = 0$ because the individual is still alive at time t . However, when a death is observed $\delta_i = 1$, both the survival and hazard functions contribute to the likelihood. The likelihood for \mathbf{t} is given by

$$[\mathbf{t}|\lambda, \alpha, \boldsymbol{\beta}, \mathbf{z}] = \prod_{i=1}^I h(t_i)^{\delta_i} S(t_i).$$

where the survival times, t_i , are assumed to follow a Weibull distribution.

Separate survival and hazard functions were used for CWD susceptible and infected deer. The survival function for CWD susceptible deer was $S(t_i) = \exp(-\lambda_1 t_i^{\alpha_1})^{\exp(\boldsymbol{\beta} \mathbf{x}_i)}$ with the corresponding hazard function $h(t_i) = \lambda_1 \alpha_1 t_i^{\alpha_1 - 1} \exp(\boldsymbol{\beta} \mathbf{x}_i)$. Age and wintering population unit affected survival. The covariate vector for the i th deer \mathbf{x}_i included the age of each deer when initially captured and wintering population unit membership. The covariate for the age of entry for fawns (6 mo) was coded using the value 0. Therefore, juveniles were

allowed lower survival than adults. For CWD infected deer, we used the survival function $S(t_i) = \exp(-\lambda_2 t_i^{\alpha_2})$ with the corresponding hazard function $h(t_i) = \lambda_2 \alpha_2 t_i^{\alpha_2 - 1}$. The vector $\boldsymbol{\lambda} = [\lambda_1, \lambda_2]^t$ was the monthly hazard rate for susceptible and infected deer. The vector $\boldsymbol{\alpha} = [\alpha_1, \alpha_2]^t$ were parameters affecting the degree to which these hazards increased over time. Note, values of $\boldsymbol{\alpha}$ near one indicate constant hazard over time, whereas values greater than one show increasing hazards.

We define the indicator variable W_i coded using the reference value of 0 for CWD susceptible and 1 for infected animals. We specify diffuse $N(0,1000)$ prior distributions for elements of $\log(\boldsymbol{\alpha})$, $\log(\boldsymbol{\lambda})$, and β .

To evaluate the projection matrix \mathbf{A} , we approximated the posterior distribution of annual survival probabilities using the survival functions for CWD susceptible and infected deer. For infected deer, we set $t_i=36$ (e.g., 36 months) and evaluated the survival function using posterior estimates of α_2 and λ_2 . We used a 36 month time step because monthly hazards increased over time. Therefore, annual survival was progressively lower each year after initially becoming infected. The 36 month survival was then raised to the one third power to approximate the posterior distribution of s_{inf} . For susceptible deer, we approximated the posterior distribution of annual survival for each age $s_{\text{sus},0.5} \dots, s_{\text{sus},10.5}$ by setting elements of \boldsymbol{x}_i equal to the desired covariate levels, $t_i=12$ (e.g., 12 months), and evaluating the survival function using posterior estimates of α_1 , λ_1 , and β .

Fertility: Elements of the top row of \mathbf{A} are fertilities in a Leslie matrix. To align model updates that occurred in January with the timing of fawning in June, fertility elements were the product of female survival from census to the birth pulse $s_{6,\text{inf}}, s_{6,\text{sus},1.5} \dots, s_{6,\text{sus},10.5}$, birth rate b , and neonate survival to census s_{neo} . CWD infection has small effects on birth rate and neonate survival and we simplified our model by defining recruitment as $r = b s_{\text{neo}}$. It follows that fertility elements were $f_{\text{inf}} = s_{6,\text{inf}} r$ for infected deer and $f_{\text{sus},j} = s_{6,\text{sus},j} r$ for a susceptible deer of the j^{th} age.

We began by generating age- and disease- specific survival probabilities for a six month period from census to the birth pulse. We used the approach outlined in the above section on survival modeling, except that we set $t_i=6$ (e.g., 6 months).

Second, we used a Poisson model fit to consecutive annual counts of adult females and fawns to estimate r . Fawns and adult females were counted in separate groups encountered during helicopter surveys. We assumed an equal sex ratio of fawns and only included half of the fawns counted in our analysis. The vector \mathbf{y}_f is half the sum of fawns observed in groups each year. The corresponding vector \mathbf{a} is the sum of females observed in groups in each year. Elements of these vectors correspond to observations from the t^{th} year.

It follows that the proportion of female fawns at t is y_{f_t}/a_t . The number of female fawns observed at t , y_{f_t} , can be approximated as the product of the number of CWD infected and susceptible adult females alive at $t - 1$ that survive to the birthing pulse, $(1 - \psi_0)s_{6,\text{sus}}a_{t-1} + \psi_0s_{6,\text{inf}}a_{t-1}$, and r . The number of adult females observed at t , a_t , can be approximated as the number of CWD infected and susceptible adult females alive at $t - 1$ that survive to t , $(1 - \psi_0)s_{\text{sus}}a_{t-1} + \psi_0s_{\text{inf}}a_{t-1}$, plus the number of reproductively immature deer alive at $t - 1$ that survive to t , $s_{\text{sus},0.5}y_{f_{t-1}}$. It follows that the proportion of female fawns is given by,

$$\frac{y_{f_t}}{a_t} = r \frac{((1 - \psi_0)s_{6,\text{sus}}a_{t-1} + \psi_0s_{6,\text{inf}}a_{t-1})}{(1 - \psi_0)s_{\text{sus}}a_{t-1} + \psi_0s_{\text{inf}}a_{t-1} + s_{\text{sus},0.5}y_{f_{t-1}}} = r d.$$

Continuing, y_{f_t} follows a Poisson distribution with intensity $a_t r d$.

Survival and infection probabilities in the above expression were generated as described in the preceding sections, except for one notable exception. Helicopter surveys did not differentiate adult ages. Therefore, we estimated s_{sus} using a survival function that did not include adult age effects.

To evaluate the projection matrix \mathbf{A} , we needed age- and disease specific fertilities. We derived $f_{\text{inf}} = s_{6,\text{inf}} \times r$ for infected deer and $f_{\text{sus},j} = s_{6,\text{sus},j} \times r$ for a susceptible deer of the j^{th} age.

CWD Prevalence: A Beta-binomial model was used to estimate CWD prevalence during 1997-2003 from hunter harvested deer and animals removed through management culling that overlapped the winter spatial extent of capture-mark-recapture studied deer. It follows that $p \sim \text{Beta}(y_{\text{cwd}} + 1, N_{\text{cwd}} - y_{\text{cwd}} + 1)$ where y_{cwd} is the number of CWD positive deer and N_{cwd} is the total number of tested deer.

Abundance: Quadrats that were one quarter land section were counted semiannually to estimate population abundance. The vector \mathbf{y}_{quad} is the sum of annual counts across quadrats. We assumed each element of \mathbf{y}_{quad} follows a negative binomial distribution with average count γ_k and over dispersion σ_k . We specify diffuse $N(0,1000)$ distributions for $\log(\boldsymbol{\gamma})$ and $\log(\boldsymbol{\sigma})$.

Posterior Distribution: The posterior distribution for the complete model is,

$$\begin{aligned}
& [\psi_0, \boldsymbol{\zeta}, \pi, \mathbf{Z}, \boldsymbol{\beta}, \boldsymbol{\lambda}, \boldsymbol{\alpha}, r, p, \boldsymbol{\gamma}, \boldsymbol{\sigma} | \mathbf{Y}, \mathbf{T}, \mathbf{y}_f, \mathbf{a}, y_{\text{cwd}}, N_{\text{cwd}}, \mathbf{y}_{\text{quad}}] \propto \\
& \prod_{i=1}^I \left([y_{i,1} | \pi]^{z_{i,1}} [z_{i,1} | \psi_0] \right) \prod_{t=2}^T \prod_{i=1}^I \left\{ \left([y_{i,t} | \pi]^{(z_{i,t}) V_{i,t}} \right) \left([z_{i,t} | \boldsymbol{\zeta}]^{(1-z_{i,t-1}) U_{i,t}} \right) \right\} [\psi_0] [\boldsymbol{\zeta}] [\pi] \\
& \times \prod_{i=1}^I \left([t_i | \lambda_1, \alpha_1, \boldsymbol{\beta}]^{1-W_i} [t_i | \lambda_2, \alpha_2]^{W_i} \right) [\boldsymbol{\beta}] [\boldsymbol{\lambda}] [\boldsymbol{\alpha}] \\
& \times \prod_{n=2}^N [y_{f_n} | r, a_n] [r] \\
& \times [y_{\text{cwd}} | p, N_{\text{cwd}}] [p] \\
& \times \prod_{k=1}^K [y_{\text{quad}_k} | \gamma_k, \sigma_k] [\boldsymbol{\gamma}] [\boldsymbol{\sigma}].
\end{aligned}$$

The joint posterior distribution is not available in closed form. We use a Markov chain Monte Carlo (MCMC) algorithm to simulate from the posterior distribution and to estimate the unknown parameters of interest and the latent variables. Samples were drawn from the posterior distribution of each parameter and latent state using a hybrid Gibbs sampler. All analyses were completed using program R (R Core Development Team 2013). Each of three MCMC chains was run for 100,000 iterations and the first 25,000 iterations were discarded to allow for burn-in. We confirmed convergence using the Gelman and Rubin test statistic by assuring that the potential scale reduction factor was <1.02 for each variable. Trace plots of marginal posterior distributions were inspected to ensure reasonable exploration of the parameter space. Metropolis-Hastings acceptance rates were tracked to assure values near 0.40.

A variety of tools were used to assess our model. We used posterior predictive checks to confirm whether observed data were consistent with the model. Bayesian p-values were calculated for mean and standard deviation of various data, including numbers of positive follicles in capture-mark-recapture studied deer and months till death of capture-mark-recapture studied deer. Bayesian p-values indicated an ability of our model to replicate data with similar means to the observed data. We found some inability for our model to replicate data with similar standard deviations. Cox Snell residuals were also used to confirm the proportional hazards assumption of our survival analysis.

Overview of MCMC algorithm: The MCMC algorithm proceeds as follows:

1. Initialize each parameter and the elements of the latent infection matrix with a starting value.
2. Sample $[z_{i,1}|\cdot]$ when $y_{i,1} = 0$ otherwise $z_{i,1} = 1$.

$$[z_{i,1}|\cdot] \propto \text{Brn} \left(\frac{\psi_0(1 - \pi)^{J_{i,1}}}{\psi_0(1 - \pi)^{J_{i,1}} + 1 - \psi_0} \right)$$

3. Sample $[z_{i,2}|\cdot]$ when $y_{i,1} = 0$ and $y_{i,2} = 0$ otherwise $z_{i,2} = 1$. Note that if deer i during occasion t is in the study, but not tested, then $y_{i,t}$ and $J_{i,t}$ was coded as 0.

$$[z_{i,2}|\cdot] \propto \text{Brn} \left(\frac{(1 - \pi)^{J_{i,2}V_{i,2}} \psi_i^{(1-z_{i,1})U_{i,2}}}{(1 - \pi)^{J_{i,2}V_{i,2}} \psi_i^{(1-z_{i,1})U_{i,2}} + \psi_i^{z_{i,3}U_{i,3}} (1 - \psi_i)^{(1-z_{i,3})U_{i,3}} (1 - \psi_i)^{(1-z_{i,1})U_{i,2}}} \right)$$

4. Sample $[z_{i,3}|\cdot]$ when when $y_{i,1} = 0$, $y_{i,2} = 0$, and $y_{i,3} = 0$ otherwise $z_{i,3} = 1$.

$$[z_{i,3}|\cdot] \propto \text{Brn} \left(\frac{(1 - \pi)^{J_{i,3}V_{i,3}} \psi_i^{(1-z_{i,2})U_{i,3}}}{(1 - \pi)^{J_{i,3}V_{i,3}} \psi_i^{(1-z_{i,2})U_{i,3}} + \psi_i^{z_{i,4}U_{i,4}} (1 - \psi_i)^{(1-z_{i,4})U_{i,4}} (1 - \psi_i)^{(1-z_{i,2})U_{i,3}}} \right)$$

5. Sample $[z_{i,4}|\cdot]$ when when $y_{i,1} = 0$, $y_{i,2} = 0$, $y_{i,3} = 0$, and $y_{i,4} = 0$ otherwise $z_{i,4} = 1$.

$$[z_{i,4}|\cdot] \propto \text{Brn} \left(\frac{(1 - \pi)^{J_{i,4}V_{i,4}} \psi_i^{(1-z_{i,3})U_{i,4}}}{(1 - \pi)^{J_{i,4}V_{i,4}} \psi_i^{(1-z_{i,3})U_{i,4}} + \psi_i^{z_{i,5}U_{i,5}} (1 - \psi_i)^{(1-z_{i,5})U_{i,5}} (1 - \psi_i)^{(1-z_{i,3})U_{i,4}}} \right)$$

6. Sample $[z_{i,5}|\cdot]$ when when $y_{i,1} = 0$, $y_{i,2} = 0$, $y_{i,3} = 0$, $y_{i,4} = 0$ and $y_{i,5} = 0$ otherwise $z_{i,5} = 1$.

$$[z_{i,5}|\cdot] \propto \text{Brn} \left(\frac{(1 - \pi)^{J_{i,5}V_{i,5}} \psi_i^{(1-z_{i,4})U_{i,5}}}{(1 - \pi)^{J_{i,5}V_{i,5}} \psi_i^{(1-z_{i,4})U_{i,5}} + (1 - \psi_i)^{(1-z_{i,4})U_{i,5}}} \right)$$

7. Sample $[\psi_0|\cdot] \propto \text{Beta}(\sum_i z_{i,1} + 1, m - \sum_i z_{i,1} + 1)$.

8. Sample elements of $[\zeta|\cdot]$ sequentially using a Metropolis step.

9. Sample $[\pi|\cdot] \propto \text{Beta}(\sum_{z_{i,t}=1} y_{i,t} + 1, \sum_{z_{i,t}=1} (J_{i,t} - y_{i,t}) + 1)$.

10. Sample elements of $[\alpha|\cdot]$ sequentially using a Metropolis step.

11. Sample elements of $[\lambda|\cdot]$ sequentially using a Metropolis step.

12. Sample elements of $[\beta|\cdot]$ sequentially using a Metropolis step.

13. Derive annual survival estimates for susceptible deer $s_{\text{sus},0.5}, \dots, s_{\text{sus},10.5}$ using posterior estimates of λ_1 , α_1 , and β .

14. Derive annual survival of infected deer s_{inf} using posterior estimates of λ_2 and α_2 .
15. Sample $[r|\cdot]$ using using a Metropolis step.
16. Sample $[p|\cdot] \propto \text{Beta}(y_{\text{cwd}} + 1, N_{\text{cwd}} - y_{\text{cwd}} + 1)$.
17. Sample $[\gamma|\cdot]$ using a Metropolis step.
18. Sample $[\sigma|\cdot]$ using a Metropolis step.
19. We portrayed the deer population in 21 demographic and disease stages. The vector \mathbf{n}_t described the number of deer in each of these stages during January of a given year. The first element, $n_{1,t}$ was for deer that were 6 months old and CWD susceptible. The next ten elements $n_{2,t}, \dots, n_{11,t}$ represented CWD susceptible deer from in 1.5 to 10.5 years old. The final ten elements $n_{12,t}, \dots, n_{21,t}$ portrayed CWD infected deer from in 1.5 to 10.5 years old. The vector $\mathbf{A}\mathbf{n}_t$ described the deer population during the subsequent year where \mathbf{A} was a 21×21 projection matrix. Construct \mathbf{A} .

$$\mathbf{A} = \begin{bmatrix} 0 & f_{\text{sus},1.5} & f_{\text{sus},2.5} & \dots & f_{\text{sus},10.5} & f_{\text{inf}} & f_{\text{inf}} & \dots & f_{\text{inf}} \\ s_{\text{sus},0.5}(1 - \psi) & 0 & 0 & \dots & 0 & 0 & 0 & \dots & 0 \\ 0 & s_{\text{sus},1.5}(1 - \psi) & 0 & \dots & 0 & 0 & 0 & \dots & 0 \\ \vdots & \vdots \\ 0 & 0 & 0 & \dots & 0 & 0 & 0 & \dots & 0 \\ s_{\text{inf}}\psi & 0 & 0 & \dots & 0 & 0 & 0 & \dots & 0 \\ 0 & s_{\text{inf}}\psi & 0 & \dots & 0 & s_{\text{inf}} & 0 & \dots & 0 \\ \vdots & \vdots \\ 0 & 0 & 0 & \dots & 0 & 0 & 0 & \dots & 0 \end{bmatrix}$$

This step was repeated for each wintering population unit.

20. Derive the population growth rate for a CWD infected population λ_{cwd} by calculating the dominant eigenvalue of \mathbf{A} . Also derive CWD prevalence under equilibrium

conditions (p^*) from the dominant eigenvector of \mathbf{A} . This step was repeated for each wintering population unit.

21. Derive the population growth rate for a CWD free population λ_{free} by calculating the dominant eigenvalue of the upper left 12x12 sub matrix of \mathbf{A} and setting ψ equal to zero. This step was repeated for each wintering population unit.
22. Repeat steps 2 through 19 many times.

This completes the MCMC algorithm.

Monte Carlo estimates of i) differences in population growth rates with and without CWD and ii) differences in prevalence during intense surveillance (1997-2001) and under disease equilibrium:

1. Derive the difference between population growth rates λ_{cwd} and λ_{free} . This quantity was a measure of the effect of CWD on deer population growth. Select with replacement an element of λ_{cwd} and λ_{free} and calculate the difference of these values. This step was repeated for each wintering population unit.
2. Derive the difference between prevalence recorded during intense surveillance efforts p and predicted under disease equilibrium p^* . Select with replacement an element of p and p^* and calculate the difference of these values. This step was repeated for each population unit where surveillance data were available.
3. Repeat steps 21 through 23 many times.

APPENDIX 3: SUPPLEMENTARY MATERIAL

We define \mathbf{Z} as the true infectious status matrix. We define \mathbf{Y} as an observation matrix of the observed number of follicles exhibiting PrP^{Sc}. We define the corresponding matrix, \mathbf{J} , as total numbers of follicles. There are I total individuals which were in the study for a variable number of years. We define the indicator variable $U_{i,t}$ coded using the reference value of 0 when an individual i was no longer in the study on occasion t and with the value of 1 when individual i was in the study. Similarly, we define the indicator variable $V_{i,t}$ coded as 0 when individual i was not tested and 1 when individual i was tested. Model parameters are annual infection probability (ψ), population prevalence (ψ_0), and probability that a follicle tests positive in deer i on occasion t ($\pi_{i,t}$). We treated $\pi_{i,t}$ hierarchically. That is, $\text{logit}(\pi_{i,t}) = \mathbf{X}\boldsymbol{\beta} + \epsilon_{i,t}$ where $\boldsymbol{\beta}$ were logistic model coefficients, \mathbf{X} was a matrix of covariate levels, and $\epsilon_{i,t}$ were additional unstructured error. Errors $\epsilon_{i,t}$ followed a $N(0, \sigma^2)$ distribution. Then, the posterior distribution follows,

$$\begin{aligned}
 [\psi, \psi_0, \boldsymbol{\beta}, \sigma^2, \mathbf{Z} | \mathbf{Y}] \propto & \\
 & \prod_{i=1}^I \left([y_{i,1} | \boldsymbol{\beta}, \sigma^2]^{z_{i,1}} [z_{i,1} | \psi_0] \right) \\
 & \prod_{t=2}^T \prod_{i=1}^I \left\{ \left([y_{i,t} | \boldsymbol{\beta}, \sigma^2]^{(z_{i,t}) V_{i,t}} \right) \left([z_{i,t} | \psi]^{(1-z_{i,t}-1) U_{i,t}} \right) \right\} \\
 & [\psi_0] [\psi] [\boldsymbol{\beta}] [\sigma^2]
 \end{aligned}$$

The first product in the posterior refers to the initial testing occasion. The mixture distribution for the number of observed positive tests is expressed $[y_{i,1} | \boldsymbol{\beta}, \sigma^2]^{z_{i,1} V_{i,t}}$. When $z_{i,1} = 1$ (e.g., an infected individual) the probability density of the number of positive tests reduces to $[y_{i,1} | \boldsymbol{\beta}, \sigma^2]$ otherwise, when $z_{i,1} = 0$ (i.e., a susceptible individual) or $V_{i,t} = 0$ (i.e., individual i not tested), the probability density reduces to 1. The second product refers to the

subsequent testing occasions. The mixture distribution for the infection status is expressed $[z_{i,t}|\psi]^{(1-z_{i,t-1})U_{i,t}}$. When $z_{i,t-1} = 1$ (e.g., individual i was found to be infected in a previous time period) or $U_{i,t} = 0$ (e.g., individual i is no longer in the study), then the probability density reduces to 1 otherwise the probability density equals $[z_{i,t}|\psi]$.

We specify a diffuse Beta(1,1) prior distribution for ψ_0 and ψ , and a diffuse N(0,1000) prior distribution for elements of β and $\log(\sigma^2)$. Marginal posterior distributions of latent states $z_{i,t}$ and parameters were estimated using Markov chain Monte Carlo (MCMC) methods. Full conditional distributions were found in closed form for $z_{i,t}$, ψ_0 , and ψ . These derivations can be found in Chapter 3. Full conditional distributions for logistic model coefficients were not found in closed form and updated using a Metropolis step. Samples were drawn from the posterior distribution of each parameter and latent state using a hybrid Gibbs sampler. Each of three MCMC chains was run for 100,000 iterations and the first 25,000 iterations were discarded to allow for burn-in. We confirmed convergence using the Gelman and Rubin test statistic by assuring that the potential scale reduction factor was <1.01 for each variable. We confirmed ability of our model to replicate the observed data using posterior predictive checking.

APPENDIX 4: SUPPLEMENTARY MATERIAL

We define \mathbf{Z} as an infectious status matrix. We define \mathbf{Y} as an observation matrix of the observed number of follicles exhibiting PrP^{Sc}. We define the corresponding matrix, \mathbf{J} , as total numbers of follicles. There are I total individuals which were in the study for a variable number of years. We define the indicator variable $U_{i,t}$ coded using the reference value of 0 when an individual i was no longer in the study on occasion t and with the value of 1 when individual i was in the study. Similarly, we define the indicator variable $V_{i,t}$ coded as 0 when individual i was not tested and 1 when individual i was tested. Model parameters are annual infection probability of the i^{th} individual on the t^{th} occasion $\psi_{i,t}$, population prevalence ψ_0 , and probability that a follicle tests positive π . We treated infection probability hierarchically. That is, $\text{logit}(\psi_{i,t}) = \mathbf{X}\boldsymbol{\beta}$ where $\boldsymbol{\beta}$ were logistic model coefficients and \mathbf{X} was a matrix of covariate levels. The posterior distribution follows,

$$\begin{aligned}
 [\pi, \psi_0, \boldsymbol{\beta}, \mathbf{Z} | \mathbf{Y}] \propto & \\
 & \prod_{i=1}^I \left([y_{i,1} | \pi]^{z_{i,1}} [z_{i,1} | \psi_0] \right) \\
 & \prod_{t=2}^T \prod_{i=1}^I \left\{ \left([y_{i,t} | \pi]^{(z_{i,t})V_{i,t}} \right) \left([z_{i,t} | \boldsymbol{\beta}]^{(1-z_{i,t-1})U_{i,t}} \right) \right\} \\
 & [\psi_0][\pi][\boldsymbol{\beta}]
 \end{aligned}$$

The first product in the posterior refers to the initial testing occasion. The mixture distribution for the number of observed positive tests is expressed $[y_{i,1} | \pi]^{z_{i,1}V_{i,t}}$. When $z_{i,1} = 1$ (e.g., an infected individual) the probability density of the number of positive tests reduces to $[y_{i,1} | \pi]$ otherwise, when $z_{i,1} = 0$ (i.e., a susceptible individual) or $V_{i,t} = 0$ (i.e., individual i not tested), the probability density reduces to 1. The second product refers to the subsequent testing occasions. The mixture distribution for the infection status is expressed

$[z_{i,t}|\boldsymbol{\beta}]^{(1-z_{i,t-1})U_{i,t}}$. When $z_{i,t-1} = 1$ (e.g., individual i was found to be infected in a previous time period) or $U_{i,t} = 0$ (e.g., individual i is no longer in the study), then the probability density reduces to 1 otherwise the probability density equals $[z_{i,t}|\boldsymbol{\beta}]$.

We specify diffuse Beta(1,1) prior distributions for ψ_0 and ψ , and diffuse N(0,1000) prior distributions for elements of $\boldsymbol{\beta}$ and $\log(\sigma^2)$. Marginal posterior distributions of latent states $z_{i,t}$ and parameters were estimated using Markov chain Monte Carlo (MCMC) methods. Full conditional distributions were found in closed form for $z_{i,t}$, ψ_0 , and ψ . These derivations can be found in Chapter 3. Full conditional distributions for logistic model coefficients were not found in closed form and updated using a metropolis step. Samples were drawn from the posterior distribution of each parameter and latent state using a hybrid Gibbs sampler. Each of three MCMC chains was run for 100,000 iterations and the first 25,000 iterations were discarded to allow for burn-in. We confirmed convergence using the Gelman and Rubin test statistic by assuring that the potential scale reduction factor was <1.01 for each variable. We confirmed ability of our model to replicate the observed data using posterior predictive checking.